

Biological ice nucleating particles at tropospheric cloud height

Inauguraldissertation

zur

Erlangung der Würde eines Doktors der Philosophie

vorgelegt der

Philosophisch-Naturwissenschaftlichen Fakultät

der Universität Basel

von

Emiliano Stopelli

von Italien

Basel, 2016

Originaldokument gespeichert auf dem Dokumentenserver der Universität Basel: edoc.unibas.ch



Dieses Werk ist unter dem Vertrag "Creative Commons Attribution-NonCommercial-NoDerivatives 4.0 International License" lizenziert. Die vollständige Lizenz kann eingesehen werden unter: creativecommons.org/licenses/by-nc-nd/4.0/

Genehmigt von der Philosophisch-Naturwissenschaftlichen Fakultät

Auf Antrag von

Fakultätsverantwortliche: Prof. Dr. Christine Alewell

Dissertationsleiterin: Prof. Dr. Cindy E. Morris

Korreferent: Dr. Benjamin J. Murray

Basel, 21.06.2016

Dekan der Fakultät
Prof. Dr. Jörg Schibler

Summary

Airborne ice nucleating particles (INPs) promote the freezing of cloud droplets, which is relevant for the radiative properties of clouds and for the development of precipitation. A quantitative assessment of the impact of INPs on cloud processes and on their responsiveness to climate and land use change is still missing. This is particularly true for INPs of biological origin. They are made of molecules produced by bacteria, fungi, plants, lichens, which promote the freezing of droplets at temperatures above $-15\text{ }^{\circ}\text{C}$. Bottom-up modelling studies based on the release of ice nucleation active cells from crops and plants have excluded any chance for biological INPs to impact climate. Nevertheless, recent observations point at the ubiquity across ecosystems of species capable of producing INPs and at the fact that such INPs can be released from cells and maintain their activity for instance when linked to soil particles.

Here we employed a top-down approach to improve our understanding of the variability of biological INPs in precipitation. 16 sampling campaigns were organised between 2012 and 2014 and over 100 precipitation samples were collected at the High Altitude Research Station Jungfraujoch (3580 m a.s.l., Switzerland). They have been analysed for their content in INPs active at moderate supercooling directly in field with our new immersion freezing apparatus LINDA. Several environmental parameters have been studied to derive more information on the most relevant factors responsible for the variability of INPs. The abundance of bacterial cells and the presence of the nucleation active plant pathogen bacterium *Pseudomonas syringae* have been determined as well, to know more on the nature of biological INPs in precipitation.

By means of stable water isotopes, we demonstrate that INPs are rapidly and selectively removed by precipitating clouds. Focusing on INPs active at $-8\text{ }^{\circ}\text{C}$ (INPs₋₈), their concentrations varied between 0.21 and 434 INPs₋₈ mL⁻¹. Up to 75% of this large temporal variability can be modelled and predicted by multiple linear regression models based on the combination of a few environmental parameters. These models point at the interaction of “source” (uptake) and “sink” (removal) processes as relevant to determine the variability of INPs₋₈. Large abundance of INPs₋₈ can be best expected with a coincidence of high wind speed and little precipitation lost from an air mass prior to sampling. Bacterial cells present more constant concentrations than INPs, from $2.4 \cdot 10^3$ to $6.8 \cdot 10^4$ cells mL⁻¹, with their numbers increasing mainly under high wind speed. INPs are more efficiently removed than bacterial cells by precipitation, which implies a larger variability, a shorter residence time in the atmosphere and shorter lengths of dispersal for INPs rather than for bacterial cells. *P. syringae* has been successfully isolated at high-altitude and its presence seems to be influenced by uptake and removal processes, as it happens for INPs₋₈.

This study constitutes a strong improvement of our understanding of the abundance, variability and nature of biological INPs in precipitation and points at the potential for this group of INPs to impact cloud processes. In fact, a coincidence of high wind speed and first precipitation often occurs at the passage of a front, where the meteorological conditions are also favourable to precipitation. This can be the ideal and frequent context where to expect large numbers of INPs₋₈ and to study their effects on cloud processes. Furthermore, bacterial cells can contribute to the number of INPs₋₈, but a large fraction of INPs₋₈ is potentially due to cellular fragments and macromolecules, both freely floating and attached to mineral and soil dust. This multiplies the possibility for biological INPs to be released and be present in the atmosphere.

Table of contents

Summary	I
Table of contents	III
1. Introduction	1
1.1 Ice nucleating particles (INPs): impact on clouds and precipitation	1
1.2 INPs of biological origin and open issues	3
1.3 Objectives of the thesis	4
1.4 Outline of the thesis	5
2. Freezing nucleation apparatus puts new slant on study of biological ice nucleators in precipitation	7
Abstract	8
2.1 Introduction	9
2.2 Description of the apparatus (LINDA)	10
2.3 New applications	13
2.3.1 Evolution of a sample upon storage at low temperature	13
2.3.2 Progressive isolation of ice nucleators from a sample	15
2.4 Conclusions	16
2.5 Acknowledgements	17
3. Ice nucleation active particles are efficiently removed by precipitating clouds ...	19
Abstract	20
3.1 Introduction	21
3.2 Methods	22
3.2.1 Sample collection	22
3.2.2 $\delta^{18}\text{O}$ analysis and modelling of f_v values	22
3.2.3 Total number of particles $N_{>0.5}$	23
3.2.4 Statistics	24
3.3 Results	24
3.3.1 General overview	24
3.3.2 INPs get rapidly lost from a precipitating cloud	25
3.3.3 Selective removal of INPs	27

3.4 Discussion	28
3.5 Acknowledgements.....	29
3.6 Authors Contributions	29
4. Predicting abundance and variability of ice nucleating particles in precipitation at the high-altitude observatory Jungfraujoch.....	31
Abstract	32
4.1 Introduction.....	33
4.2 Methods.....	34
4.2.1 Sample collection and analysis of INPs.....	34
4.2.2 Parameters related to the concentration of INPs.....	35
4.2.3 Statistical analyses and modelling.....	36
4.3 Results and discussion	38
4.3.1 Model calibration.....	38
4.3.2 Model validation	41
4.3.3 Source and sink effects	42
4.4 Conclusions	43
4.5 Acknowledgements.....	44
4.6 Author contributions.....	44
5. Bacteria at tropospheric cloud heights and potential impact on ice nucleation ..	45
Abstract	46
5.1 Introduction.....	47
5.2 Materials and methods	48
5.2.1 Sampling and bacterial cell counts	48
5.2.2 Selective isolation of <i>P. syringae</i>	49
5.2.3 Environmental parameters and INPs _g	50
5.2.4 Statistics.....	50
5.3 Results and discussion	50
5.3.1 Bacterial cells and successful isolation of <i>P. syringae</i>	50
5.3.2 Factors influencing the abundance of bacterial cells.....	51
5.3.3 Behaviour of INPs _g compared to bacterial cells	54
5.3.4 Role of bacterial cells in precipitation	55
5.4 Conclusions	56
5.5 Supplementary material.....	57
5.5.1 INPs _g and progressive heating/filtration	57
5.5.2 Heat sensitivity of INPs _g	58
5.5.3 Potential forms of aggregation of INPs _g	58

6. Clues that decaying leaves enrich Arctic air with ice nucleating particles	61
Abstract	62
6.1 Introduction	63
6.2 Material and methods	63
6.3. Results and discussion	64
6.4 Acknowledgements	66
7. Conclusions and Outlooks.....	67
7.1 Conclusions.....	67
7.2 Outlooks	69
7.2.1 Networking observatories to study the spatial variability of INPs	69
7.2.2 Shape of the freezing profiles and source region fingerprints.....	69
7.2.3 Approaches to distinguish groups of biological INPs	69
7.2.4 Strategies to link biological INPs to the development of precipitation	70
Additional contents	73
A1 NICE project and airborne INPs	73
A2 Rain collection at the station Opme	77
A3 Shape of the freezing profiles - first trials	77
A4 Table of data.....	78
References	83
Acknowledgements/Ringraziamenti	93

Introduction

1.1 Ice nucleating particles (INPs): impact on clouds and precipitation

Airborne particles impact climate on Earth both directly, absorbing and scattering radiation, and indirectly, influencing the radiative properties and the lifetime of clouds by originating precipitation. According to the latest scientific report of the Intergovernmental Panel on Climate Change (IPCC, 2013a) a precise quantification of the indirect role of these particles on climate and their responsiveness to climate and land-use change remains largely impossible.

In a low warm cloud, water is formerly condensed around particles acting as cloud condensation nuclei (CCN). The larger is the number of CCN, the more droplets will be formed, increasing the scattering of solar radiation and the lifetime of the cloud, since such tiny droplets may be too small and too many to effectively coalesce and originate raindrops. A fraction of CCN is acting also as ice nucleating particles (INPs). INPs provide a surface where the aggregation of water molecules into ice crystals is enhanced. Without INPs, the freezing of water would spontaneously occur by random aggregation of water molecules at temperature below $-36\text{ }^{\circ}\text{C}$. This is what happens in high cold cirrus clouds, which are composed of ice crystals only and are optically thin to incoming solar radiation, promoting net warming of the Earth. As a warm cloud progressively cools down, ice crystals are progressively formed around INPs. Such crystals tend to grow rapidly at the expense of cloud droplets, because of the smaller saturation pressure of water vapour over ice than over the liquid phase, leading to a diffusion gradient of water molecules. Therefore, with INPs precipitation can be originated at a faster rate, reducing the lifetime of clouds. Moreover, the presence of the ice phase in clouds changes their optical thickness, that is to say their interaction with radiation. Between low warm clouds (made of liquid droplets formed around CCN) and high cold cirrus clouds (where only ice crystals are present), mixed-phase clouds exist. These clouds contain variable amounts of liquid water and ice, are present in the troposphere and are relevantly

1.1 Ice nucleating particles (INPs): impact on clouds and precipitation

connected to climate and to the development of precipitation. It has been demonstrated that the large majority of precipitation on Earth is generated from ice- or mixed-phase clouds (Lau and Wu, 2003; Mülmenstädt, et al., 2015).

A quantitative assessment of the feedbacks on climate and on precipitation is specifically difficult for INPs in the atmosphere (IPCC, 2013b, chapter 7 and paragraph 7.3.3.4), which depends on several factors:

- A range of natural and anthropogenic particles are known as efficient INPs in the atmosphere, like mineral dust, volcanic ashes, bioaerosols and soot. Still, all these groups of particles show ice nucleating activities at different temperatures. While minerals, soot and salts tend to be dominantly active below $-15\text{ }^{\circ}\text{C}$, INPs of biological origin, such as pollen, fungal spores, soil organic matter and bacteria, initiate freezing above $-15\text{ }^{\circ}\text{C}$ (Murray et al., 2012);
- Several nucleation mechanisms exist, like immersion freezing, contact freezing and deposition nucleation. Ice multiplication processes like rime splintering and the production of ice fragments by breakings and collisions multiply the freezing potential of INPs (Cantrell and Heymsfield, 2005);
- The composition of INPs can change in time and space, providing different nucleation possibilities in clouds. This has a strong impact on the presence of the ice-phase in clouds, which determines their radiative properties, their vertical development and the formation of precipitation;
- Measurements on INPs in the environment are concentrated at some points and for a limited time period.

To merge this gap of knowledge and observations, recent years have seen a “resurgence” in the measurements of INPs in the laboratory and in the atmosphere (DeMott et al., 2011).

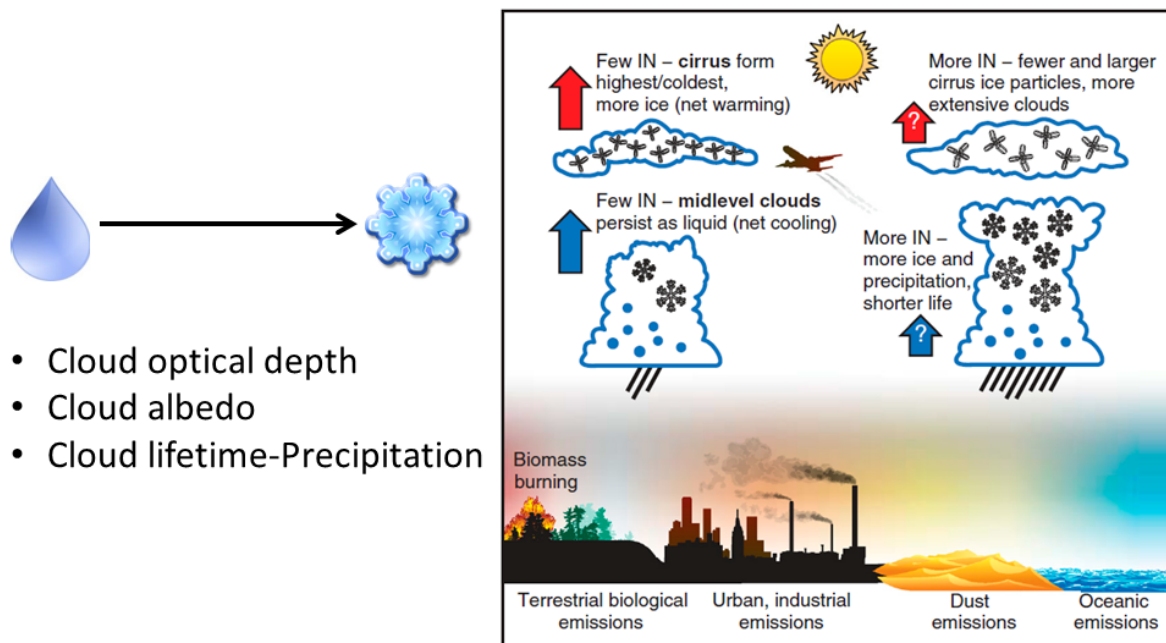


Figure 1.1 The freezing of droplets changes the optical properties of clouds, their interactions with radiation and increases the chance for precipitation. Large uncertainties exist in modelling the effect of INPs on the radiative budget of clouds and precipitation, as well as in predicting the feedbacks between the emissions of INPs from several sources and climate change (adapted from DeMott et al., 2010, where INPs are indicated as IN).

1.2 INPs of biological origin and open issues

Particularly intriguing is the assessment of the relevance of INPs of biological origin on cloud processes and on the onset of precipitation. The most efficient ice nucleating substance discovered so far comes from the protein produced by the plant pathogen bacterium *Pseudomonas syringae* (Maki et al., 1974), capable of freezing water at temperatures up to -2 °C. This bacterium has been progressively isolated from both crops and non-agricultural ecosystems (Morris et al., 2008) and along with INPs of biological origin in precipitation samples (Monteil et al., 2014). This promoted the necessity to assess the relevance of microorganisms showing ice nucleating activity for climate on Earth. This question has been firstly addressed with a bottom-up approach, where microorganisms were analysed for their ice nucleating properties and the results were fed into numerical models to predict their likely atmospheric abundances and their impacts on climate. The results indicate that the expected airborne concentrations of these cellular INPs are numerically lower than those of more abundant INPs like mineral dust, soot and ashes, but dominant for temperatures warmer than -15 °C (Murray et al., 2012). When fed into models simulating global climate, particles of biological origin (simulated as single bacterial, fungal and pollen cells emitted from several ecosystems) resulted to have a very small effect on cloud glaciation (Burrows et al., 2009; Hoose et al., 2010a; Hoose et al., 2010b; Sesartic et al., 2012).

In the recent years this perspective has significantly changed. More and more species of bacteria, fungi, plants, lichens have been discovered to promote ice nucleation, as means for damaging host species or neighbouring cells, accessing new sources of food, surviving at cold temperatures, collecting water in moisture-limited environments (Fröhlich-Nowoisky et al., 2015; Joly et al., 2013; Moffett et al., 2015; Morris et al., 2013a; O'Sullivan et al., 2015; Pummer et al., 2015). These organisms either host ice nucleation active molecules on the surface of the cell or even release them in the environment. Moreover, once a cell dies, ice nucleating molecules seem to maintain their activity when linked to mineral particles. This is reflected in the fact that organic matter produced from living and dead organisms can significantly increase the ice nucleating properties of soil, with a different behaviour according to the geographical origin of the soil itself (Conen et al., 2011; O'Sullivan et al., 2014).

In addition to this, some top-down studies have been carried out to determine the role of biological INPs in the atmosphere, based on the analysis of INPs captured in the atmosphere or in precipitation samples. Precipitation samples collected around the world confirm that INPs active at moderate supercooling are less abundant than those active at lower temperatures, but their concentrations vary over several orders of magnitude (Petters and Wright, 2015). Biological particles can make up a relevant amount of ice residuals in clouds (Pratt et al., 2009), are found associated to dust in precipitation samples (Creamean et al., 2013; Prenni et al., 2009) and are dominant among the INPs active at moderate supercooling in precipitation (Joly et al., 2014). Their local abundance increases with an increase in relative humidity and after a precipitation event (Prenni et al., 2013; Wright et al., 2014). This has promoted the question whether and on which scale bioprecipitation feedbacks occur (Morris et al., 2014), that is to say to what extent ecosystem can biologically enhance precipitation, which turns to be positive for maintaining the ecosystem itself. It is realistic to think that changes in land use and in climate can influence the proportion of biological and mineral material released in the atmosphere, with a direct feedback on climate and land characteristics themselves (Conen and Leifeld, 2014; Morris et al., 2014). Last, but not of least importance, INPs of biological origin are active at temperatures where ice multiplication through riming and ice splintering can take place (Hallett and Mossop, 1974).

All these recent findings on the variability of the species producing biological INPs, on the multiplicity of forms of such biological INPs in the environment and on the variable presence of biological INPs in the atmosphere and in precipitation have reopened the debate on the role of biological INPs on cloud processes and on precipitation. This still remains largely unclear and it is crucial to assess the abundance of biological INPs in the atmosphere and to understand the sources of their quantitative and qualitative variability (DeMott and Prenni, 2010). This will improve also the understanding on the processes of spreading of some ice nucleation active plant pathogenic species like *P.syringae* and to understand to which extent land use change and climate change alter regional and global weather patterns.

1.3 Objectives of the thesis

This thesis project started in September 2012, pointing at the necessity to obtain more information on the abundance of INPs of biological origin, on the factors responsible for their variability and on their relevance for cloud processes. Four main goals were set:

- Determine the abundance and nucleation spectra of warm-temperature ice nucleating particles at tropospheric cloud height;
- Identify the conditions associated with high number concentrations of INPs active at warm-temperature;
- Quantify the relative contributions of intact microorganisms and biological residues on soil dust for conditions when INPs active at moderate supercooling are particularly abundant;
- Isolate *Pseudomonas syringae* from samples with large numbers of INPs active at warm temperatures.

Following a top-down approach, core activity of the thesis has been the periodical collection of precipitation samples at the High Altitude Research Station Jungfrauoch (3580 m a.s.l., Switzerland) and their analysis for the content of INPs active at moderate supercooling (fig. 1.2). This site offers the possibility to collect precipitation directly inside clouds, avoiding the contamination of the sample by the scavenging of particles, which generally occurs between the bottom of the cloud and the ground. Falling snow samples have been collected on the terrace of the Sphinx observatory on a baking tin and successively analysed directly in field with a new LED-based immersion freezing apparatus LINDA, in order to do the analysis of the samples as soon as possible after their collection. In fact, immersion freezing is the dominant mechanism of nucleation for INPs active at moderate supercooling (Hoose and Möhler, 2012) Information on the meteorological conditions associated with the air masses originating precipitation have been collected and new measurements have been integrated into the thesis project, like:

- The content of ^{18}O and ^2H in precipitation;
- The total number of bacterial cells and the living ones by double staining and epifluorescence microscopy.



Figure 1.2 a) Location of the Research Station Jungfrauoch; b and c) example of snow collection on the terrace of the Sphinx building; d) LINDA apparatus brought on site to directly measure INPs active at moderate supercooling.

1.4 Outline of the thesis

The starting point of the work was the familiarisation with the analysis of INPs by immersion freezing with the new apparatus LINDA (LED-based Ice Nucleation Detection Apparatus). This instrument offers the possibility to automatically detect the freezing of droplets, improving the precision and rapidity of analysis of a sample. LINDA was firstly tested in the laboratory and a second model was successively brought in field at Jungfrauoch. **Chapter 2** provides a detailed description of LINDA and of its potential applications, setting the methodological background of the whole thesis work.

Relevant information, which is generally missing when collecting rain and snow samples, is the quantity of precipitation lost from the air mass prior to sampling. To derive this information we started measuring the content of ^{18}O in precipitation collected at Jungfrauoch. Under simple modelling assumptions it is possible to use $\delta^{18}\text{O}$ values from snow to derive the fraction of water vapour lost as precipitation from a cloud prior to sampling. This approach is described in detail in **Chapter 3**. By using water stable isotopes we managed to demonstrate that INPs are efficiently removed by precipitating clouds.

Chapter 4 presents the results of sampling campaigns done at Jungfraujoch to determine the abundance of INPs active at moderate supercooling (specifically at $-8\text{ }^{\circ}\text{C}$, hereafter INPs₈) in precipitation and the conditions associated with large abundance of INPs₈. The set of data belonging to a first year of sampling campaigns has been employed to construct models capable of describing the variability of INPs₈, while data coming from a second year of observations have been used to test the predictive power of these statistically built models. Results of this modelling point at the best conditions when to expect large numbers of INPs₈.

In order to improve our understanding on the sources of biological INPs in precipitation, we also looked for the number of bacterial cells (total and living) and for the presence of culturable *P. syringae*. Relating bacterial cells and *P. syringae* to INPs₈ helped a better assessment of the behaviour of such organisms once airborne and their role in biological ice nucleation activity. These data are presented in **Chapter 5**.

Chapter 6 is an added activity to this thesis and shows a sampling campaign done in North Norway in July 2015. The objective of this work was to study the abundance of airborne INPs in the Arctic, which is known to be an INP-limited place, causing the persistence of thin clouds with low rates of precipitation. The Arctic is a perfect place also to study the effects of climate change on INPs. In fact, warming is causing the progressive greening of areas around the Arctic, with unknown effect on the load of airborne biological INPs and their impact on cloud properties.

The conclusions of the thesis are drawn in **Chapter 7**, along with the depiction of several outlooks on future activities to improve top-down approaches, ultimately aimed at assessing the impact of biological INPs on the properties of clouds and on the onset of precipitation.

Freezing nucleation apparatus puts new slant on study of biological ice nucleators in precipitation

This chapter has been published as article:

Stopelli, E.¹, Conen, F.¹, Zimmermann, L.¹, Alewell, C.¹, and Morris, C. E.²: Freezing nucleation apparatus puts new slant on study of biological ice nucleators in precipitation, *Atmospheric Measurement and Techniques*, 7, 129–134, doi.org/10.5194/amt-7-129-2014, 2014.

¹ Environmental Geosciences, University of Basel, CH-4056 Basel, CH

² INRA, UR 0407 Plant Pathology Research Unit, 84143 Montfavet, FR

Abstract

For decades, drop-freezing instruments have contributed to a better understanding of biological ice nucleation and its likely implications for cloud and precipitation development. Yet, current instruments have limitations. Drops analysed on a cold stage are subject to evaporation and potential contamination. The use of closed tubes provides a partial solution to these problems, but freezing events are still difficult to be clearly detected. Here, we present a new apparatus where freezing in closed tubes is detected automatically by a change in light transmission upon ice development, caused by the formation of air bubbles and crystal facets that scatter light. Risks of contamination and introduction of biases linked to detecting the freezing temperature of a sample are then minimized. To illustrate the performance of the new apparatus we show initial results of two assays with snow samples. In one, we repeatedly analysed the sample (208 tubes) over the course of a month with storage at +4 °C, during which evidence for biological ice nucleation activity emerged through an increase in the number of ice nucleators active around -4 °C. In the second assay, we indicate the possibility of increasingly isolating a single ice nucleator from a precipitation sample, potentially determining the nature of a particle responsible for a nucleation activity measured directly in the sample. These two seminal approaches highlight the relevance of this handy apparatus for providing new points of view in biological ice nucleation research.

2.1 Introduction

Certain particles suspended in the atmosphere provide surfaces for nucleating ice in rising and cooling air masses. These small activated ice fractions can enlarge through the Wegener-Bergeron-Findeisen process of accretion by water vapor deposition. Secondary processes of collision and collection then may lead to the formation of ice fragments sufficiently large to fall and develop into precipitation. The only naturally occurring particles active at temperatures warmer than $-12\text{ }^{\circ}\text{C}$ are mainly biological ice nucleators (IN) (Murray et al., 2012), such as bacteria and parts thereof. Their potential to facilitate precipitation is still under debate, particularly their impact on global or on regional scales (Hoose et al., 2010a; Möhler et al., 2007; Morris et al. 2011). Bacteria are in fact minor constituents of aerosols, moreover only a fraction of them is capable of ice nucleation activity. However, in the temperature window between -3 and $-8\text{ }^{\circ}\text{C}$ a process of ice multiplication through splintering (Hallett and Mossop, 1974) can effectively multiply a very small number of initial ice particles ($< 10\text{ m}^{-3}$) and lead to the full glaciation of supercooled cumulus clouds (Mason, 1996).

All these open questions are part of a recent “resurgence in ice nuclei measurement research” (DeMott et al., 2011), where measurements at temperatures above $-12\text{ }^{\circ}\text{C}$ are clearly a remaining research issue. The objectives of that research are to reliably quantify the abundance of IN in the air that are active above $-12\text{ }^{\circ}\text{C}$, to obtain information on their temporal dynamics, on their sources, on the environmental factors determining their numbers, and on the scale of their influence (DeMott and Prenni, 2010; Möhler et al., 2007; Morris et al., 2011).

Different instruments have been developed to assess the concentration of IN in the atmosphere and to study their behaviour. Cloud chambers have seen substantial improvements in recent decades (DeMott et al., 2011), but there has not been the same progress with drop freeze instruments. These instruments are the only ones that can be used to estimate the very small numbers of IN in environmental samples active at temperatures warmer than $-10\text{ }^{\circ}\text{C}$. Typically, a sample (melted snow, rain or cloud water, impinger liquid with trapped aerosol) is divided into aliquots in the form of small drops on plates or larger aliquots in tubes. These are then allocated in a cooling bath where temperature decreases over time. The temperature of nucleation of each drop is recorded through direct observation of increased turbidity due to freezing of the water sample. Probably the most widely used instrument of this kind is the one described by Vali and Stansbury (1966), which continues to provide new insights into freezing nucleation at temperatures above $-15\text{ }^{\circ}\text{C}$ (e.g. Attard et al., 2012; Joly et al., 2013; Vali, 1995, 2008). Drop freeze assays provide no sharp discrimination among all classes of IN present in a sample and on micro-scale mechanisms of freezing. However, they allow the analysis of larger quantities of sample (typically 1–10 mL) than microfluid instruments (0.065 mL h^{-1} ; Stan et al., 2009), and this at cooling rates similar to those in slowly ascending clouds ($< 1\text{ m s}^{-1}$) where precipitation is initiated by the formation of ice crystals ($< 1\text{ }^{\circ}\text{C min}^{-1}$). The cumulative number $K_{(\theta)}$ of IN active at a temperature θ present in a unit volume of the sample can thus be calculated (Vali, 1971), considering the total number of drops/tubes analysed, N_T , the number of unfrozen ones at a certain temperature, N_{θ} , and the volume analysed, V :

$$K_{(\theta)} = \frac{[\ln N_T - \ln N_{\theta}]}{V} \quad (1)$$

2.2 Description of the apparatus (LINDA)

The major limitations of testing drops on a cold stage are the potential evaporation of the droplets over time, their contamination from the surrounding air and the risk of cross-contamination of drops on the plate through ice growth among the drops or splintering. When these problems are overcome by putting the drops into closed tubes, new challenges emerge. One is the difficulty of detecting freezing in a closed tube. For that purpose, tubes are usually taken out of the cold bath after a relevant temperature change and inspected visually across their radial axis, where ice formation leaves visible traces of entrapped gas or solutes (“milky” appearance of tube content, or part thereof). Problems hereby are that condensation on the outside of the supercooled tube may be mistaken for frozen content and that removal from the cold bath temporarily increases the tube temperature.

Here, we present a new freezing apparatus that overcomes these problems. It is equipped with an automatic detection system for nucleation events, based on the reduction of light transmission upon freezing of a liquid sample. We present the example of an assay conducted with this new apparatus that would not have been possible to achieve with previous instruments and, in addition, we describe another interesting application that could be realized with it in the future.

2.2 Description of the apparatus (LINDA)

The core of the LINDA (LED-based Ice Nucleation Detection Apparatus) device is a 7 x 8 array of red LEDs (645 nm wavelength), surface mounted on a printed circuit board cast into a polycarbonate housing (128 x 113 x 10 mm, Fig. 2.1b) and submersed in a cold bath (Lauda RC6, Lauda-Königshofen, Germany). A total of 52 sample tubes (0.5 mL Eppendorf Safe-Lock) containing each between 40 and 400 μ L of liquid sample are held in another polycarbonate plate (Fig. 2.1b) and placed onto the LED array so that each tube is vertically centered on an LED. Four sample tubes with cast-in Pt₁₀₀₀ temperature sensors are placed in the corner positions of the tube holder (Fig. 2.1c). A USB CMOS Monochrome Camera (DMK 72BUC02, The Imaging Source Europe GmbH, Bremen, Germany) mounted in a black hood placed above the sample array is directed toward the lids of the tubes, which are illuminated from below (Fig. 2.1a). Images are recorded every six seconds. Light intensity in the area of each tube lid is extracted from each image and recorded into a text file together with the temperature at the time the image was taken. Further analysis of the data collected can be easily done with little effort through a spreadsheet to obtain the very precise freezing temperature for each tube allocated in the cooling bath. More detailed technical information on hardware and software components are available at the website: <http://azug.minpet.unibas.ch/~lukas/FNA/index.html>.

The apparatus was devised based on the principle that the transfer of light through water is reduced upon freezing when light gets scattered by inclusions and impurities in ice, such as air bubbles, brine pockets or crystal facets (Perovich, 2003). Pure water freezes without these inclusions and impurities, so no relevant change in light transmission upon freezing is noticeable. Hence, it is essential that samples contain a small amount of salt (or buffer), which is also recommendable for reasons of sample stability and to avoid eventual osmotic stress on living cells. To see whether the addition of small amounts of salt has a noticeable impact on freezing temperatures, we tested fresh snow samples with and without addition of NaCl (0.9 % final concentration, equal to physiological solution). Analyses were done by removing the tubes from the cold bath and inspecting them by

eye. The resulting freezing spectra (Fig. 2.2) suggest no systematic suppression of freezing at this salt concentration. Later trials with the apparatus described in the following showed that much lower NaCl concentrations (0.11 %) were already sufficient for reliably detecting change in light transmission.

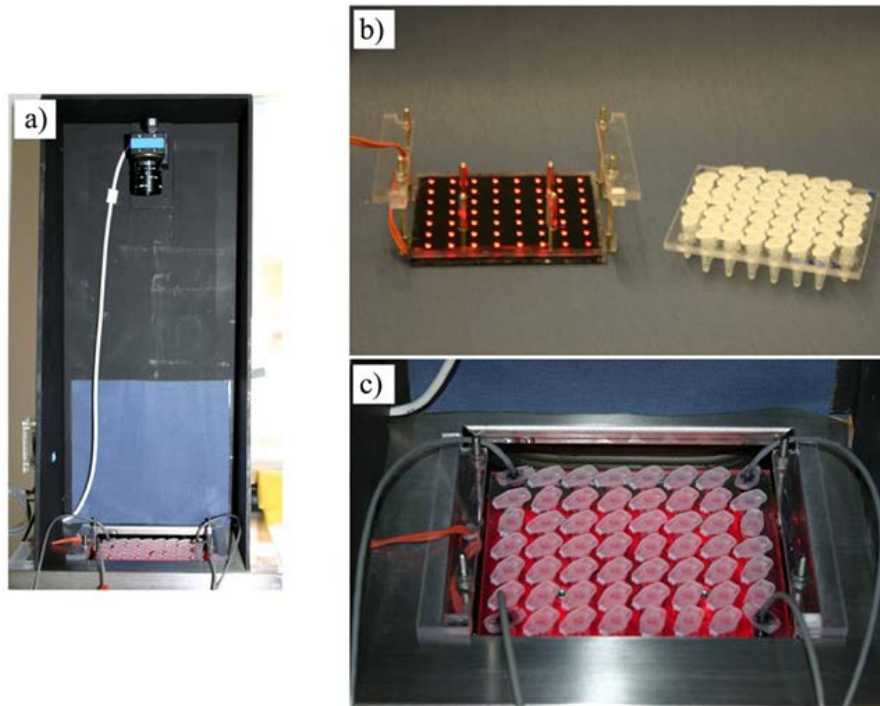


Figure 2.1 a) Cold bath set-up, ready for analysis with camera recording from above; b) LED array and polycarbonate plate holding 52 sample tubes; c) Detail of tubes and Pt1000 sensors in the corners of the grid inside the cooling bath.

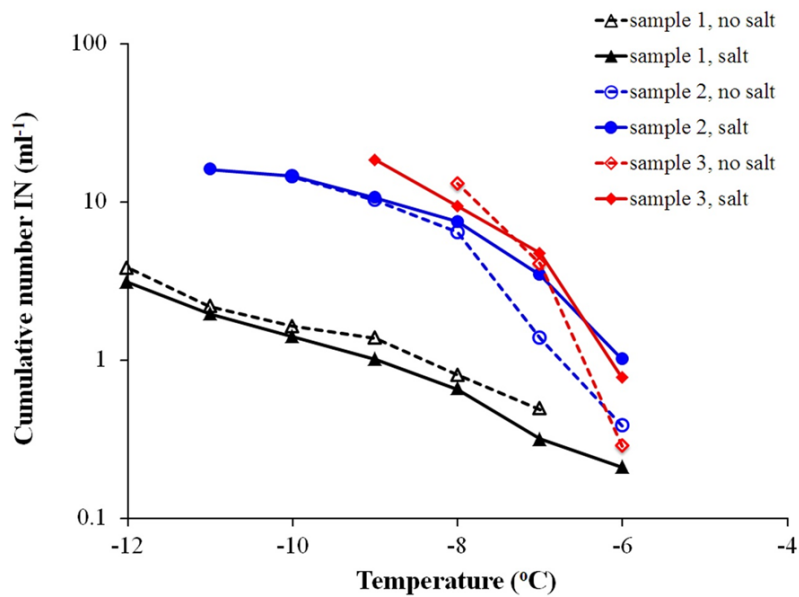


Figure 2.2 Paired snow water samples without (open symbols) and with (closed symbols) NaCl (0.9 %). Each spectrum based on manual/visual analysis of 54 tubes at $200 \mu\text{L}$.

2.2 Description of the apparatus (LINDA)

The phase change from liquid to ice is clearly detectable by a sudden decrease in transmitted light (Fig. 2.3). It is not necessary to have identical light intensities for each tube at the beginning of an analysis, since freezing is determined by the relative change in light intensity and not by its absolute value. The upper limit for the number of IN detectable is determined by the total number of aliquots analysed (52) and the smallest volume that still results in a clearly detectable change in light transmission when changing from liquid to frozen (40 μL). In a given sample it is 98.8 IN mL^{-1} $((\ln(52)-\ln(1))/0.04 \text{ mL})$, but can be extended by orders of magnitude through proper dilution. The part of the tube containing the sample is still fully surrounded by cooling liquid when containing a sample of 400 μL , which can be considered the largest volume for the analysis. This provides for a lower detection limit of 0.05 IN mL^{-1} $((\ln(52)-\ln(51))/0.4 \text{ mL})$. For the operational conditions described from here on, the background due to container characteristics, water quality and working environment could become an issue at temperatures around $-15 \text{ }^\circ\text{C}$ or lower. The employment of other methods based on different materials and smaller volume quantities is then recommended to investigate colder temperature intervals, simultaneously allowing the detection of higher abundance of ice nucleators with a reduced background (for instance, Iannone et al., 2011).

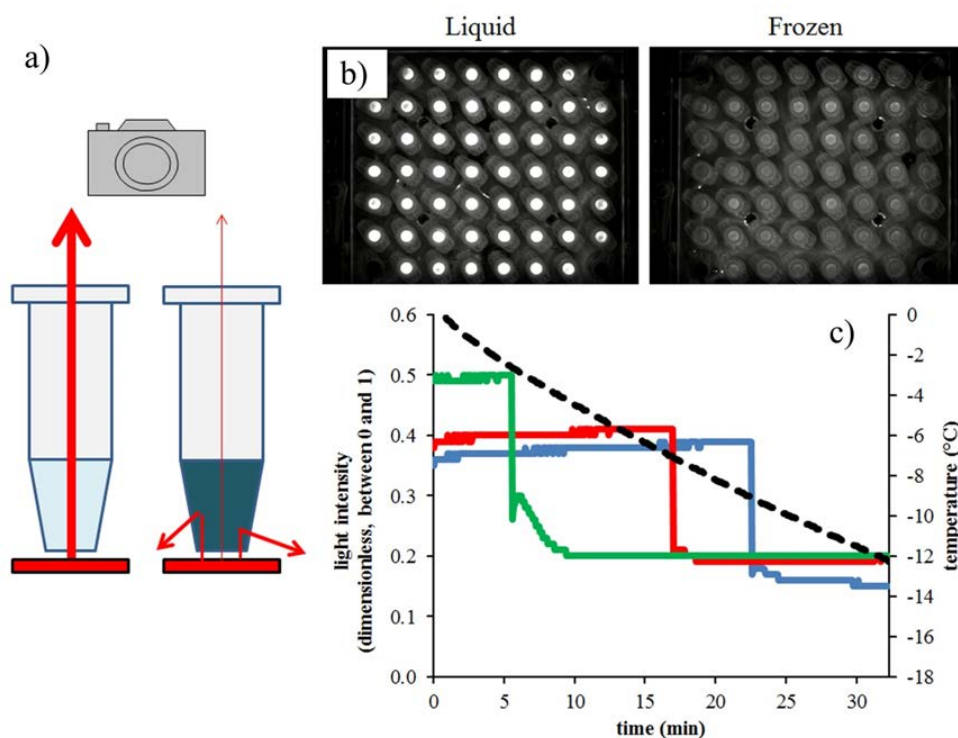


Figure 2.3 a) Schematic representation of the principle of freezing detection by a decrease in light transmission associated with the passage from liquid water (light blue) to ice (dark blue); b) Images taken by the camera at the beginning and the end of a test run when all samples were liquid (left panel) and frozen (right panel); c) Time record of temperature (black dashed line) and light intensities of three tubes (coloured solid lines) showing the sudden and sharp decrease in recorded light intensity (full line), associated with ice nucleation. As shown in the graph, this system provides good detection of freezing events without loss of reliability also at temperatures close to $0 \text{ }^\circ\text{C}$, where visual detection may be more difficult (Vali, 1995).

Pure substances with a known freezing temperature range were tested to assess the repeatability in the detection of nucleation events. For this purpose we repeated five times the analysis of the same array of 52 tubes containing 200 μL of sample each. Samples tested were montmorillonite (at the concentration of $50 \mu\text{g mL}^{-1}$) and SNOMAX[®] ($0.1 \mu\text{g mL}^{-1}$), showing a freezing temperature range from $-7.1 \text{ }^{\circ}\text{C}$ to $-13.0 \text{ }^{\circ}\text{C}$ (median $-11.9 \text{ }^{\circ}\text{C}$) and from $-4.3 \text{ }^{\circ}\text{C}$ to $-5.4 \text{ }^{\circ}\text{C}$ (median $-5.0 \text{ }^{\circ}\text{C}$), respectively. For both substances, the median value of the standard deviation in freezing temperatures of repeatedly frozen individual tubes was $0.20 \text{ }^{\circ}\text{C}$, comparable to the value reported in Vali (2008) for a soil suspension. This standard deviation in repeated analyses is a combination of the precision of the apparatus and the stochastic element in freezing nucleation. Hence, we can say that the precision of the apparatus (1 standard deviation) must be smaller than $0.2 \text{ }^{\circ}\text{C}$.

2.3 New applications

This section illustrates two kinds of freezing nucleation assays that are facilitated by use of the described apparatus. It is intended as an outlook on opportunities. The first example makes use of the possibility to store and repeatedly analyse the same sample without risk of contamination or evaporation. The second example demonstrates how the sample may be recovered after freezing analysis for other subsequent characterization.

2.3.1 Evolution of a sample upon storage at low temperature

In the first example, we follow the dynamics of biological IN in a snow sample over several weeks. Ice nucleators active at temperatures warmer than $-10 \text{ }^{\circ}\text{C}$ in precipitation samples are efficiently deactivated by heat through boiling and to some extent by the addition of lysozyme, an enzyme that partially destroys the microbial cell wall. This has led to the conclusion that ice nuclei in environmental samples are associated with microbial cells (Christner et al., 2008b). Here, we try to approach the same issue, but from the opposite direction. Effectively, certain conditions are known to activate the ice nucleating property of bacterial cells. Modifications in temperature and nutrient supply lead to the aggregation of individual IN proteins on the outer cell membrane into larger units able to catalyse freezing at warmer temperatures than before (Nemecek-Marshall et al., 1993; Ruggles et al., 1993). Hence, if IN active cells are present in a sample of snow water, which is naturally poor in nutrients, aggregation of IN proteins into larger units may be stimulated during storage at a cool temperature and result in an onset of freezing at increasingly warmer temperatures with time.

To test this assumption, snow was collected on 22 January 2013 from an open field in the northern part of the Jura mountains ($47^{\circ}28'30'' \text{ N}$, $07^{\circ}40'07'' \text{ E}$, 700 m a.s.l.) in Switzerland, where it had accumulated the night before in a powdery layer (4 cm) on top of an older, frozen snow layer. The snow was melted at room temperature and divided into 4 aliquots. Different quantities of 9 % NaCl solution were added to each aliquot (0.11 %, 0.23 %, 0.45 % and 0.9 % as final salt concentrations). Aliquots were then divided into 52 tubes at 200 μL each and analysed with the apparatus, at a cooling rate of $0.4 \text{ }^{\circ}\text{C min}^{-1}$. A blank sample of 52 tubes of pure water with NaCl added (0.9 %) was treated in the same way but did not show a single freezing event throughout the trial. To determine the dynamics of IN activity of the samples over time, freezing assays were

2.3 New applications

conducted at increasing time intervals. Between freezing assays, the samples were stored at +4 °C. Since no differences were observed among salt concentrations, we pooled the data for further analysis, resulting in a total of 208 observed tubes. Freezing temperatures were approximately normally distributed among the tubes on the day of sampling (Fig. 2.4, day 0). When analysed the following day, 90 % of the tubes froze within a range of ± 0.7 °C of the temperature at which they had frozen the previous day. However, 13 tubes which had frozen at lower temperatures during the first analysis, subsequently froze at -5 °C or warmer after one day (Fig. 2.4, signed as red dots on day 0 and as green dots from day 1 on). After one week, 37 new tubes moved into this temperature range, while after one month 14 tubes still showed this increase (Fig. 2.4, red dots), suggesting the appearance of more active IN over time. On the other hand, in some tubes IN started to lose efficiency, thus leading to a lower temperature of freezing (Fig. 2.4, green dots progressively decreasing towards colder temperatures).

The results seem to correspond to what is expected according to the aggregational model for microbial IN proteins, in particular they suggest the likely active aggregation of small subunits into larger structures effectively catalysing ice formation at warmer temperatures and a parallel disaggregation of medium-sized structures into smaller, less efficient IN. A multiplication of IN active cells seems unlikely, because the total number of IN active at -12 °C had actually declined (Table 2.1) and freezing cycles may have reduced the viability of cells. Observing a sample over longer time could thus provide compelling evidence for the presence and number of living biological ice nucleators.

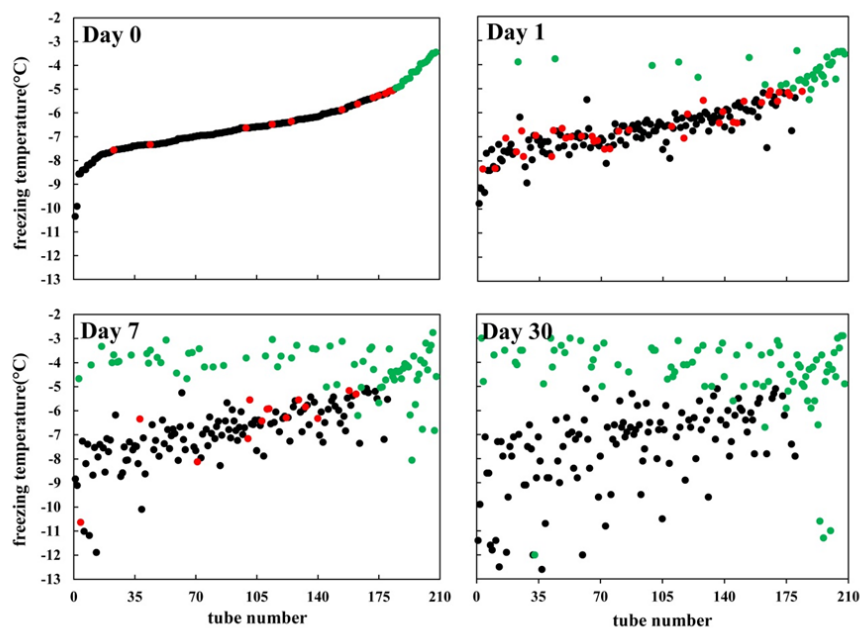


Figure 2.4 Evolution of freezing temperature of 208 tubes filled with 200 μ L of snow water and stored at +4 °C. Tubes were analysed on the day of snow sampling (day 0) and 1, 7, and 30 days later. They were ranked by freezing temperatures on day 0 and this rank was allocated as a tube identity number for the rest of the trial. Freezing temperatures were determined between 0 °C and -12 °C. Points were coloured according to different behaviours of associated tubes: black for those not frozen at or above -5 °C and not doing so the next time they are analysed; red for those not frozen at or above -5 °C, but which do so the next time they are analysed; green for those frozen at or above -5 °C during the current or one of the previous analyses.

Table 2.1 Development of IN in snow water over 30 days during storage at 4 °C. To observe the development, the same 208 sample tubes were repeatedly subjected to freezing tests. The lower limit of detection in this trial was 0.03, the upper limit was 27.80 IN mL⁻¹. The number of IN active at -4 °C quadruplicated, while the number of IN active at -8 °C halved (indicated in *italic*).

T (°C)	Cumulative number of ice nucleators (mL ⁻¹)					
	day 0	day 1	day 3	day 7	day 15	day 30
-3				0.05		0.15
-4	<i>0.26</i>	<i>0.42</i>	<i>0.47</i>	<i>0.99</i>	<i>0.47</i>	<i>1.05</i>
-5	0.67	0.99	1.27	2.02	1.84	2.33
-6	1.99	2.17	2.25	3.41	3.00	3.51
-7	5.98	6.14	5.45	6.83	4.72	5.90
-8	<i>15.31</i>	<i>14.86</i>	<i>11.70</i>	<i>12.20</i>	8.85	8.72
-9	24.19	22.08	22.08	18.47	13.04	11.03
-10	27.80		27.80	19.42	15.31	13.04
-11			27.80	24.19	18.47	14.86
-12			27.80		22.08	22.08

2.3.2 Progressive isolation of ice nucleators from a sample

In a second application, we demonstrate how the sample may be recovered after freezing analysis for other subsequent characterization and in particular to progressively isolate an IN active at temperatures above -12 °C from an environmental sample. To demonstrate this, a fresh snow sample was collected in March 2013 from a rooftop in Basel. The snow was melted at room temperature, NaCl was added to a final concentration of 0.9 % and analysis of the sample was carried out to a minimum temperature of -8 °C after it had been divided into 52 tubes at 200 µL each. The five tubes (from here on called samples 1 to 5, Table 2.2) that had frozen first were further topped up, after they had melted, with 0.9 % NaCl (in pure sterile water) to a total volume of 500 µL and split into 10 portions (tubes) at 50 µL for a second freeze test. From each series of 10 tubes, the tube that froze first was topped up to 500 µL and split into 10 tubes at 50 µL for further analysis. The same scheme was followed until a fourth dilution step. Handling was carried out in cold conditions (0-5 °C). In a series of blank samples (52 tubes at 50 µL filled with the 0.9 % NaCl solution used to top up) none of the tubes froze at -10 °C or warmer. In two out of the five samples the putative initial ice nucleator could be followed to a dilution of 10⁻⁴ (Table 2.2). In the other three cases ice nucleators either shifted their onset of freezing to temperatures colder than -8 °C or were completely lost. This loss may be due either to an incomplete recovery of all particles present in a tube or to the manipulating conditions destroying the ice nucleation active sites. Improvement of this methodology to optimize IN recovery is currently under study.

Snow samples previously collected in Basel during winter showed a total number of bacteria (epifluorescence microscopy, SYBR green staining) ranging from 10³ to 10⁵ cells mL⁻¹ of melted snow. Through four dilution steps, so by a factor of 10⁴, 1 to 10 bacterial cells remained in the last series of dilution and the solution also included the most active IN. Thus, this sequential isolation can help to reduce the background of the non-ice nucleation active microbial community in the sample and provides a first step towards an identification of most active IN. At that stage, either selective cultivation-based methods may allow the recovery of the biological agent responsible for the nucleation, or molecular approaches such as amplification of key genes may be applied, since

2.4 Conclusions

extraction and amplification of DNA even from single cells seems to become an increasingly feasible method (Gao et al., 2011).

Table 2.2 Freezing temperatures of five samples (200 μ L each of the same snow water) repeatedly diluted (1:10 with 0.9 % NaCl) and split into ten portions each. A freeze test was performed after the first dilution step and the freezing temperature is indicated for those of the ten sub-samples that froze at temperatures warmer than to -8 °C. Only the sub-sample with the warmest freezing temperature was taken to the next dilution step (marked in *italic*). Those freezing at colder temperatures were discarded. A total of 4 dilution steps were carried out.

Sample	Dilution step				
	0	1	2	3	4
1	-5.0	-7.5	-7.9	-8.0	
2	-5.4	-6.0 -6.3 -7.3 -7.4	-6.5 -6.9	-6.5	-6.5
3	-5.6	-6.8 -7.2 -7.7	-7.0		
4	-5.7	-5.6 -7.1 -7.2	-5.8	-5.9	-6.1
5	-5.9	-6.7 -7.2 -7.7	-6.6		

2.4 Conclusions

We have developed the traditional immersion freezing nucleation method further by detecting the phase change from liquid to ice in closed test tubes through the reduction of light transmission upon freezing. The change in signal upon freezing is abrupt and clear. Manipulation of the sample before and during analysis is minimised, parameters of analysis can be accurately controlled, reliably recorded and risk of contamination is negligible, even during prolonged storage. This extends the possibilities of traditional immersion freezing tests. One interesting new application is the possibility of detecting the presence of living biological ice nucleators in a sample by storing it at low temperatures and observing over the course of days or weeks an increase in the number of IN active around -4 °C. Moreover, it could be possible to recover and isolate warm IN directly from a sample with known nucleating activity through subsequent dilution steps during which the number of particles not active as IN is successively reduced from a sample. Thus, this new apparatus could help to bridge the gap between the analysis of environmental samples collected in field and laboratory assays in ongoing and future research on biological ice nucleation.

2.5 Acknowledgements

The work reported here was supported by the Swiss National Science Foundation (SNF) through grant number 200021_140228.

Ice nucleation active particles are efficiently removed by precipitating clouds

This chapter has been published as article:

Stopelli, E.¹, Conen, F.¹, Morris, C. E.², Herrmann, E.³, Bukowiecki, N.³, and Alewell, C.¹: Ice nucleation active particles are efficiently removed by precipitating clouds, *Scientific Reports*, 5, 16433, doi.org/10.1038/srep16433, 2015.

¹ Environmental Geosciences, University of Basel, CH-4056 Basel, CH

² INRA, UR 0407 Plant Pathology Research Unit, 84143 Montfavet, FR

³ Laboratory of Atmospheric Chemistry, Paul Scherrer Institut, CH-5232 Villigen PSI, CH

Abstract

Ice nucleation in cold clouds is a decisive step in the formation of rain and snow. Observations and modelling suggest that variations in the concentrations of ice nucleating particles (INPs) affect timing, location and amount of precipitation. A quantitative description of the abundance and variability of INPs is crucial to assess and predict their influence on precipitation. Here we used the hydrological indicator $\delta^{18}\text{O}$ to derive the fraction of water vapour lost from precipitating clouds and correlated it with the abundance of INPs in freshly fallen snow. Results show that the number of INPs active at temperatures ≥ -10 °C (INPs_{-10}) halves for every 10 % of vapour lost through precipitation. Particles of similar size (> 0.5 μm) halve in number for only every 20 % of vapour lost, suggesting effective microphysical processing of INPs during precipitation. We show that INPs active at moderate supercooling are rapidly depleted by precipitating clouds, limiting their impact on subsequent rainfall development in time and space.

3.1 Introduction

Ice formation in clouds contributes to the development of precipitation at mid-latitudes (Creamean et al., 2013; Möhler et al., 2007; Mülmenstädt et al., 2015; Phillips et al., 2003). Ice nucleating particles (INPs) of biological origin can be effective in promoting ice nucleation at temperatures around $-10\text{ }^{\circ}\text{C}$ or warmer (Christner et al., 2008a; Christner et al., 2008b; Joly et al., 2014), whereas at colder temperatures inorganic substances are likely to be responsible for an increasing fraction of ice particles formed in the atmosphere (Murray et al., 2012). Here we focus on the cumulative number of INPs active at temperatures warmer than $-10\text{ }^{\circ}\text{C}$ ($\text{INPs}_{>10}$), the range where the activity of INPs of biological origin seems to be dominant. Such INPs include certain bacteria, fungal spores and pollen, but a large fraction of INPs from biological sources in the atmosphere may also be composed of ice nucleation active macromolecules associated with mineral and soil particles (O'Sullivan et al., 2015; Pummer et al., 2015). Because of usually very small number concentrations in the atmosphere, the potential role of such particles in conditioning precipitation is still contentious (Hoose et al., 2010a; Morris et al., 2014).

Elevated concentrations of INPs associated with dust from desert storms on other continents and with far away and regionally emitted INPs were recently found to contribute to precipitation over the Western USA (Creamean et al., 2013) and the Amazon basin (Prenni et al., 2009) respectively. Overall, it is likely that there is a coincidence in time and space of the concentration of INPs and the intensity of precipitation events (Chongyi et al., 2014), raising the general question of where and when cloud glaciation and subsequent precipitation are limited or facilitated by INPs. To address this question, it is crucial to understand the major factors driving the variation of atmospheric concentrations of INPs, which have been observed to range over several orders of magnitude (DeMott and Prenni, 2010; Möhler et al., 2007).

Feedbacks between human activities and climate modifications could be, or become, partly influenced by INPs. In fact, intensifying land use and climatic change are likely to increase future emissions of INPs associated with wind-blown soil dust (Conen and Leifeld, 2014). Changes in vegetation cover, crop type and management may also affect emissions of ice nucleating particles from vegetation (Morris et al., 2014). In this study we intend to quantify the relation between the fraction of water lost from air masses and the residual concentrations of $\text{INPs}_{>10}$. This could help to assess the range of influence that a change in the source strength of INPs in a particular region may have on precipitation downwind.

3.2 Methods

3.2.1 Sample collection

During sampling events the Research Station Jungfraujoch was always inside clouds and the temperature of the air at the Station was ranging from -27.3 °C to 0.4 °C. Snow samples were collected with a teflon-coated tin (0.1 m², 8 cm deep) carefully rinsed ethanol and sterile Milli-Q water. Sampling duration lasted from 1.5 to 8 hours (median time = 2 hours). Snow was melted at around 16 °C and analysed within less than 4 hours after its collection. The cumulative number of INPs was determined between -2 °C and -12 °C in immersion freezing mode, using an automated drop freeze apparatus (Stopelli et al., 2014) loaded with 52 tubes containing 100 µL of sample each. In our analyses we concentrated on the warmest temperature at which all samples had a detectable number of INPs, which was -10 °C. The smallest number concentration of INPs that can be detected with this configuration is 0.21 INPs mL⁻¹. Blanks were periodically prepared by sprinkling Milli-Q water into the tin and analysed with the same material and method as the snow samples, at 200 µL per tube to obtain more conservative results. Blank values for INPs active at -10 °C were on average 0.11 INPs mL⁻¹, with only 7 blanks showing some freezing activity on a total of 39 blanks analysed.

3.2.2 δ¹⁸O analysis and modelling of f_v values

Aliquots of snow (equivalent to about 5 mL of water) were immediately loaded from the sampling tin into 15 mL sealed polypropylene Falcon tubes and stored at 4 °C until analysis with a tunable, off-axis integrated-cavity laser spectrometer (DLT-100, Los Gatos Research, Inc. (LGR), Mountain View, California). Standards used for calibration were provided by LGR and all results presented here were related to the standard VSMOW. The local meteoric water line obtained from the whole set of yearly data fits well with the equation associated to the global meteoric water line ($\delta^2\text{H} = 7.7 \delta^{18}\text{O} + 10.6$; $R^2 = 0.98$). This indicates the absence of significant disequilibrium conditions at Jungfraujoch compared to the global behaviour of precipitations. The remaining water vapour fraction (f_v) was calculated from $\delta^{18}\text{O}$ ‰ values measured in snow (δ_L) following the method described in Rowley et al. (2001).

The evolution of $\delta^{18}\text{O}$ in vapour (δ_v) can be described by a Rayleigh-type fractionation model (Sinclair et al., 2011; Yamanaka et al., 2007):

$$\frac{\delta_v}{1000} = \left(1 + \frac{\delta_{v,0}}{1000}\right) \cdot f_v^{\alpha_{L/V}} - 1 \quad (2)$$

In our calculations, the fractionation factor from liquid to vapour $\alpha_{L/V}$ along the trajectory of the cloud was assumed constant during the entire path of a precipitating cloud and proportional to the average value between the temperature of the air at Jungfraujoch and the estimated temperature at the sea surface from where the air mass originated. The dependence of $\alpha_{L/V}$ from absolute temperature (T) was calculated according to Majoube (1971):

$$\ln \alpha_{L/V} = 1.14 \cdot 10^3 \cdot T^{-2} - 0.42 \cdot T^{-1} - 2.07 \cdot 10^{-3} \quad (3)$$

The isotopic ratio of the vapour at Jungfraujoch (δ_V) was calculated from the isotopic ratio of snow (δ_L) and the fractionation factor liquid-vapour at the temperature of the air recorded at the station:

$$\delta_L = \alpha_{L/V} \cdot (\delta_V + 1000) - 1000 \quad (4)$$

Seawater was considered the principal and constant source of moisture in calculating the isotopic ratio of the initial water vapour ($\delta_{V,0}$):

$$\delta_{V,0} = \alpha_{V/L} \cdot (\delta_{L,0} + 1000) - 1000 \quad (5)$$

with the isotopic $\delta^{18}\text{O}$ ratio of seawater ($\delta_{L,0}$) homogeneously equal to 0 ‰, since it coincides with the standard reference for water stable isotopes measurements and the fractionation factor between seawater and vapour $\alpha_{V/L}$, equal to $1/\alpha_{L/V}$. Over the year, the station is affected by intermittent influence of the boundary layer (Ketterer et al., 2014), with air masses coming from different geographical regions and its location in a saddle allows air systems to be channelled along two main directions, mainly North-West and South-East (Collaud Coen et al., 2011). Vapour source regions were derived from source sensitivity plots calculated with a Lagrangian particle dispersion model and made available online by Stephan Henne at the Swiss Federal Laboratories for Materials Science and Technology (EMPA), Dübendorf, Switzerland (individual results are available on the webpage http://lagrange.empa.ch/FLEXPART_browser/). The surface average temperatures of source areas in the North Atlantic and the Mediterranean Sea were derived from a National Oceanic and Atmospheric Administration NOAA database, grouped per season, and used to calculate $\alpha_{V/L}$ (<http://www.nodc.noaa.gov/OC5/indprod.html>).

A constant relative humidity factor (h) of 0.8 was used for the North Atlantic and for Mediterranean Sea, a value reasonably analogous to those recently reported in Pfahl and Sodemann (2014) since the local meteoric water line shows a deuterium excess comparable to the average precipitations on Earth. Consequently, $\alpha_{V/L}$ values were corrected for disequilibrium processes occurring during evaporation from the sea, which tend to increase isotopic fractionation, according to the relationship (IAEA, 2001b):

$$\alpha_{L/V \text{ TOTAL}} = \alpha_{L/V \text{ EQUILIBRIUM}} + 0.0142 \cdot (1 - h) \quad (6)$$

Obtained values for $\delta_{V,0}$ ranged from -13.76 ‰ (North Atlantic, winter) to -12.16 ‰ (Mediterranean Sea, summer), comparable to what is reported in IAEA (2001a, 2001b).

3.2.3 Total number of particles $N_{>0.5}$

The total number of particles with a diameter larger 0.5 μm ($N_{>0.5}$) was measured with an optical particle counter (GrimmTM, Dust Monitor 1.108). Particles up to 40 μm size are aspirated through a heated sample inlet, dried and detected, even when activated as cloud condensation nuclei and part of hydrometeors or ice (Weingartner et al., 1999; WMO/GAW 2003). Since the values of $N_{>0.5}$ correspond to unit volume of air, a conversion of INPs per mL of snow into INPs per m^3 of air was necessary in order to calculate the ratio $\text{INPs}_{>0.5}/N_{>0.5}$ presented here. By dividing the precipitation rate measured with the sampling tin by an average deposition velocity of snowflakes (1 m s^{-1}) (Szyrmer, 2010; Zawadzki, 2010), we obtained a value for the snow water equivalent present in 1 m^3 of air for each sampling interval. A median of 0.25 mL m^{-3} of snow water equivalent was

obtained, well within the range reported by Muhlbauer et al. (2010) and by Deguillaume et al. (2014).

3.2.4 Statistics

Statistical analyses presented here were done with PAST software version 2.17 (Hammer et al., 2001) and refined with the use of R software version 3.0.1. (R Development Core Team, 2011). Parametric regression was done on logarithmic values of INPs as correction for normality to understand how much of the total variability was covered by our tests and R^2 values have been reported. These results are accompanied by non-parametric Spearman's correlation results (r coefficient and p values expressing the probability that variables are not correlated), as a more robust test for the significance of the relationships found. For the comparison among months for the values of INPs a Kruskal-Wallis test was done.

3.3 Results

3.3.1 General overview

The concentration of INPs in an air mass is principally a function of (a) the accumulation of INPs from sea and land surfaces that the air mass has contacted, (b) the degree of mixing with other air masses, richer or poorer in INPs, and (c) the cumulative loss of INPs, most importantly by wet deposition processes, across its trajectory. Here we focus on the proportion of variation in the abundance of INPs that the last factor (c) might explain when (a) and (b) are presumed to be constant. Presuming (a) to be constant, we assume a temporally steady and spatially homogenous cumulative mix of INPs from several sources. Our presumption of (b) to be constant does not account for possible cumulative enhancement of INPs by falling and evaporating hydrometeors.

Observations and direct measurements relate to the conditions at the High Altitude Research Station Jungfraujoch (7°59'06'' E, 46°32'51'' N, 3580 m a.s.l.).

Water precipitating at Jungfraujoch generally originates from evaporation from either the North Atlantic or the Mediterranean Sea, depending on trajectories of air masses (Sodemann and Zubler, 2010). Upon its approach over land, moist air picks up additional dust and biogenic particles from various sources. Through precipitation it loses varying proportions of water and particles before arriving at Jungfraujoch, which is on the highest mountain ridge between the Mediterranean and the Atlantic water source regions. Isotopic fractionation leads to a preferential condensation and loss of heavier isotopes (^{18}O and ^2H) compared to the lighter ones (^{16}O and ^1H ; for sake of brevity we will refer hereafter only to oxygen). This results in increasingly smaller values of the ratio $^{18}\text{O}/^{16}\text{O}$, expressed as $\delta^{18}\text{O}$, both in cloud water and rain or snow during the progressive development of precipitation (IAEA, 2001a; Moran et al., 2007; Rowley et al., 2001; Sinclair et al., 2011). Although the isotopic signal is sensitive to the integrated amount of precipitation deposited from an air mass, it provides no details about the specific conditions that have triggered a precipitation event (e.g. temperature) or whether the integrated precipitation was lost in one or in several events. Not only $\delta^{18}\text{O}$, but also the number of INPs in precipitation is influenced by the

cumulative history of water loss from the air mass, since INPs active at the warmest supercooling are the first to be activated as a cloud progressively cools down, and are potentially removed with precipitation. Therefore, the larger the fraction of water that has precipitated, the greater the chance that INPs active at moderate supercooling have been removed, hence the smaller the fraction of such INPs among other particles in later precipitation (Fig. 3.1).

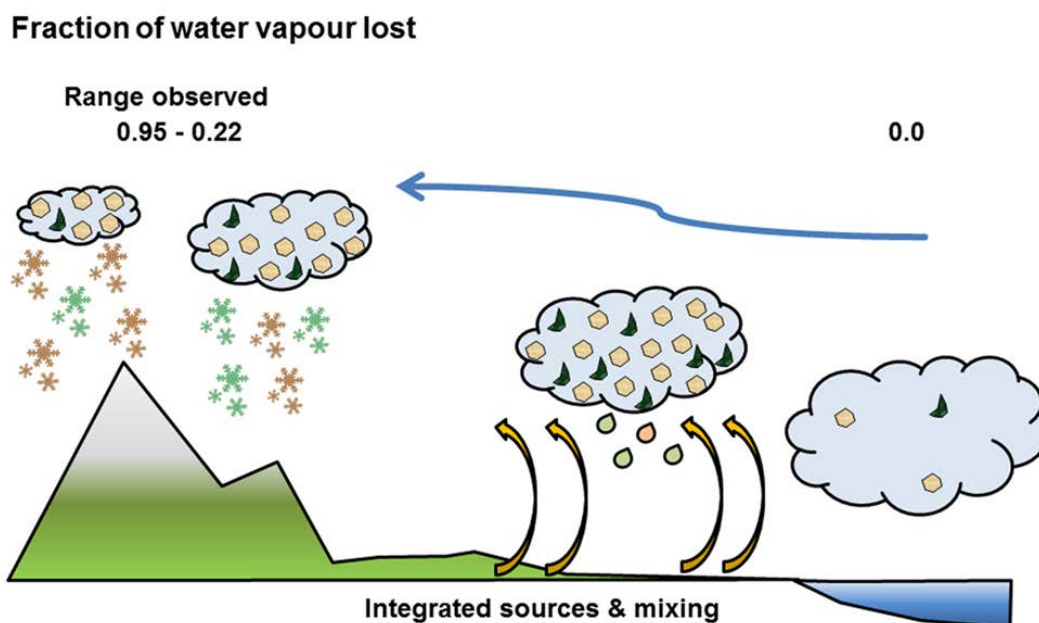


Figure 3.1 Relationship between the fraction of water vapour lost from a precipitating cloud (derived from stable isotope ratios in snow ($\delta^{18}\text{O}$)) and ice nucleating particles (INPs, measured in snow). As the cloud precipitates, the progressive loss of water vapour (from right to left) is accompanied by a loss of INPs which have been uplifted from the sea and land surfaces (yellow arrows). INPs of biological origin (green half-moons) are activated at more moderate supercooling, hence typically earlier than inorganic INPs (brown hexagons). The values 0.22 and 0.95 correspond to the minimum and maximum fractions of water vapour lost that we observed at Jungfrauoch (drawn by E. Stopelli).

3.3.2 INPs get rapidly lost from a precipitating cloud

Over a 10-month period (December 2012 to September 2013) we sampled snow within precipitating air masses that had lost between 22 and 95 % of their initial water content before arriving at the observatory (Fig. 3.2). The decision to initiate a sampling campaign depended on weather forecasts that predicted snowfall for at least two full days in a row, to assure that we could collect multiple samples within the same campaign. A total of 304 mm were collected, reaching approximately 20 % of the total amount of precipitation fallen in the same period of 10 months at the closest station recording precipitation (1640 mm, Kleine Scheidegg, 2060 m a.s.l., 4.6 km North from Jungfrauoch). A trend of $\text{INPs}_{-10} \text{ mL}^{-1}$ of snow with minimum values in winter and maximum values in summer appears from the data collected (comparison among months, Kruskal-Wallis $p < 0.001$). Nevertheless, similarly large variations of INPs_{-10} are apparent even among samples collected within a single sampling campaign, as for instance in June and August 2013.

The predominant factor with a similarly marked variability that correlates with the abundance of $INPs_{-10}$ observed in precipitation is the fraction of residual water vapour in clouds (Fig. 3.2).

The abundance of $INPs_{-10}$ in snow declines exponentially with increasing proportions of water lost before arrival of an air mass at Jungfraujoch (Fig. 3.2b), and is best described by equation (1):

$$INPs_{-10} (mL^{-1}) = 1.12 \cdot 10^3 \cdot e^{(-7.57 \cdot (1-f_v))} \quad (1)$$

$$(R^2 = 0.52; \text{Spearman's } r = -0.61, p < 0.001, n = 91)$$

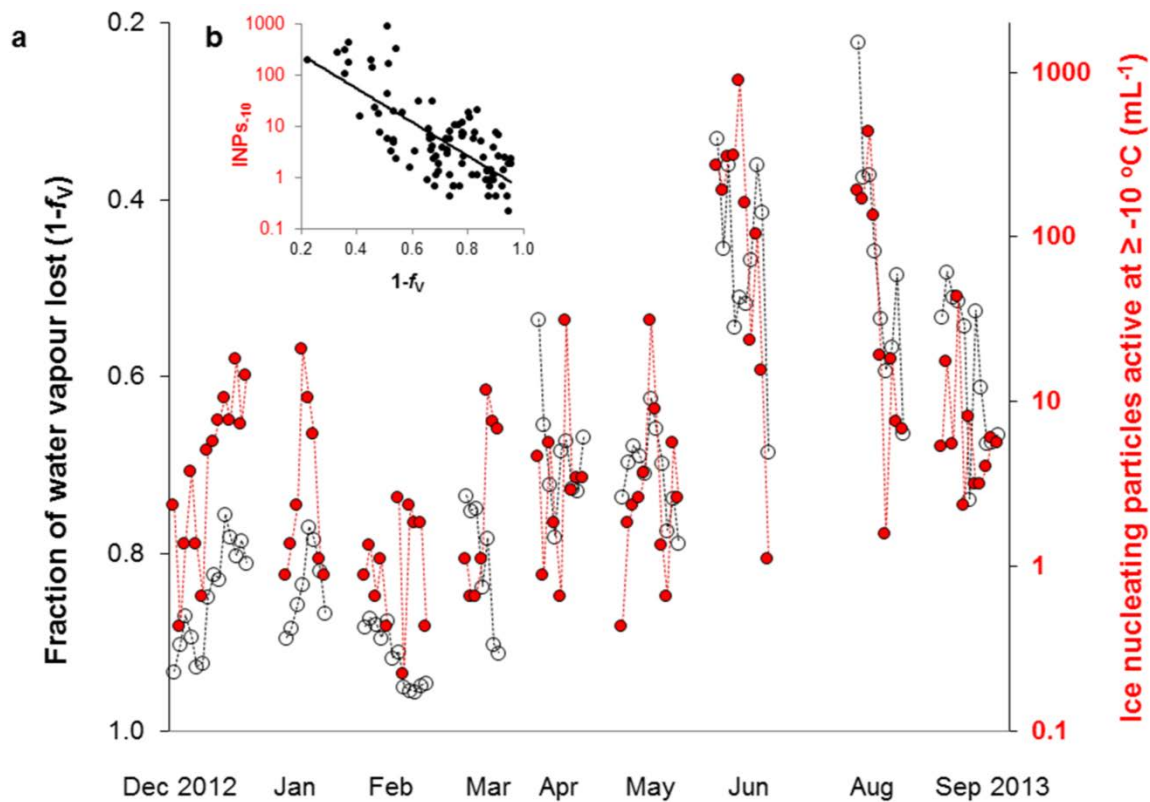


Figure 3.2 a) Covariation over time of concentrations of $INPs_{-10}$ in snow (red, log scale) and the estimated fraction of water vapour lost from an air mass prior to its arrival at the Jungfraujoch observatory (black). Time proceeds from left to right, intervals are not to scale. Each symbol signifies a snow sample with a median sampling duration of 2 hours. Each campaign (symbols connected by dotted lines, one campaign per month) lasted from 3 to 5 subsequent days. A total of 91 samples were collected between December 2012 and September 2013 (exception of July 2013 due to the lack of considerable precipitation events); b) Relationship between $INPs_{-10}$ and $1-f_v$; the function of the fitted exponential curve is reported in equation (1).

We can derive from this empirical equation, fitted to our data, an estimate for the largest number of $INPs_{-10}$ to expect in 1 mL of precipitation at Jungfraujoch. If the very first precipitation from an air mass is just about triggered at the observatory ($1-f_v = 0$) we would expect it to contain around 10^3 $INPs_{-10} mL^{-1}$. This number is probably a consequence of the strength of the sources of INPs influencing Jungfraujoch. Nevertheless, we can presume the exponential relationship to hold also in

other places because of a generally geometric behaviour observed in precipitating particles (Limpert et al., 2008). Physical processes during the course of precipitation define the factor -7.57 in the exponent, which might have a similar value also at other locations where the same physical processes are at work. It suggests that the concentration of $\text{INPs}_{.10}$ halves with about every 10 % of moisture lost from a precipitating air mass (e.g. moving $1-f_V = 0.5$ to $1-f_V = 0.6$ results in: $e^{(-7.57 \cdot 0.6)} / e^{(-7.57 \cdot 0.5)} = 0.47$).

3.3.3 Selective removal of INPs

The question remains whether there is experimental evidence for an INP being more likely to be deposited from an air mass than a particle of similar size that is not ice nucleation active. INPs should, in principle, be the starting point for snowflakes precipitating from a cloud. The average activation diameter for cloud condensation nuclei at Jungfraujoch is about $0.1 \mu\text{m}$ and most INPs are probably larger than $0.5 \mu\text{m}$ (DeMott et al., 2010; Hammer et al., 2014). Relating concentrations of $\text{INPs}_{.10}$ in precipitating snow to all particles larger than $0.5 \mu\text{m}$ ($N_{>0.5}$) in the same air volume reveals a significant negative trend in the ratio of $\text{INPs}_{.10}$ to $N_{>0.5}$ with an increasing fraction of vapour lost, despite the large scatter of data (Fig. 3.3).

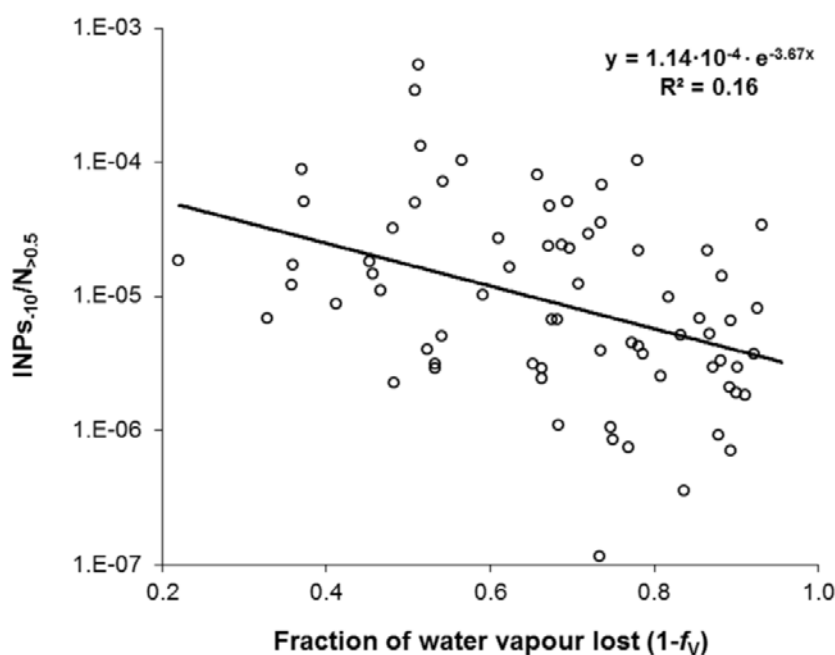


Figure 3.3 Ratio of $\text{INPs}_{.10}$ to the total number of particles $> 0.5 \mu\text{m}$ ($N_{>0.5}$, on log scale) as a function of the fraction of water vapour lost from the air mass prior to arrival at the observatory ($n = 71$; Spearman's $r = -0.42$, $p < 0.001$).

If the ratio of $\text{INPs}_{.10}$ to $N_{>0.5}$ were independent from the fraction of water vapour lost, we could say that both kinds of particles are removed with equal efficiency from a precipitating cloud. This is clearly not the case. The function fitted to our data (Fig. 3.3) suggests that the ratio of $\text{INPs}_{.10}$ to particles of similar size $N_{>0.5}$ is reduced to 0.69 times of what it was before with every 10 % of initial water vapour lost from a precipitating cloud (e.g.: $e^{(-3.67 \cdot 0.6)} / e^{(-3.67 \cdot 0.5)} = 0.69$). With the same 10 % loss of vapour, the absolute number of $\text{INPs}_{.10}$ almost halves (0.47, equation (1)) and the

absolute number of $N_{>0.5}$ is consequently reduced to 0.68 times of what it was before (reduction of $INPs_{.10}$ in absolute terms (factor 0.47) divided by the change in the ratio $INPs_{.10}/N_{>0.5}$ (factor 0.69) = 0.68). Hence, to halve the number of $N_{>0.5}$ ($0.68 \times 0.68 = 0.46$, approximately the half) requires about 20 % moisture loss, almost twice the amount of water vapour lost to what is necessary to halve the number of $INPs_{.10}$, suggesting active microphysical processing of particles (Phillips et al., 2008). This selective loss of INPs is highly significant, but explains only about one sixth of the total variation in the ratio of $INPs_{.10}$ to $N_{>0.5}$. The remaining variation might be due to source-related factors and could reflect temporal and spatial differences in $INPs_{.10}$, $N_{>0.5}$ and in the proportion of INPs among particles $N_{>0.5}$ emitted to the atmosphere before precipitation. Part of the scattering of $INPs_{.10}$ and $N_{>0.5}$ data may be also due to differences in the dimensions of INPs and total particles in each sample. In fact, not only nucleation but also impaction scavenging of aerosols can contribute to the simultaneous removal of particles, with an efficiency largely depending on the size of aerosols and precipitation intensity (Andronache, 2003; Santachiara et al., 2013; Schumann, 1991).

3.4 Discussion

Land use and climate change alter the distribution, the quality and the size of soil and vegetation cover in a landscape, and with it the strength and distribution of sources of different INPs (Conen and Leifeld, 2014; Morris et al., 2013b; Morris et al., 2014). As we illustrate here, the ratio of stable water isotopes in precipitation can be used in novel way to characterize the history of air masses in terms of residual abundance of INPs. Despite simplifying assumptions, our approach explains more than 50 % of the large variation of $INPs_{.10}$ observed in snow both within short sampling campaigns and over the year. Much of the unexplained variation is probably due to variations in the initial concentration of INPs before precipitation, which depends both on the source strength of INPs and on the degree of the mixing of air masses with different initial concentrations of INPs (e.g. from different altitudes or regions). Source strength in the lowland north of Jungfrauoch is scattered over two orders of magnitude during most of the year, but does not seem to change with season (Conen et al., 2015). In the same study the seasonal variation observed on Jungfrauoch seemed to be driven by microphysical processing of INPs through activation and deposition from approaching air masses. The same process may explain much of the observed temporal variation of INPs in this study (Fig. 3.2). It is in fact supported by the finding that $INPs_{.10}$ are deposited more efficiently than other particles of similar size (Fig. 3.3).

Carrying out similar measurements on stable water isotopes and on INPs also at other stations will firstly lead to the constant improvement and refinement of our calculations and, secondly, it will shed new light on the evolution of concentrations of INPs before and during precipitation events over the trajectories of air masses.

This will provide an important contribution for mapping the probabilities of the abundance of INPs and their exchanges across regions, in particular the estimation of how far from a source and along a specific trajectory INPs might have an impact. Furthermore, the fact that INPs active at moderate supercooling get rapidly lost through precipitation adds a significant constraint to the role of such INPs on the development of cloud processes in time and space, fostering a deeper understanding of the effects of different land use strategies on rainfall distributions. Therefore, predictive modelling of precipitation patterns, and eventually of water supply and climate change could be improved

through enhanced precision about where and when INPs are incorporated into air masses and subsequently parachute with rain and snow along their trajectory over landscapes.

3.5 Acknowledgements

We are grateful to the International Foundation for High Altitude Research Stations Jungfraujoch and Gornergrat (HFSJG) for making it possible for us to do our measurements at Jungfraujoch, and to Mark Rollog for the analyses of stable isotopes ratios in snow water. We thank MeteoSwiss for providing data on meteorological conditions at the observatory Jungfraujoch, and Dr. Stephan Henne (EMPA) for high-resolution particle transport simulations (FLEXPART) which enabled us to identify the main source regions of air masses. The work reported here was supported by the Swiss National Science Foundation (SNF) through the grant 200021_140228. Measurements of total solid particles were performed by Paul Scherrer Institute in the framework of the Global Atmosphere Watch (GAW) programme funded by MeteoSwiss with further support provided by the European FP7 project BACCHUS (grant agreement no. 49 603445).

3.6 Author Contributions

E.S. and F.C. did the field measurements at Jungfraujoch on the abundance of INPs, analysed and interpreted the stable isotope data and wrote the manuscript. E.H. and N.B. provided data and support for the interpretation of the concentrations of $N_{>0.5}$ at Jungfraujoch. C.M. and C.A. provided strong conceptual frameworks and contributed to writing the paper.

Predicting abundance and variability of ice nucleating particles in precipitation at the high-altitude observatory Jungfraujoch

This chapter has been published as article:

Stopelli, E.¹, Conen, F.¹, Morris, C. E.², Herrmann, E.³, Henne, S.⁴, Steinbacher, M.⁴, and Alewell, C.¹: Predicting abundance and variability of ice nucleating particles in precipitation at the high-altitude observatory Jungfraujoch, *Atmospheric Chemistry and Physics*, 16, 8341-8351, doi.org/10.5194/acp-16-8341-2016, 2016.

¹ Environmental Geosciences, University of Basel, CH-4056 Basel, CH

² INRA, UR 0407 Plant Pathology Research Unit, 84143 Montfavet, FR

³ Laboratory of Atmospheric Chemistry, Paul Scherrer Institut, CH-5232 Villigen PSI, CH

⁴ Empa, Laboratory for Air Pollution/Environmental Technology, 8600 Dübendorf, CH

Abstract

Nucleation of ice affects the properties of clouds and the formation of precipitation. Quantitative data on how ice nucleating particles (INPs) determine the distribution, occurrence and intensity of precipitation are still scarce. INPs active at $-8\text{ }^{\circ}\text{C}$ (INPs₋₈) were observed for 2 years in precipitation samples at the High-Altitude Research Station Jungfraujoch (Switzerland) at 3580 m a.s.l. Several environmental parameters were scanned for their capability to predict the observed abundance and variability of INPs₋₈. Those singularly presenting the best correlations with observed number of INPs₋₈ (residual fraction of water vapour, wind speed, air temperature, number of particles with diameter larger than $0.5\text{ }\mu\text{m}$, season and source region of particles) were implemented as potential predictor variables in statistical multiple linear regression models. These models were calibrated with 84 precipitation samples collected during the first year of observations; their predictive power was successively validated on the set of 15 precipitation samples collected during the second year. The model performing best in calibration and validation explains more than 75% of the whole variability of INPs₋₈ in precipitation and indicates that a high abundance of INPs₋₈ is to be expected whenever high wind speed coincides with air masses having experienced little or no precipitation prior to sampling. Such conditions occur during frontal passages, often accompanied by precipitation. Therefore, the circumstances when INPs₋₈ could be sufficiently abundant to initiate the ice phase in clouds may frequently coincide with meteorological conditions favourable to the onset of precipitation events.

4.1 Introduction

Ice nucleating particles (INPs) play an essential role in the formation of precipitation on Earth, specifically on the continents, where most precipitation comes from ice- or mixed-phase clouds (Mülmenstädt et al., 2015). INPs catalyse the first aggregation of water molecules into ice crystals, which progressively grow larger by diffusion of surrounding water vapour and by collision with water droplets and other ice crystals until they reach a sufficient size to precipitate. In the absence of INPs, spontaneous freezing would occur only at temperatures below $-36\text{ }^{\circ}\text{C}$ (Cantrell and Heymsfield, 2005; Murray et al., 2012).

The scarcity of data about the atmospheric abundance and distribution of INPs prevents a quantitative assessment of their effect on cloud properties, on the development of precipitation and subsequently on climate. Several studies have shown the co-occurrence of INPs from local or faraway sources with precipitation at sites in the Amazon forest (Pöschl et al., 2009; Prenni et al., 2009), in the Sierra Nevada region (Creamean et al., 2013), and at a forested site in Colorado (Huffman et al., 2013; Prenni et al., 2013). The prediction of atmospheric concentrations of INPs from more easily accessible parameters would allow for a more thorough evaluation of the influence of INPs on clouds and precipitation. This approach merits attention in light of results showing the correlation of specific meteorological and environmental parameters with the abundance of INPs, such as air temperature (Conen et al., 2015), wind speed (Jiang et al., 2014; Jones and Harrison, 2004), relative humidity (Wright et al. 2014), season and geographical source (Christner et al., 2008a), and the abundance of airborne particles of micrometre size (DeMott et al., 2010). In addition, we have recently shown that the abundance of INPs active at moderate supercooling negatively correlates with the amount of water that has been lost from an air mass prior to sampling (Stopelli et al., 2015). All these studies indicate statistical relations between INPs and the mentioned parameters, but each tends to focus predominantly on the role of a single parameter.

Here our objective is to describe and foresee the variations in the concentration of INPs active at $-8\text{ }^{\circ}\text{C}$ or warmer (INPs_{-8}) in falling precipitation at the high-altitude observatory Jungfraujoch (Swiss Alps, 3580 m a.s.l.) by means of multiple linear regression models. INPs_{-8} are of particular interest since it has been proposed that the ice phase in clouds could be initiated by relatively few INPs_{-8} (10 m^{-3} or less) through the Hallet-Mossop process of riming and ice splintering (Crawford et al., 2012; Mason, 1996). To attain our objective, we firstly identified the strongest predictors for the abundance of INPs_{-8} in precipitation among all the environmental parameters measured at the observatory. Secondly, we implemented these predictors in three multiple linear regression models built on the temporal variations in INPs_{-8} occurred during the first year of observations ($n = 84$). The predictive power of these statistical models was subsequently tested on an independent set of samples from the second year of measurements ($n = 15$). Prediction of the quantity of INPs_{-8} provides useful means to understand the factors responsible for their large variability in precipitation (Petters and Wright, 2015) and to indicate the circumstances when and where INPs_{-8} may be sufficiently abundant to impact the formation of the ice phase in clouds and conduce to precipitation.

4.2 Methods

4.2.1 Sample collection and analysis of INPs

Falling snow was collected at the High Altitude Research Station Jungfraujoch in the Swiss Alps (7°59'06'' E, 46°32'51'' N; 3580 m a.s.l.) from December 2012 until October 2014. A total of 106 precipitation samples were collected over these 2 years, with a median sampling duration of about 2 hours per sample (sampling time between 1.5 and 8 hours), depending on the intensity of the precipitation events. We started sampling campaigns when the forecasts predicted 2 or more days of precipitation to assure the collection of several samples during each campaign. The station was always inside clouds while sampling, allowing us to collect falling snow as close as possible to where it formed. Samples were collected with a Teflon-coated tin carefully rinsed with ethanol and sterile Milli-Q water to avoid cross-contamination.

Snow samples were analysed for the concentrations of INPs₈ directly on site, using the automated drop freeze apparatus LINDA (LED-based Ice Nucleation Detection Apparatus) loaded with 52 tubes containing 100 µl of sample each (prepared adding 2 ml of 9 % NaCl sterile solution to 18 ml of sample and gently shaken, to ensure a final physiological saline concentration and improve the detection of freezing events, dilution 1:1.1; Stopelli et al. 2014; Stopelli et al., 2015). Blanks were periodically prepared distributing sterile Milli-Q water onto the rinsed tin and analysed with the same procedure as the snow samples, with 200 µl per tube to obtain more restrictive results. Out of 29 blanks analysed during the sampling campaigns reported here, only two blanks contained 0.11 INPs₈ mL⁻¹, confirming the accuracy of our analyses.

Error bars for values of 1, 10, 100, and 1000 INPs₈ mL⁻¹ are shown in the figures of the article. Confidence intervals were calculated as errors in counting frozen tubes, following Poisson's distribution (depending on the number of frozen tubes, they account for 30 % to 50 % increase or decrease of the calculated concentrations of INPs₈). These intervals were propagated into the uncertainty associated with the maximum error in the determination of the freezing temperature of the tubes of ± 0.2 °C (assuming a doubling of INPs per °C of decrease in the freezing temperature, an error of 0.2 °C accounts for a change in 14 % of the measured concentrations) to provide more cautious confidence intervals.

The collection of precipitation allows for the sampling of INPs that either formed precipitating ice particles or were scavenged by precipitation. It is difficult to distinguish between these contributions in field studies, where scavenging, riming, and crystal growth by vapour deposition can alter the abundance of INPs in precipitation. Nevertheless, the station was always inside clouds while sampling, allowing us to collect falling snow as close as possible to where it formed. Furthermore, precipitation was immediately analysed, in order to minimise the chance for biases due to artefacts like the production (i.e. the release in solution of INPs or cellular multiplication) and the loss (i.e. settling or increased molecular weakness of biological INPs detached from mineral and soil dust) of INPs₈.

4.2.2 Parameters related to the concentration of INPs

To analyse and understand more on the factors responsible for the variability of INPs₈ in precipitation, several environmental parameters were considered in relation with the number of INPs₈.

INPs are efficiently removed by precipitating clouds (Stopelli et al., 2015). Therefore, important information on the residual abundance of INPs in rain and snow samples is contained in the value of the residual fraction of water vapour in the sampled air mass f_V . Water molecules containing the stable isotope ^{18}O have a greater propensity to condense, hence to precipitate, than those containing the more abundant stable isotope ^{16}O . Consequently, the $^{18}\text{O}:^{16}\text{O}$ ratio (indicated as δ) in an air mass decreases during precipitation. f_V can be easily calculated comparing the isotopic ratio of the initial water vapour content of an air mass at the moment of its formation with the ratio at the moment of sampling according to Rayleigh's fractionation model (IAEA, 2001a):

$$\frac{\delta_V}{1000} = \left(1 + \frac{\delta_{V,0}}{1000}\right) \cdot f_V^{\alpha_{LV} - 1} - 1$$

In this study δ_V is the isotopic ratio of the vapour at Jungfraujoch, calculated from the isotopic ratio of sampled snow, $\delta_{V,0}$ is the modelled isotopic ratio of the vapour in an air mass at the moment of its formation in contact with seawater and α_{LV} is the fractionation factor from liquid to water along the trajectory of a cloud. Further details on the calculation of these parameters are presented in Stopelli et al., 2015.

Wind speed, air temperature and relative humidity are continuously measured at Jungfraujoch by MeteoSwiss and are stored as 10 min averages. An optical particle counter (GrimmTM, Dust Monitor 1.108) mounted in series with a heated inlet regularly measures the total number of particles with a dry optical diameter larger than 0.5 μm ($N_{>0.5}$) (Weingartner et al., 1999; WMO/GAW, 2003). To produce robust statistics, it was important to assign a single value of air temperature, wind speed and $N_{>0.5}$ to each snow sample. These parameters had a finer temporal resolution compared to the measurements of INPs₈; therefore, they were averaged over the time interval during which each snow sample was collected. To fill gaps due to instrument failures, missing $N_{>0.5}$ values (26 out of 106 samples) were estimated by linear regression from measured PM_{10} concentrations ($R^2 = 0.40$, $p < 0.001$), which are continuously determined at Jungfraujoch by Empa (the Swiss Federal Laboratories for Materials Science and Technology) through a beta-attenuation method (Thermo ESM Andersen FH62 IR). Due to the usually low PM_{10} concentrations at Jungfraujoch, data are aggregated to hourly averages to achieve better signal to noise ratios. In this case, the PM_{10} concentration corresponding to each snow sample was calculated averaging the hourly values including the whole duration of the collection of the sample. Empa also provided hourly concentrations of CO and total reactive nitrogen NO_y in the air. The ratio NO_y/CO is a common proxy of the age of an air mass; thus, it was used as indicator of planetary boundary layer influence and recent land contact of air masses sampled at the observatory (Griffiths et al., 2014; Pandey Deolal et al., 2013). Due to different susceptibility to photochemical transformation in the atmosphere, NO_y/CO ratios decrease during transport after being emitted from anthropogenic sources. Therefore, a larger ratio of NO_y/CO is associated with a more recent contact of the air masses with land surface. Threshold values in the range 0.002 to 0.008 have been proposed to distinguish between conditions influenced by planetary boundary layer and free tropospheric air masses (Fröhlich et al., 2015; Pandey Deolal et al., 2013).

Precipitation intensity (mm h^{-1}) was calculated by dividing the water-equivalent volume of precipitation collected in the sampling tin by its horizontal surface and the sampling duration.

Potential regions where air masses could have picked up particles on their way to Jungfraujoch were determined by the analysis of source sensitivities simulated with FLEXPART, a Lagrangian particle dispersion model used in backward mode (Stohl et al., 2005). FLEXPART was driven with analysed meteorological fields taken from the ECMWF integrated forecasting systems with a horizontal resolution of 0.2° by 0.2° over the Alpine area and 1° by 1° elsewhere (more details on the specific set-up for Jungfraujoch simulations can be found in Brunner et al., 2013). A “source region score” was assigned to each sample, combining information derived from the visual inspection of potential source regions in FLEXPART plots with the prevailing wind direction during sampling. This categorical parameter was conceived to mirror the potential differences in source quality and source strength of INP populations between northern and southern Europe. Three groups were identified: north, south and mixed/uncertain conditions. *A priori* it was hypothesised that a higher score should be given to samples from southern Europe, assuming a larger influence of warmer air masses, enriched in larger mineral dust and organic material emissions, also linked to a more prolonged duration of agricultural activities (Kellogg and Griffin, 2006; Lindemann et al., 1982; Morris et al., 2014). Therefore *a priori* the larger value should be assigned to events from South, followed by mixed conditions and by events from northern Europe. Several combinations of values ranging from 1 to 3 (2-1.5-1, 3-2-1, etc.) were tested and the best combination of values was determined through comparisons with the numbers of $\log(\text{INPs}_g \text{ mL}^{-1})$. It corresponds to the following: south is for 3; mixed condition for 2, and north for 1.

A similar approach was used to insert the “season score” a categorical parameter mirroring the potential effects of seasonality on the release and abundances of INPs_g . *A priori* the highest value was assigned to samples collected in summer, assuming both a larger release of soil and organic material containing INPs, associated with the growth of vegetation, agricultural activity, and warmer air masses (Jones and Harrison, 2004; Lindow et al., 1978; Morris et al., 2014) and a greater chance for INPs to reach the observatory before being removed by precipitation (Conen et al., 2015). In the ranking, summer was followed by autumn and spring as intermediate seasons, and finally by winter. Once this *a priori* classification was established, the precise values for each class were again determined by comparing different possible combinations of numbers from 1 to 9 (3-2-2-1, 9-6-3-1, 4-3-2-1, etc.) with measured values of $\log(\text{INPs}_g \cdot \text{mL}^{-1})$. The best fit with the data was found for the combination: summer is for 4; autumn for 3; spring for 2; winter for 1.

4.2.3 Statistical analyses and modelling

Univariate statistics were carried out with PAST software version 2.17. The R software version 3.0.1 was used to build multiple linear regression models (Hammer et al., 2001; R Team, 2011).

The first step in model building consisted of a preliminary screening of the environmental parameters that had a significant relation with the variability in INPs_g . This was done considering both the results of parametric linear regression and Spearman’s non-parametric correlation test. For the categorical parameters “season score” and “source region score” the results of parametric regression were conservatively substituted with Kruskal-Wallis non-parametric test for the comparison among groups, because this test takes into account the presence of different numbers of data among groups. Normal distribution of variables is required for parametric statistics. In particular, the concentrations of INPs_g were approximately log-normally distributed over several

orders of magnitude. Therefore, they were \log_{10} transformed to normalise their distribution. This led to the exclusion of 7 of 106 samples with no measurable activity (< 0.21 INPs₈ mL⁻¹): the arbitrary assignment of small concentrations would have resulted in a bias when projected on the log scale. Similarly, the number of particles $N_{>0.5}$, precipitation intensity and the ratio NO_y/CO were \log_{10} transformed to improve the distribution of their data. Non-parametric correlation was added to draw more robust and stricter conclusions, independent from parameter distributions.

Multiple linear regression models were built on the parameters presenting the best correlations with INPs₈. Criteria to build up the models were (a) to start from the addition of two parameters which we *a priori* suspected could be descriptors of environmental processes impacting INPs₈ in different ways, such as proxies for their production and removal; (b) to add further parameters only if resulting in a significant gain in explained variability and improved distribution of the residuals; and (c) to prefer combinations of parameters weakly correlated among themselves (Table 4.1), to avoid collinearity.

Table 4.1 Pairwise correlations among predictors for the concentrations of INPs₈. The upper panel indicates the pairwise Spearman's r_s correlation coefficient, the lower panel its statistical significance (*, **, and *** stand for a probability smaller than 0.05, 0.01, and 0.001 respectively).

	f_v	Wind speed	Temperature	$\log(N_{>0.5} \text{ m}^{-3})$	Season	Source region	Relative humidity	$\log(\text{mm h}^{-1})$	$\log(\text{NO}_y/\text{CO})$
f_v		0.10	0.88	0.33	0.89	0.42	0.72	0.07	0.13
Wind speed			0.02	0.21	-0.04	0.17	0.04	0.08	0.31
Temperature	***			0.18	0.85	0.58	0.70	-0.03	-0.28
$\log(N_{>0.5} \text{ m}^{-3})$	**	*	*		0.35	0.32	0.28	-0.11	0.37
Season	***		***	***		0.38	0.77	-0.04	0.15
Source region	***		***	**	***		0.42	-0.12	-0.23
Relative humidity	***		***	**	***	***		-0.12	0.23
$\log(\text{mm h}^{-1})$									0.24
$\log(\text{NO}_y/\text{CO})$		*	*	**		*	*	*	

The normal distribution of independent and dependent variables is not considered necessary for assessing the quality of multiple linear regression models, but it can improve the quality of the results of the model. Consequently, the variables, which were log transformed for univariate statistics, were kept transformed also in multiple linear models. The quality of a multiple linear regression model is evaluated by the significance of the whole model as well as of the regression coefficients of each parameter. Particular care was taken in analysing the residuals of the models. All the models presented here fulfilled the conditions of normally distributed residuals, with an average value of zero and no significant trends. Furthermore, we assumed that the parameters could be added in linear combinations. The correctness of this assumption was verified by the method of

partial regression plots of the residuals. Given an ideal model $y \sim x_1 + x_2$ (x_1 and x_2 used to derive the dependent variable y) it is possible to test whether i.e. x_2 is linearly linked to y . To do that, the residuals of the regression of y with x_2 are plotted against the residuals of the regression of x_1 with x_2 . A linear distribution of the residuals confirms the correctness of the linear relationship between x_2 and y . On the contrary, the presence of a different trend implies a different relationship between x_2 and y , like, for example, a quadratic one. Interactions between independent variables were tested as well as potential ways to improve the models. This means that the additional factor $x_1 \cdot x_2$ was inserted in a model to test whether the effect of the independent variable x_1 (or x_2) on the dependent variable y changes according to different levels of the other independent variable x_2 (or x_1). No interaction we tested resulted in a significant improvement of the models.

4.3 Results and discussion

4.3.1 Model calibration

The observations used to create the models consist of 84 snow samples with measurable concentrations of INPs₈ collected in the Swiss Alps at 3580 m altitude between December 2012 and September 2013. Measured values of INPs₈ ranged from the lower limit of detection (0.21 mL⁻¹) to a maximum of 434 mL⁻¹. Interestingly, these values are comparable to, or even greater than those recently found in cloud water samples in central France at 1465 m altitude (Joly et al., 2014) and well within the range of values and variability observed in precipitation samples collected all around the world (Petters and Wright, 2015).

The best correlations found at Jungfraujoch agree with our current understanding of the factors that are related to the abundance of INPs in the environment (Fig. 4.1, black dots). In particular, the relationships with the remaining fraction of water vapour f_v and air temperature are coherent with the observation that INPs are rapidly lost by precipitating clouds; hence, they are more abundant at early stages of precipitation (Stopelli et al., 2015) and that colder air masses tend to be more depleted in INPs₈ (Conen et al., 2015). A better linear fit suggests that f_v is a factor capable of better representing the temporal variability in INPs₈ than air temperature, which shows a threshold trend. Specifically, it is possible to find more than 10 INPs₈ mL⁻¹ in precipitation for temperatures around 0 °C, indicating that when at the station the temperature is warm then also the temperature of precipitation formation in clouds above the Station can be compatible with residual large abundance of INPs₈, but not exclusively associated only to large values of INPs₈. Therefore, whilst air temperature appears more like a local snapshot-value for the potential activation of INPs₈, f_v is a broader descriptor of the cumulative precipitation history of an air mass.

Wind speed is a good proxy of the energy and turbulence associated with an air mass, promoting the transport and mixing of airborne particles (Jiang et al., 2014; Jones and Harrison, 2004). This is confirmed by the correlation between wind speed and $\log(N_{>0.5} \text{ m}^{-3})$ (Table 4.1). Wind speed is not correlated to the direction of air masses, expressed by the source region score, indicating that the local morphology plays a minor role regarding this parameter. Coherently, the correlation between INPs₈ and $N_{>0.5}$ suggests that the more particles $N_{>0.5}$ are present in the air, the greater is also the probability of finding a greater abundance of INPs₈. This relationship proved significant for INPs

active at $-15\text{ }^{\circ}\text{C}$ or colder (DeMott et al., 2010). Here we show its validity for INPs active at $-8\text{ }^{\circ}\text{C}$ measured in precipitation at Jungfraujoch.

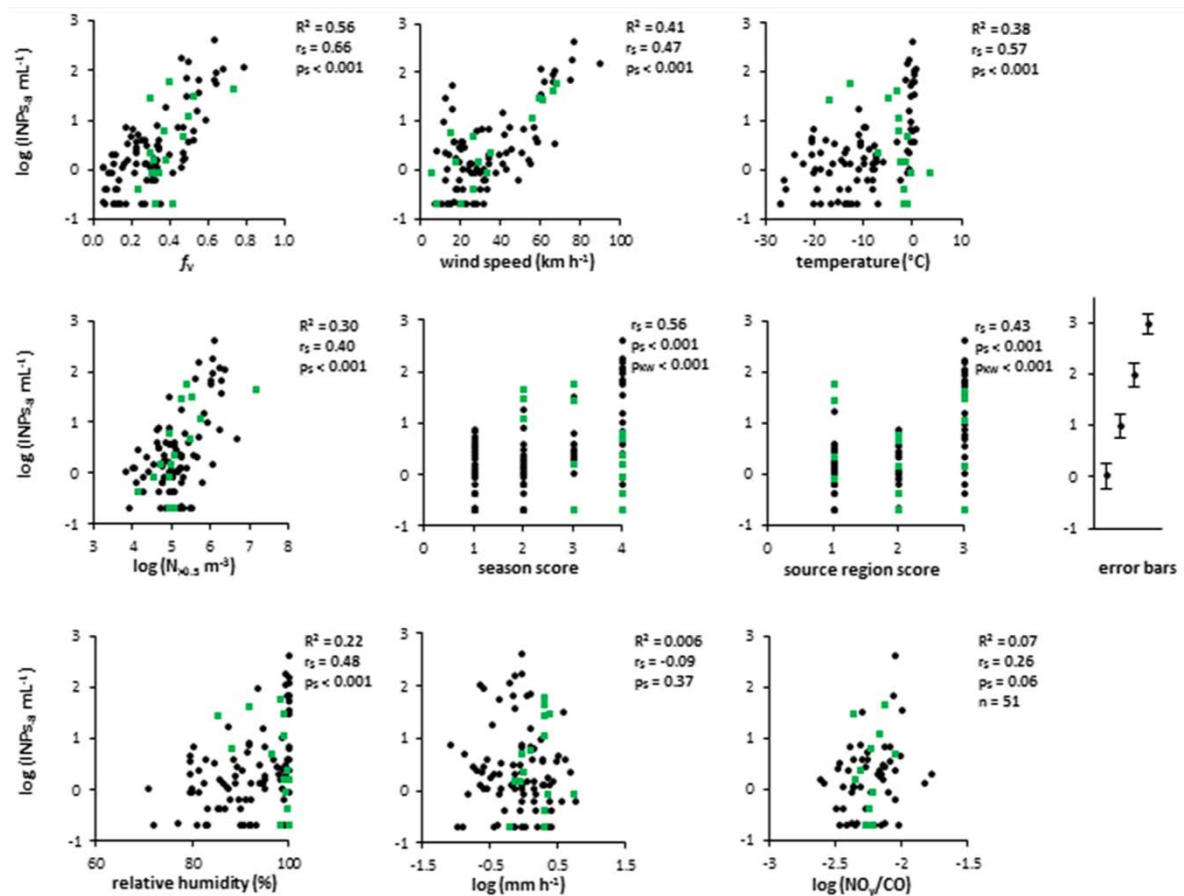


Figure 4.1 Relationships between $\text{INPs}_{.8}\text{ mL}^{-1}$ and singular environmental parameters for the first year of observations (black dots, $n = 84$, exception for the ratio NO_y/CO with $n = 51$ due to missing data of trace gases). Shown are R^2 values, the coefficient of Spearman's correlation r_s and its probability p_s calculated for the data belonging to the first year of observations. f_v indicates the remaining fraction of water vapour in a precipitating air mass. In the panel "season score" 1 is for winter, 2 for spring, 3 for autumn, and 4 for summer. In the panel "source region score" 1 is for northern Europe, 2 for mixed conditions, and 3 for southern Europe. For both "season score" and "source region", values of Kruskal-Wallis' test probability p_{kw} are shown instead of R^2 . Data belonging to the second year of observations are represented as green squares ($n = 15$, $n = 12$ for the ratio NO_y/CO). Error bars associated to the measurement of 1, 10, 100, and 1000 $\text{INPs}_{.8}\text{ mL}^{-1}$ are represented close to the graphs.

$\text{INPs}_{.8}$ found in precipitation confirmed the expectations to be more abundant in summer and in air masses coming from southern Europe. Relative humidity appears as a threshold for the abundance of $\text{INPs}_{.8}$ (Bowers et al., 2009; Wright et al., 2014), with a similar distribution of the data to the one shown by temperature. Therefore, the relationship between the relative humidity and $\text{INPs}_{.8}$ may reflect the role of particle processing in the residual abundance of $\text{INPs}_{.8}$. This process can be better represented by temperature or f_v ; thus, preference was given to the latter parameters in building multiple linear regression models. $\text{INPs}_{.8}$ are not correlated with the intensity of precipitation, suggesting that different amounts of precipitation can be generated per INP. The ratio NO_y/CO

presents a relatively low and homogeneous range of values, which are related to air masses with slightly recent contact with land surfaces (the most recent threshold value presented in literature for Jungfraujoch is 0.004, -2.4 on log scale; Fröhlich et al., 2015). Nevertheless, the sampling happened always inside precipitating clouds, which suggested the occurrence of the uplift of planetary boundary layer air to the height of the station. Therefore, it is realistic to speculate that the precipitation collected was generally originating from air masses integrating several source regions and distances before reaching the observatory. Furthermore, the ratio NO_y/CO is positively correlated with wind speed and $N_{>0.5}$ (Table 4.1), suggesting that at high wind speed clouds at Jungfraujoch may be charged with particles taken up during recent contact of the air mass with a land surface. This suggestion could explain larger numbers of $\text{INPs}_{.8}$ in precipitation at high NO_y/CO ratios (Fig. 4.1).

The parameters presenting the best correlations with $\text{INPs}_{.8}$ were successively added into multivariate linear regression models and the three models predicting the concentrations of $\text{INPs}_{.8}$ best are

$\log(\text{INPs}_{.8} \text{ mL}^{-1}) =$

- 1) $2.84 * f_v + 0.02 * \text{wind speed (km h}^{-1}) - 1.12$
- 2) $0.36 * \text{season} + 0.02 * \text{wind speed (km h}^{-1}) + 0.13 * \text{source region} - 1.39$
- 3) $0.02 * \text{wind speed (km h}^{-1}) + 0.05 * \text{temperature (}^\circ\text{C)} + 0.34 * \log(N_{>0.5} \text{ m}^{-3}) - 1.54$

They were all capable of describing about 75% of the observed variability for the calibration period (year 1, Table 4.2) and of reproducing observations equally well, where an apparent seasonal trend with maximum values of $\text{INPs}_{.8}$ in summer is recognisable (Fig. 4.2, upper panel). Yet, model 1, based on two variables only - f_v and wind speed -, performed slightly better than the other two models, which are based on three parameters. It also provided the smallest maximum absolute error (Table 4.2). The range of potential concentrations of $\text{INPs}_{.8}$ which can be predicted from model 1 is also the closest to observations. Inserting in the model the smallest, and largest, observed values of f_v and wind speed results in a range of calculated concentrations of $0.11 \text{ INPs}_{.8} \text{ mL}^{-1}$, and $750 \text{ INPs}_{.8} \text{ mL}^{-1}$. Doing the same with model 2 results in a maximum value of $250 \text{ INPs}_{.8} \text{ mL}^{-1}$, and with model 3 of $400 \text{ INPs}_{.8} \text{ mL}^{-1}$, underestimating the range of measured concentrations for at least one event. The observed rapid changes in the abundance of $\text{INPs}_{.8}$ may explain the slightly better performance of model 1. Differences in the concentration of $\text{INPs}_{.8}$ of more than 2 orders of magnitude were found not only on a seasonal timescale, but also within the same precipitation event over a couple of hours. The variables “season” and, to a lesser extent, “source region”, “temperature” and “ $\log(N_{>0.5} \text{ m}^{-3})$ ” could not always reproduce such sudden changes, as can be seen from the broader distribution of these parameters in Fig. 4.1.

The pattern of residuals over time is almost the same for all three models (Fig. 4.2, lower panel). Thus, it is unlikely to result from random noise and suggests the presence of at least one further driver of the abundance of $\text{INPs}_{.8}$ in precipitation. Given the lack of any relationship with precipitation intensity, a likely candidate is the average mass (equivalent liquid volume) of hydrometeors formed by individual INPs. For snow crystals it spans over more than an order of magnitude (Mason, 1957). INPs generating larger hydrometeors, such as those grown through riming, will be diluted in a larger volume of water and result in an overestimation of modelled numbers of $\text{INPs}_{.8} \text{ mL}^{-1}$. Smaller than average ice crystals will do the opposite.

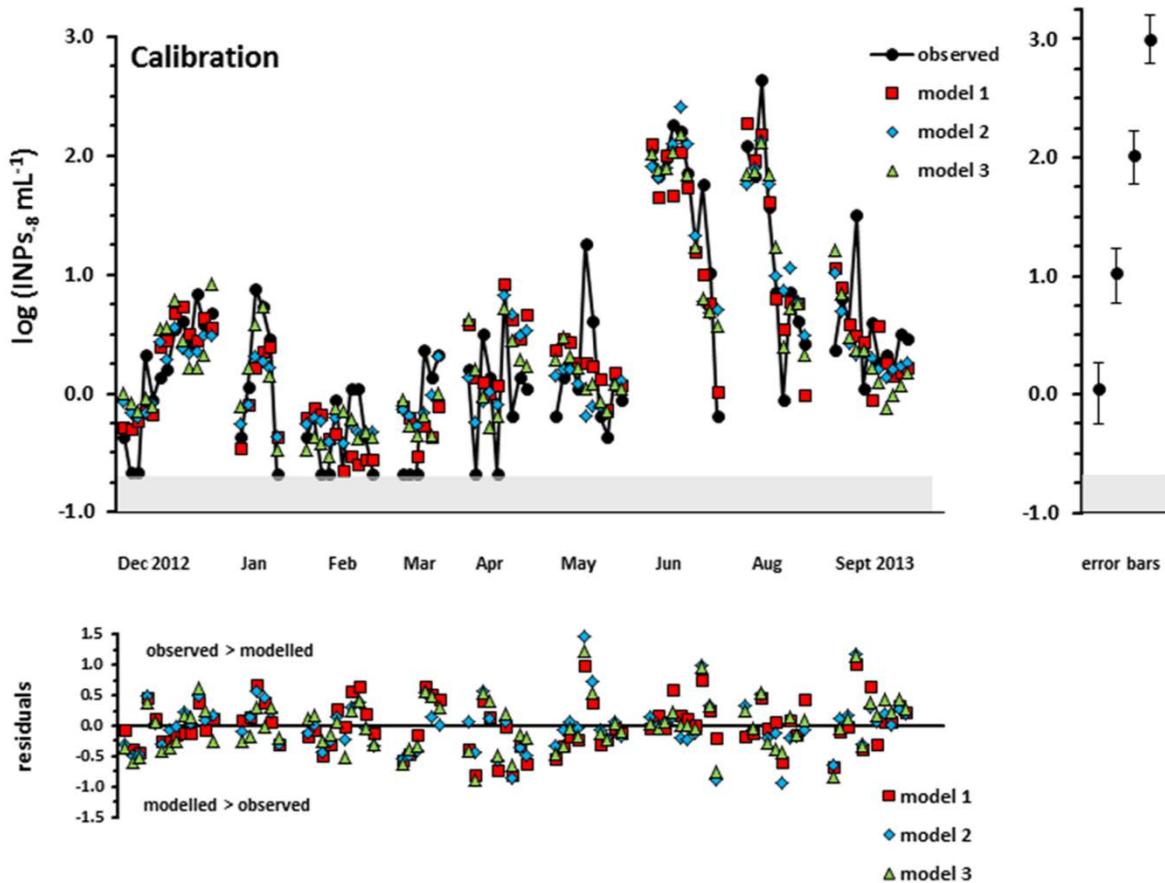


Figure 4.2 Comparison of observed concentrations of $\text{INPs}_{.8}$ with the values predicted by models (absolute values in upper panels, residuals in lower panels) for the data set used for calibration ($n = 84$). The grey area in the upper panel indicates the range below the detection limit of our observation method. Time proceeds from left to right, intervals are not to scale, dots belonging to the same sampling campaign are connected by lines. Error bars associated to the measurement of 1, 10, 100, and 1000 $\text{INPs}_{.8} \text{ mL}^{-1}$ are represented close to the graph

4.3.2 Model validation

We validated the three models with observations from 15 precipitation samples collected between May 2014 and October 2014. The values of the environmental parameters associated with these 15 independent samples (f_v , air temperature, etc.) were directly inserted in the equations of the three models as derived from the calibration step and used to predict values of $\text{INPs}_{.8} \text{ mL}^{-1}$.

The observed concentrations of $\text{INPs}_{.8}$ during this second period of measurements ranged from 0.21 mL^{-1} to a maximum of 60 mL^{-1} . Interestingly, the samples collected in 2014 presented a completely different pattern compared to the previous year of observations (Fig. 1, green squares; Fig. 4.3 upper panel). The lowest concentrations of $\text{INPs}_{.8}$ were observed during summer, whilst the highest concentrations occurred in May during a Saharan dust event and in October when a cold front from northern Europe reached Jungfraujoch (air temperature dropped to $-16 \text{ }^\circ\text{C}$). For the sampling campaigns carried out in June, July, and September the local air temperature was relatively warm (between -7 and $+3 \text{ }^\circ\text{C}$). Still, f_v values were low, between 0.23 and 0.47, suggesting that air masses had already lost substantial parts of their initial water vapour prior to

arrival at Jungfraujoch, even if season, source region, and local temperature could have been favourable for an abundant residual presence of INPs₈.

As a consequence, models 2 and 3, which are based either on season, source region, or air temperature, predicted a smaller variability of INPs than observed and overestimated the low concentrations measured in summer 2014 causing larger residual values (Fig. 4.3 lower panel, Table 4.2). Model 1, based only on the two parameters f_v and wind speed, provided better results in predicting the variability of INPs₈ observed during the second year of sampling, producing lower absolute errors, less than 1 log unit (Table 4.2).

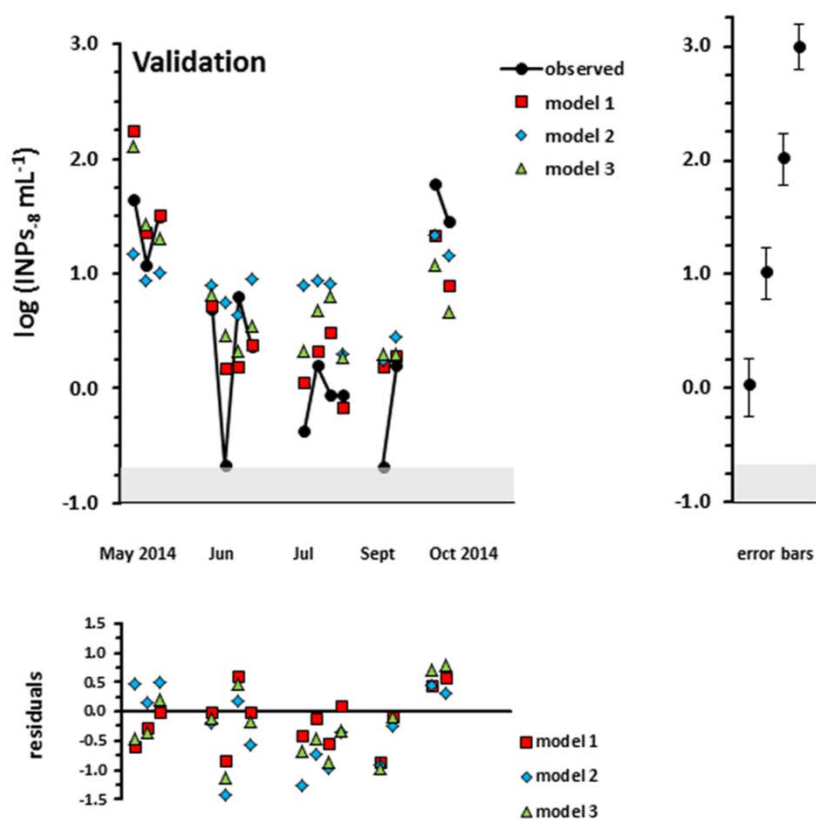


Figure 4.3 Comparison of observed concentrations of INPs₈ with the values predicted by models (absolute values in upper panels, residuals in lower panels) for the data set used for validation ($n = 15$). The grey area in the upper panel indicates the range below the detection limit of our observation method. Time proceeds from left to right, intervals are not to scale, dots belonging to the same sampling campaign are connected by lines. Error bars associated to the measurement of 1, 10, 100, and 1000 INPs₈ mL⁻¹ are represented close to the graph.

4.3.3 Source and sink effects

Even if the linear coefficients are site specific, the three models presented in this paper point at important general indications. Wind speed is a necessary parameter to describe INPs₈ in precipitation and is related to $N_{>0.5}$ and to a more recent land contact represented by the ratio NO_y/CO (table 4.1). Other factors can be combined to wind speed obtaining models of comparable quality. These factors are f_v , temperature, season, source region, and $N_{>0.5}$ and are all well correlated among themselves (table 4.1). This means that their relation with INPs₈ can be linked to the same process, which can be particle processing in precipitating clouds. This can act as a “sink”

force for INPs_g and is best represented by f_v . On the other hand, wind speed can strengthen the “source” of airborne particles. To different degrees, surfaces on Earth, such as oceans, forests, crops, soils, freshwaters and snowpack, host organisms with ice nucleating activity (Després et al., 2012) and may contribute to the airborne population of INPs_g. In this perspective, source region and seasonality may relate more to the likelihood for an air mass to reach Jungfraujoch with a lot of particles and little prior precipitation rather than to a different background number of airborne INPs_g. Therefore it is possible to imagine that, independent from a more or less constant and widespread reservoir of INPs_g, it is the combination of the energy of an air mass with the amount of precipitation generated by this air mass that determines the residual abundance of INPs_g in precipitation samples.

Table 4.2 Summary of the main statistics employed to evaluate the quality of the models. “ R^2_{adj} ” is the fraction of the observed variance reproduced by a model. It is adjusted to account for the number of variables and samples considered. All models, parameters, and constants are highly significant ($p < 0.001$), except the parameter “source region” ($p = 0.06$). “ β^* ” is the value of the standardised regression coefficients, expressing the relative importance of each parameter in a model. The “residuals” column shows the median residual value “med” and the maximum absolute residual as maximum estimation error “ABS” (the corresponding factors of error estimate on linear scale are shown in brackets). “MSE” is the value of the mean squared error.

	Calibration			Validation
	R^2_{adj}	β^*	residuals	residuals
1	0.76	f_v : 0.62 wind speed: 0.47	Med: -0.04 (0.9) ABS: 1.02 (10.4) MSE: 0.16	Med: -0.08 (0.8) ABS: 0.87 (7.4) MSE: 0.25
2	0.73	season: 0.52 wind speed: 0.52 source region: 0.12	Med: 0.00 (1.0) ABS: 1.45 (28.4) MSE: 0.17	Med: -0.25 (0.6) ABS: 1.42 (26.1) MSE: 0.56
3	0.74	wind speed: 0.49 temperature: 0.48 $\log(N_{>0.5} \text{ m}^{-3})$: 0.26	Med: -0.02 (0.9) ABS: 1.22 (16.5) MSE: 0.17	Med: -0.33 (0.5) ABS: 1.13 (13.5) MSE: 0.43

4.4 Conclusions

Large variability in the abundance of INPs_g has been found in over a hundred precipitation samples collected at Jungfraujoch (3580 m a.s.l.), with values ranging from 0.21 INPs_g mL⁻¹ to 434 INPs_g mL⁻¹. Strikingly, with simple multiple linear regression models based on some easily measurable environmental parameters it was possible to describe and predict up to 75 % of the observed variability in INPs_g. All these models indicate that the variability of INPs_g is determined by the interaction of “source” and “sink” processes, such as the potential for air masses to pick up and transport INPs_g from several sources and for INPs_g to be removed by precipitation. Our investigation indicates that a large abundance of INPs_g in precipitation at Jungfraujoch is present

4.5 Acknowledgements

whenever there is a coincidence of high wind speed and moist air mass with little or no prior precipitation. Based on the results of the present study, INPs active at moderate supercooling are expected to be abundant whenever high wind speed coincides with first (initial) precipitation from an air mass. These conditions can be met when an air mass is suddenly forced to rise, for instance at the boundary of a front or due to thermal updrafts or when crossing a mountain ridge. Specifically during the passage of a cold front, gusty winds promote the uptake of particles and the first clouds that form will still retain a large fraction of the initial water vapour of the warm air mass (Gayet et al., 2009; Wright et al., 2014). Simultaneously, physical conditions along a cold front are favourable for cloud formation. Therefore, frequent systematic coincidences of high numbers of INPs with meteorological conditions conducive to precipitation may be expected. Due to this frequent co-occurrence, the potential impact on precipitation by INPs active at slight supercooling - such as INPs of biological origin - may be larger than previously estimated. Their role in the water cycle might therefore best be studied under such conditions.

4.5 Acknowledgements

We thank the International Foundation for High Alpine Research Station Jungfraujoch and Gornergrat (HFSJG) for making it possible for us to conduct our measurements at Jungfraujoch. Urs and Maria Otz, and Martin and Joan Fischer provided helpful support during field activity. Corinne Baudinot measured the abundance of INPs in snow samples during the second year of observations. Dr Thomas Kuhn and Mark Rollog analysed the stable isotope ratio in our snow water samples. We thank MeteoSwiss for providing data on meteorology at Jungfraujoch. The work described here was supported by the Swiss National Science Foundation (SNF) through grant no 200021_140228 and 200020_159194. Measurements of total solid particles were performed by Paul Scherrer Institute in the framework of the Global Atmospheric Watch (GAW) programme funded by MeteoSwiss with further support provided by the European FP7 project BACCHUS (grant agreement no. 49603445). Trace gases and PM₁₀ measurements at Jungfraujoch are performed as part of the Swiss National Air Pollution Monitoring Network which is operated by Empa in collaboration with the Swiss Federal Office for the Environment.

4.6 Author contributions

E.S. and F.C. did the field measurements at Jungfraujoch on the concentrations of INPs, analysed data, did statistical modelling and wrote the manuscript. E.H., S.H. and M.S. respectively provided data and support for the interpretation of N_{>0.5}, FLEXPART modelling, PM₁₀ and trace gases and contributed to writing the paper. C.M. and C.A. provided strong conceptual frameworks and contributed to writing the paper.

Abstract

The impact of ice nucleating particles (INPs) of biological origin on cloud processes remains largely uncertain. Some plant pathogenic bacteria, like *Pseudomonas syringae*, have been originally addressed and as major INPs of biological origin in the atmosphere. This perspective has been recently enriched by the discovery of INPs produced and released from more bacterial species and even fungi, plants, lichens. Here we studied the abundance of bacterial cells in more than 50 precipitation samples collected at the High Altitude Research Station Jungfraujoch. Furthermore, we looked for the presence of culturable *Pseudomonas syringae* at tropospheric height. Results show that the majority of bacterial cells is living in the atmosphere, their abundance is generally constant ($2.4 \cdot 10^3 - 6.8 \cdot 10^4$ cells mL⁻¹) and increases under high wind speed. Comparison with the number of INPs active at -8 °C (INPs₋₈) in the same samples indicates that both bacteria and INPs₋₈ can be reinjected in the atmosphere under high wind speed, but INPs₋₈ are preferentially removed by precipitation than bacterial cells. This implies a shorter residence time in the atmosphere and shorter scales of distribution of INPs₋₈ compared to bacteria, which can persist longer as airborne. *P. syringae* has been successfully isolated (2 - 45 CFU L⁻¹) and its behaviour in the atmosphere is comparable to INPs₋₈. Intact bacterial cells can potentially account on average for 15 % of the whole number of INPs₋₈, pointing at cellular fragments and macromolecules, both freely floating and attached to mineral and soil particles, as relevant biological INPs. Therefore, this study provides important improvement of our understanding of the nature of airborne biological INPs and on the factors responsible for the spreading of bacteria and *P. syringae* through the atmosphere.

5.1 Introduction

The nucleation of ice in clouds is a process of primary relevance both for the radiative budget of clouds and for the development of precipitation on Earth (Mülmenstädt et al., 2015). Airborne ice nucleating particles (INPs) promote the aggregation of water molecules into ice crystals at temperatures above $-36\text{ }^{\circ}\text{C}$ (Murray et al., 2012). Particularly interesting are INPs of biological origin (DeMott and Prenni, 2010), since more and more living organisms have been discovered to show ice nucleating activity at temperatures up to $-2\text{ }^{\circ}\text{C}$, with the potential for promoting the onset of precipitation at moderate supercooling once they get airborne.

Research on biological INPs moved its first steps from the study of bacterial strains responsible for the development of crop diseases, like the bacterium *Pseudomonas syringae* (Lindemann et al., 1982; Lindow 1983; Maki et al., 1974). These bacteria belong to the G- group and carry an ice nucleating protein on their outer membrane, which can damage hosting organisms by frosting, providing access to new sources of food. These microorganisms have been isolated not only from crops, but also from water bodies, litters and even from atmospheric samples of rain and cloud water (Joly et al., 2013; Monteil et al., 2012; Morris et al., 2008), raising the question whether, once airborne, the harsh conditions met in the atmosphere induce the production of ice nucleating proteins in bacteria (Nemecek-Mashall et al., 1993), so that they can actively trigger precipitation as means to parachute and colonise new crops.

Such studies have been progressively enriched by the discovery of ice nucleating abilities in several species of fungi, pollen, lichens, algae and diatoms (DeMott et al., 2015; Fröhlich-Nowoisky et al., 2015; Moffett et al., 2015; Morris et al., 2013a; O’Sullivan et al., 2015; Pummer et al., 2015; Wilson et al., 2015). These organisms are capable of producing both proteins and polysaccharides which nucleate ice. These molecules are freely released out of the cell (Pummer et al., 2015), a mechanism which has been seen as an increased chance for accessing food sources, for surviving at cold temperatures and for facilitating the collection and local preservation of water in moisture-limited environments.

All these findings have opened new perspectives on the richness and ubiquity of living organisms producing INPs. In parallel, INPs of biological origin have been found in soils, freshwaters, forests and crops, oceans, litters as well as in precipitation (Christner et al., 2008b; Conen et al., 2011; DeMott et al., 2015; Joly et al., 2014; Morris et al., 2010; Prenni et al., 2013; Schnell and Vali, 1976). This has increased the potential for biological INPs to play a role in governing climate not only globally on Earth, but also on a more regional scale. In fact, biologically active landscapes may maintain their existence by releasing ice nucleating aerosols which would promote beneficial precipitation for the organisms living in the same landscapes, through a “bioprecipitation” feedback (Morris et al., 2014).

Nevertheless, some questions remain unanswered: whether INPs of biological origin can easily get airborne, in which forms, whether they reach cloud heights in sufficiently large concentrations to effectively promote the formation of precipitation and, if this is the case, whether it is an active process meant to survive, spread and colonise new crops or it simply a passive secondary effect of biological molecules and cellular fragments carried on mineral and soil dust. Research on airborne concentrations of bacteria and their link with precipitation is also relevant to study and predict the potential for distribution of plant pathogenic bacterial and fungal strains, in the perspective of improving the prevention of crops from the spread of diseases (Schmale and Ross, 2015).

Here we describe the factors responsible for the abundance of bacteria in precipitation collected at high altitude (Jungfrauoch, Switzerland, 3580 m a.s.l.) to find the most important drivers of the variability of airborne microorganisms. We looked for the presence of culturable *P. syringae* in precipitation to study the potential for this ubiquitous bacterium to reach cloud heights. We also compare the number of bacterial cells with the INPs_g present in the same precipitation samples to derive more information on the behaviour of these two different groups of airborne particles and to estimate to which extent bacterial cells can account for the observed number of INPs_g.

5.2 Materials and methods

5.2.1 Sampling and bacterial cell counts

Precipitation samples were collected at the High Altitude Research Station Jungfrauoch (7°59'06'' E, 46°32'51'' N, 3580 m a.s.l., Switzerland) during 11 sampling campaigns carried out from March to September 2013 and from May to October 2014. The sampling time lasted between 1.5 and 8 hours, with a median sampling duration of 2 hours. A sampling campaign was organised when weather forecasts predicted more than one day of subsequent precipitation, in order to collect multiple samples at each time.

Falling snow was collected with a Teflon-coated tin put on the terrace of the Sphinx observatory. To minimise cross-contamination among samples, the tin was always carefully rinsed with several cycles of ethanol 70% and sterile Milli-Q water. Two aliquots of the sample were collected, one for total cell counts and one for live/dead staining. For both aliquots, 18 mL of melted snow were added 2 mL of NaCl 9 % solution (dilution 1:1.1 of the sample) in order to reach a final physiological saline concentration of 9 ‰. The final 20 mL were gently shaken for 30 s to improve the homogenisation of the sample and were added to glass filtering units. Pressure difference was applied until complete collection of the sample on a 0.22 µm black polycarbonate pore filter. The glass columns were provided with a funnel of 6 mm final diameter mounted upstream of the membrane filter, to improve the concentration of the sample just on a smaller portion of the filter. 3 mL of sterile PBS buffer were used to rinse the filtering column and the staining agent added. 10 µL SYBR green (100x) was added for the total cell count, while 10 µL SYBR green and 10 µL propidium iodide (in Milli-Q water, 1‰ wt/wt) were employed to select only living cells. The filters with the staining agents were dark incubated for 10', then the strainers were filtered away and the column furtherly rinsed with 3 mL of sterile PBS to maximise the recovery of cells from the sample. Once dry, the filters were successively collected on glass slides, added with 15 µL of antifading agent (5 mL PBS, 5 mL glycerol, 10 mg p-phenyldiamine) and preserved covered with aluminium foil at -20 °C until analysis. To check the quality of the sampling method and of the filter preparation, blanks were periodically prepared with 18 mL of Milli-Q water used to rinse the tin and following all successive steps of the sample preparation. The concentrations of bacterial cells in the blanks were generally less than 10% of those present in the sample, therefore within the acceptable range of uncertainty linked with the method of direct counting of bacteria.

Filters were analysed with a fluorescence microscope (Leica DM2500) with a 100x ocular lens and an objective with 10x10 10 µm grids. Bacterial cells were recognised by shape and size. Each time,

at least 10 fields and 300 cells were counted. The final concentration of bacterial cells was calculated as follows:

$$X = \frac{N_{\text{unit}} * \text{TotalFilterSurface}}{\text{UnitFilterSurface}} * \frac{1}{\text{mL}} * \text{dilution} = \text{cells} * \text{mL}^{-1}$$

Where: N_{unit} is the average number of cells counted per unit of filter (f. i. the sum of 10 x 10 μm squares used to count the cells, from which the unit filter surface is derived), the total filter surface is related to the 6 mm funnel circle used to concentrate the sample on a smaller filter area, mL is the volume of sample filtered and dilution is the dilution factor of the sample, in our case 1.1.

The excitement wavelength was 490 nm to maximise the signal from SYBR green. SYBR green is a powerful staining agent which binds to all cells containing DNA. Once it is bound, it absorbs blue light and emits green light ($\lambda_{\text{MAX}} = 520 \text{ nm}$). Propidium iodide is on the contrary generally excluded by viable cells and can enter only in cells which are either dead or undergoing physiological stress. Once it is bound to DNA, it absorbs green light and emits red light. Therefore, a damaged or dead cell will contain both SYBR green and propidium iodide, but will not result visible anymore under blue light because the wavelength emitted by SYBR green is absorbed by propidium iodide. Therefore, in filters treated with the sole SYBR green, all cells are visible under blue light, while in filters treated with SYBR green and propidium iodide just living cells can be counted.

5.2.2 Selective isolation of *P. syringae*

Enough precipitation volume was available in 13 samples on a total of 15 collected in 2014 to study the presence of culturable *P. syringae* at tropospheric cloud heights. The method employed for the selective isolation of *P. syringae* is the one reported also in Monteil et al., 2014 and in Morris et al., 2008. Precipitation samples were collected in rinsed Teflon tins, this time also dry heated 20' at 150 °C prior to sampling. Samples were concentrated 500 times by filtration of around 1 L of melted snow on 47 mm diameter 0.22 μm pore polycarbonate sterile filters and successive resuspension of the particles by stirring the surface of the filter into 2 mL of filtered precipitation water. The concentrated samples were dilution-plated on KBC, King's medium B supplemented with boric acid, cephalixin and cycloheximide, to isolate and calculate the abundance of *P. syringae*. Plates were incubated at 20–25 °C. Putative strains of *P. syringae* were successively purified on KB and tested for the production of fluorescent pigment on King's medium B, for the absence of arginine dihydrolase and for the absence of cytochrome C oxidase. Those resulting negative both for the oxidase and arginine tests were suspended in TP1 phosphate buffer and sent at the Plant Pathology Unit, INRA, Montfavet, France for the molecular identification of *P. syringae* (PCR using primers specific for *P. syringae*: Fcb43: 5'-ATGATCGGAGCGGACAAG-3'; Rcb43: 5'-GCTCTTGAGGCAAGCACT-3', Guilbaud et al., 2016). The strains confirmed to be *P. syringae* were also tested for their ice nucleating activity. After 3 days of growth on KB, suspensions of pure colonies corresponding to around $10^8 \text{ cells mL}^{-1}$ of NaCl 0.9 ‰ solution were incubated 1 h in melting ice and subsequently tested for being ice nucleating positive at – 8 °C with immersion freezing.

5.2.3 Environmental parameters and INPs_g

The number of INPs_g per mL of precipitation was calculated by immersion freezing with the apparatus LINDA (Stopelli et al., 2014). The fraction of water vapour lost from an air mass prior to sampling, expressed as $1-f_v$, was calculated from the abundance of ^{18}O in precipitation, expressed as $\delta^{18}\text{O}$. More details on this calculation are provided in Stopelli et al., 2015. Wind speed and air temperature were measured at Jungfraujoch by MeteoSwiss and were stored as 10-minute averages. Dr. Erik Hermann from PSI provided data on the total number of particles with a dry optical diameter larger than $0.5\ \mu\text{m}$ ($N_{>0.5}$), regularly measured with an optical particle counter (GrimmTM, Dust Monitor 1.108) (Weingartner et al., 1999; WMO/GAW, 2003). Dr. Martin Steinbacher from Empa provided hourly concentrations of CO and total reactive nitrogen NO_y in the air, to calculate the ratio NO_y/CO , which is a proxy of the age of an air mass. Precipitation intensity expressed as mm h^{-1} was measured directly on site. Season and source region were treated as categorical variables in order to express different expected potentials for bacteria to be emitted from sources and to reach the observatory. A precise description on how these parameters were calculated and associated to precipitation samples is reported in Stopelli et al., 2016.

5.2.4 Statistics

Univariate and non-parametric statistics were carried out with PAST software version 2.17. (Hammer et al., 2001). Log-transformation was operated on some parameters to improve the overall distribution of the data.

5.3 Results and discussion

5.3.1 Bacterial cells and successful isolation of *P. syringae*

The total number of bacterial cells in precipitation ranged from $2.4 \cdot 10^3$ to $6.8 \cdot 10^4\ \text{mL}^{-1}$, with a median value of $7.6 \cdot 10^3$, a range which is coherent with previous observations carried out on precipitation and cloud water samples collected at several places around the world (Bauer et al., 2002; Joly et al., 2014; Šantl-Temkiv et al., 2013; Sattler et al., 2001; Vařtilingom et al., 2012; Xia et al., 2011) (fig. 5.1, black dots, $n = 58$).

The percentage of living and fit cells ranged between 35 % and 78 %, with a median value of 60 % (fig. 5.1, green bars, $n = 54$).

Pseudomonas syringae was successfully isolated from 3 out of the 13 samples analysed for its presence in 2014, specifically in two samples from Southern Europe collected in May and in one sample of a storm from Northern Europe in October. Its concentrations were 2, 4 and $45\ \text{CFU L}^{-1}$ of melted snow. It is the first time *P. syringae* has been isolated at such an altitude, confirming its ubiquity over Earth and its connection with the water cycle (Morris et al., 2008).

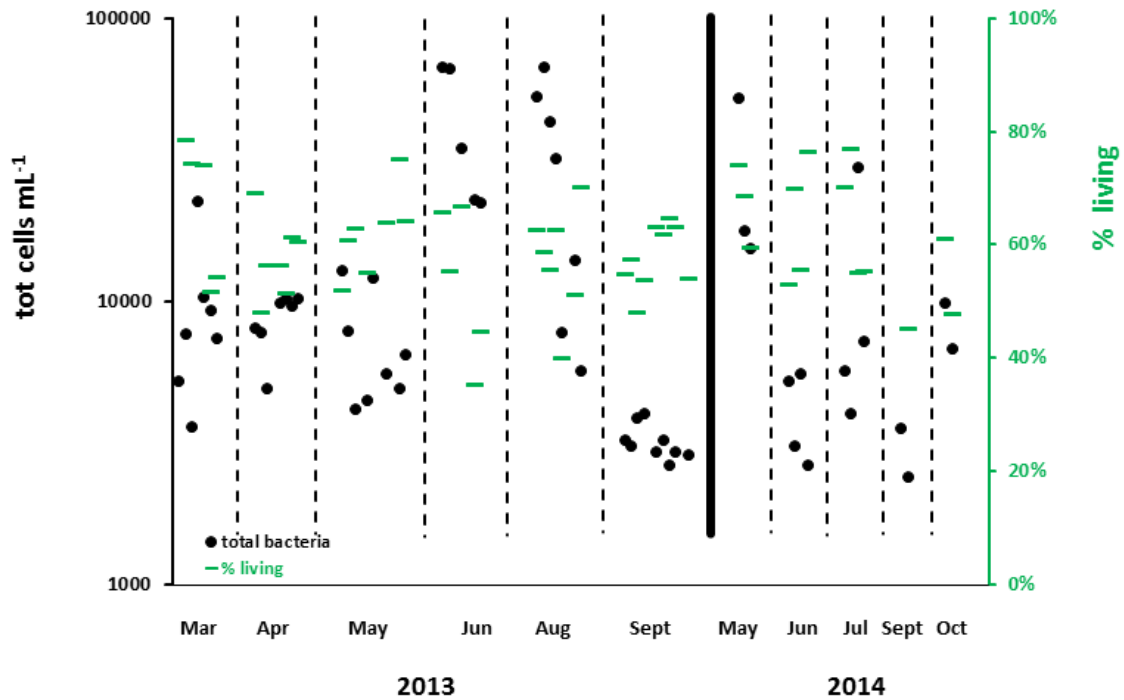


Figure 5.1 Variability of the number of total bacterial cells (black dots) and percentage of living cells (green bars) in precipitation samples collected at the observatory Jungfrauoch over 11 sampling campaigns carried out between 2013 and 2014.

5.3.2 Factors influencing the abundance of bacterial cells

The number of bacterial cells in precipitation presents generally constant background values ($5 \cdot 10^3$ to 10^4 cells per mL of precipitation), which are exceeded only under punctual events. Values of bacterial cells in precipitation increase significantly with wind speed above 50 km h^{-1} , concurrently with the parallel increase in the airborne number of particles larger than $0.5 \mu\text{m}$ ($N_{>0.5}$) (fig. 5.2). The best conditions for this to happen were represented by air masses coming in spring or summer to Jungfrauoch from southern Europe, containing also Sahara dust. This confirms the role of such events with injection of desert dust as strong carriers of microorganisms, both present in the dust itself and progressively collected over the trajectory of the air masses (Chuvochina et al. 2011; Favet et al., 2013; Kellogg and Griffin, 2006; Peter et al., 2014).

The total number of cells is not influenced by the season, the recent contact with the land (represented by the ratio NO_y/CO) and the amount of precipitation generated. It resulted independent from the local temperature of the air and weakly related to the quantity of precipitation already lost from an air mass prior to arrival at Jungfrauoch (represented by $1-f_V$) (table 5.1, fig. 5.3).

In 47 out of 54 samples the majority of bacterial cells were living, but the percentage was not correlated to any of the parameters considered. This confirms that, even if the atmosphere is a selective environment for microorganism due to the oxidative stress, the limited availability of nutrients, and extremely variable temperatures and moisture conditions, bacteria have developed strategies to successfully overcome such stress and survive in the atmosphere at cloud heights. This

expands the possibilities for bacteria to move across environments and colonise new ecosystems, for instance also to successfully cross a mountain ridge like the Alps.

Table 5.1 Correlations between bacterial cells in precipitation samples (rows) and environmental parameters (columns). Indicated are Spearman's correlation coefficient and the degree of significance of the test (*, **, *** stand for a probability of 0.05, 0.01, 0.001 respectively).

	log (INPs _{0.8} mL ⁻¹)	1-f _v	wind speed	temperature	log (N _{>0.5} m ⁻³)	season	source region	log (mm h ⁻¹)	log (NO _y /CO)
log (tot cells mL ⁻¹)	.45 ***	-.32 *	.55 ***	.20	.46 ***	.07	.34 **	.00	.29
% living	-.18	.16	-.07	-.15	.02	-.11	-.01	-.17	-.27

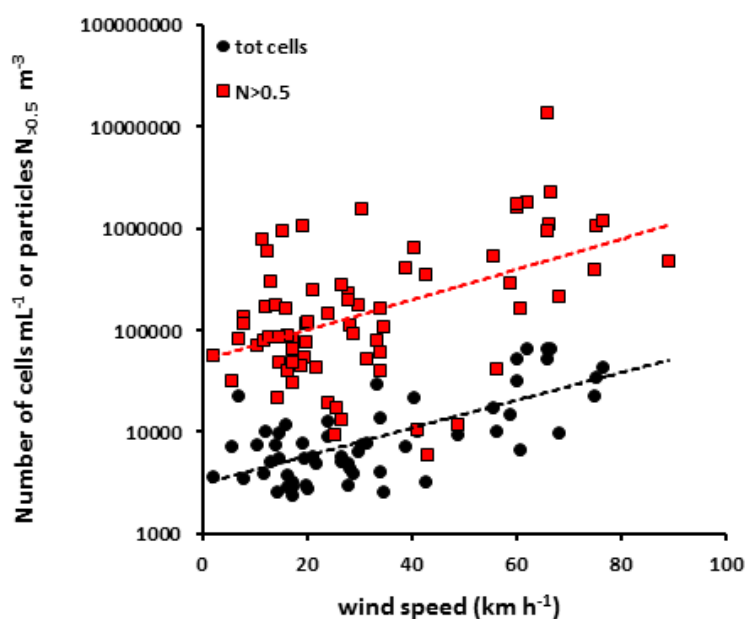


Figure 5.2 The number of total bacterial cells per mL of precipitation (black dots) increases for wind speeds larger than 50 km h⁻¹, a trend which is similar to the one shown by the number of particles of similar size N_{>0.5} per m³ of air (red squares).

Among those studied for its presence, the samples where *P. syringae* was isolated were characterised by higher concentrations of INPs_{0.8}, smaller 1-f_v and higher wind speed (fig. 5.3). This association seems to indicate that *P. syringae*, due to its nucleation properties, has a behaviour similar to that of INPs_{0.8}, which means it can be rapidly removed by precipitating clouds and re-injected in the atmosphere with high wind speed. It is interesting to compare the concentrations of

P. syringae at Jungfrauoch (2 to 45 CFU L⁻¹) with those reported for other precipitation samples collected at lower altitude between 25 and 2200 m a.s.l. (Monteil et al., 2014), where the abundance of culturable *P. syringae* ranged from 10² to 10⁶ CFU L⁻¹. Two processes can contemporarily explain this, both confirming the behaviour of *P. syringae* as INP, that is to say its possibility to be efficiently removed by precipitation. The first is that this ice nucleating bacterium is rapidly activated and lost as a cloud progressively ascend and cools down, which justifies this sort of “altitudinal gradient”. The second is that the measurement made in-cloud at Jungfrauoch may be more representative of the in-cloud abundance of *P. syringae*, with an enrichment observed at lower altitudes due to the passive scrubbing of locally airborne cells as precipitation falls down.

The results presented here confirm that the troposphere appears as a generally constant reservoir of airborne (Bowers et al., 2009) and dominantly living bacteria, with peak injections under high wind speed conditions. The arrival of air masses from southern Europe including desert dust represents the best conditions for finding several bacteria at cloud height in the Alps. The overall persistence of bacteria within precipitating air masses seems to be only moderately affected by the development of precipitation.

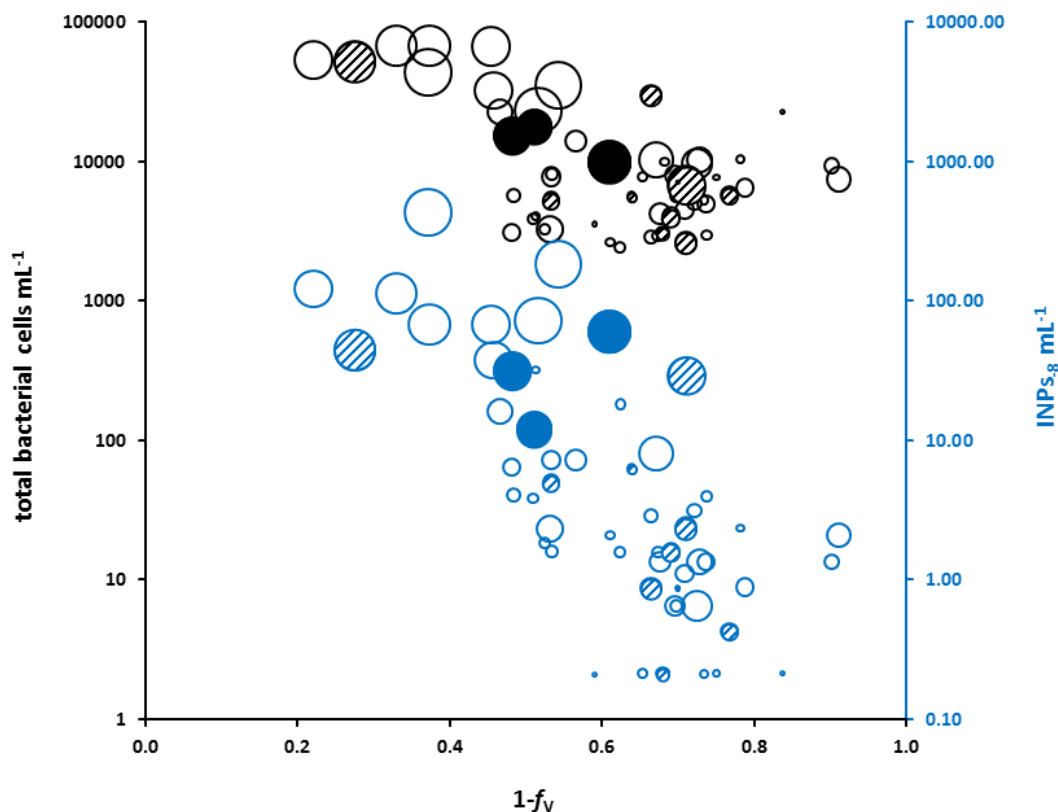


Figure 5.3 Number of total bacteria per mL of precipitation (in black) and INPs₈ mL⁻¹ (in blue) compared to the fraction of precipitation lost from a cloud $1-f_v$. Only samples where both the total number of cells and INPs₈ were available are presented in the graph, to facilitate the comparison. The width of the bubbles is proportional to wind speed. Patterned bubbles represent samples where it was looked for *P. syringae*, while filled bubbles are the 3 samples where *P. syringae* was successfully isolated.

5.3.3 Behaviour of INPs₈ compared to bacterial cells

The correlation between bacterial cells and INPs₈ merits attention, specifically in the frame of the ongoing research on the nature and abundance of airborne INPs of biological origin. INPs₈ are efficiently and rapidly removed by precipitating clouds (Stopelli et al., 2015), and their numbers declined much more rapidly with increasing amounts of water vapour lost from a cloud than the total number of bacteria (fig. 5.3). This leads to the further hypothesis that INPs₈ have a shorter residence time in the atmosphere compared to bacterial cells, that is to say a shorter range of dispersal.

The ratio INPs₈ cell⁻¹ confirms that INPs₈ are more rapidly removed than bacterial cells by precipitation (fig. 5.4). Still, looking with deeper detail at the data, it is possible to derive more information on the role of wind speed as parameter related to large abundance of INPs₈ (Stopelli et al., 2016) as well as associated to injections of bacterial cells.

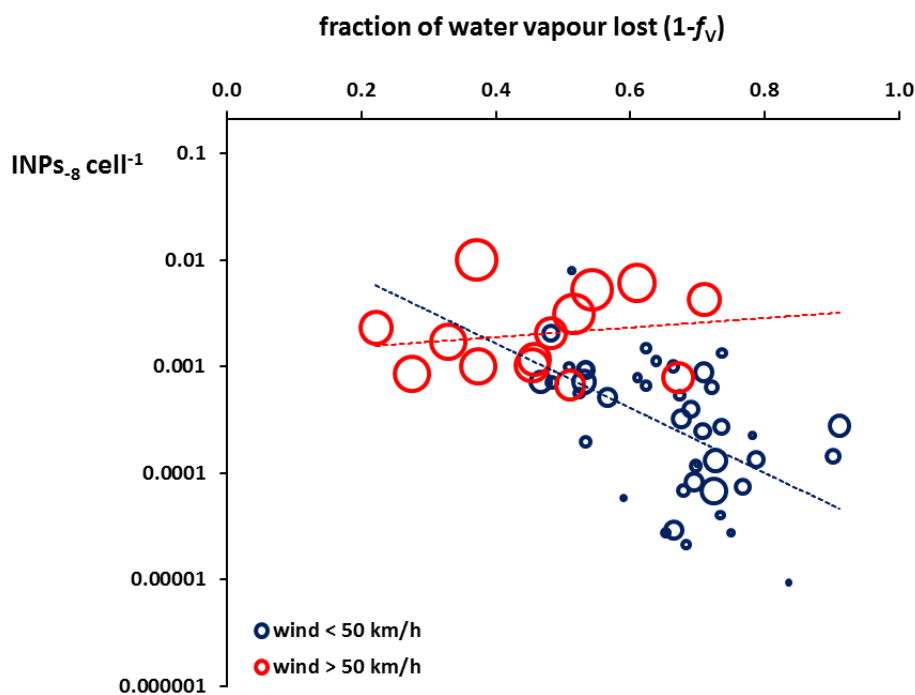


Figure 5.4 INPs₈ are removed faster than bacterial cells by precipitation, bubble width is proportional to wind speed. At wind speed larger than 50 km h⁻¹ (red bubbles) the refill of INPs₈ aerosolised from more local sources can superimpose on the preferential removal of INPs₈ to bacteria.

At high wind speeds (>50 km h⁻¹) numbers of INPs₈ were 10⁻² to 10⁻³ times the number of bacterial cells in precipitation, independently from the prior amount of precipitation lost from the air mass (red circles). At lower wind speeds, the number of INPs₈ decreased much more rapidly than the number of bacterial cells (the ratio INPs₈ cell⁻¹ decreased with increasing f_v). We could interpret this in the following way. High wind speeds at JFJ are associated with high wind speeds in source regions upwind, leading to the aerosolisation of both INPs and bacterial cells. The atmospheric lifetime of bacterial cells is longer than that of INPs₈, hence their background number is relatively large and is not changed much by the additional cells aerosolised upwind of JFJ. The much shorter

atmospheric lifetime of INPs₈ means that their number changes more substantially by the injection of new particles upwind of JFJ (air is re-charged in INPs more than in bacterial cells). Consequently, at high wind speeds our observations are more influenced by local sources, like the Po valley and the Swiss Plateau: they can either act as refill of INPs₈ into clouds with large prior precipitation (red bubbles with larger $1-f_v$ values) or constitute the injection of new INPs₈ into air masses poor of INPs₈ coming from the desert (red bubbles with smaller $1-f_v$ values) (Conen et al., 2015). At lower wind speeds, there is little recent influence of local sources and we see more clearly the effect of a preferential washout of INPs relative to bacterial cells. This washout needs to occur over a larger distance to manifest itself (over a range of f_v from 0.45 to 0.9).

5.3.4 Role of bacterial cells in precipitation

The further step was to compare the potential number of INPs derived from intact bacterial cells (either living or dead, since the viability of the cell itself is not determinant for the preservation of the activity of INPs, Möhler et al., 2007) with the number of INPs₈. Based on the data available in literature (Joly et al., 2014; Xia et al., 2012) we considered a range of 1 out of 10^5 - 10^4 total bacterial cells in the atmosphere is ice nucleation active to calculate the INPs derived from bacterial cells for all the samples collected in 2013 and 2014. Such interval fits well also to the parallel observations that 1 % to 10 % of culturable bacterial colonies are ice nucleation active (Joly et al., 2014; Šantl-Temkiv et al., 2015) but that on average only around 1 % of total cells is culturable. This number was compared with the number of INPs₈ mL⁻¹ effectively measured in precipitation (Stopelli et al., 2016). Under these two scenarios, bacterial cells are on average potentially responsible for 1.5 % or 15 % respectively of all the ice nucleation activity measured at -8 °C (10th percentile = 0.3 % - 3 %, 90th percentile = 21.3 % - 100 %). The highest potential contributions of ice nucleating bacterial cells to INPs₈ were registered during the precipitation events in March/April 2013 or summer 2014, when the abundance of INPs₈ was anyway below 40 mL⁻¹ (corresponding to around 10 INPs₈ m⁻³ of air considering a cloud liquid content of 0.25 mL m⁻³) (fig. 5.5).

When present in a sample, the percentage of colonies of *P. syringae* showing ice nucleating activity at -8 °C was 100 %, 50 % and 62 %, respectively. In laboratory pure colonies were showing activities between -2.2 and -4.9 °C. The precipitation samples where it was present were characterised by a generally higher onset temperature for freezing, between -5 and -5.5 °C, indicating a lower degree of processing of INPs. We also speculated which fraction of INPs₈ could be due to culturable *P. syringae* in the 3 samples where it was present, assuming that 62 % of the cells is always presenting ice nucleating activity. The best possibility for culturable ice nucleation active *P. syringae* is to cover just around 0.05 % of INPs₈ concentrations observed at Jungfraujoch.

All these results seem to indicate that intact bacterial cells make up a part of the whole number of INPs₈ but they cannot solely account for the whole richness of INPs₈ present in a precipitation sample, particularly when their abundance has a chance for originating the ice phase in clouds. As a consequence, macromolecules generated from living organisms, dead fractions of ice nucleation active cells and organic matter as a whole present on airborne particles must be regarded with primary interest as co-responsible for ice nucleation activity at moderate supercooling.

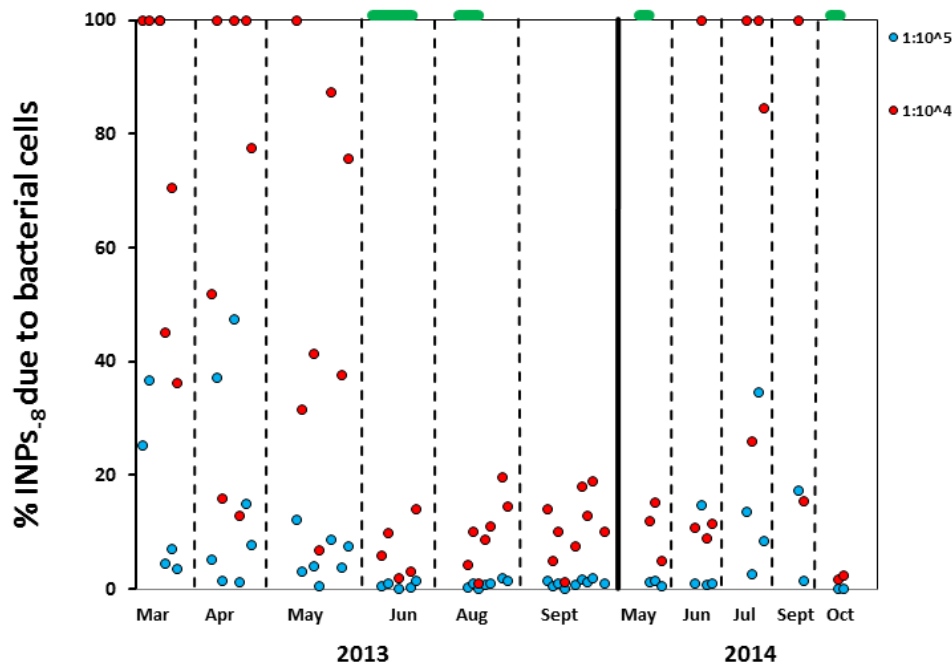


Figure 5.5 Potential relative abundance of INPs from bacterial cells to the total number of INPs₈ measured in precipitation cells, under the assumption that 1 cell out of 10⁵ (blue dots) or that 1 cell out of 10⁴ (red dots) is ice nucleation active. Green bars above the graph indicate when INPs₈ were more than 40 mL⁻¹ (more than 10 m⁻³ of air with a median value of 0.25 mL of precipitation per m³ of air; Stopelli et al., 2015)

5.4 Conclusions

The abundance of bacterial cells in precipitation samples collected at Jungfraujoch ranges between $2.4 \cdot 10^3$ and $6.8 \cdot 10^4$ cells mL⁻¹, on average the majority of bacteria is living and the ice nucleating bacterium *P. syringae* has been successfully isolated also at high altitude. Wind speeds larger than 50 km h⁻¹ promote an increase of bacteria reaching the station along with particles of similar size. Bacterial cells are not particularly sensitive to the amount of precipitation lost from an air mass prior to sampling.

Coherently, we observed a preferential removal of INPs₈ compared to bacterial cells by precipitation. This provides important information on the different dispersal potential in the atmosphere of INPs₈ and bacteria, which must be considered in modelling studies. Bacteria can persist longer in clouds, which favours more constant concentrations and transport over a longer scale. On the contrary, INPs₈ seem to have a precipitation-limited residence time, which reduces their length scale of dispersion in the atmosphere. Furthermore, thanks to these observations we interpret high wind speed as factor promoting the release of bacteria and INPs₈ from sources upwind to Jungfraujoch, compensating the removal of INPs₈ by precipitation.

Bacterial cells can account for just a part of the whole number of INPs₈ observed in precipitation. Therefore, the majority of airborne INPs₈ can be due to fragments of cells and macromolecules, either freely floating or attached to mineral dust and soil particles. The abundance of such

fragments and macromolecules in the environment has been neither intensively studied nor modelled so far and can multiply the chance for INPs.₈ to impact precipitation.

5.5 Supplementary material

5.5.1 INPs.₈ and progressive heating/filtration

The 15 samples collected during 2014 were subjected to progressive heating (10' in water bath at 40 °C and 80 °C) and filtration (5 µm, 1.2 µm, 0.22 µm meshes cellulose acetate sterile filters) and subsequently analysed for the residual activity of INPs.₈, in order to obtain more hints on the complexity of biological INPs.₈ present in precipitation. 5 out of 15 of these samples contained less than 1.5 INPs.₈ mL⁻¹ and were not considered in the following calculations, since the error on the estimation of the fractions sensitive to heating or filtration would be too large, due to the small number of tubes which effectively froze during our assays.

Given the delicate nature of INPs.₈ in solution and the interactions between organic material and mineral dust, such treatments may have introduced some modifications in the samples analysed, like creating aggregates or promoting the release in solution of INPs. Within this caveat, we believe such approach merits further attention and insights, since it provides useful indications on the nature of airborne INPs.

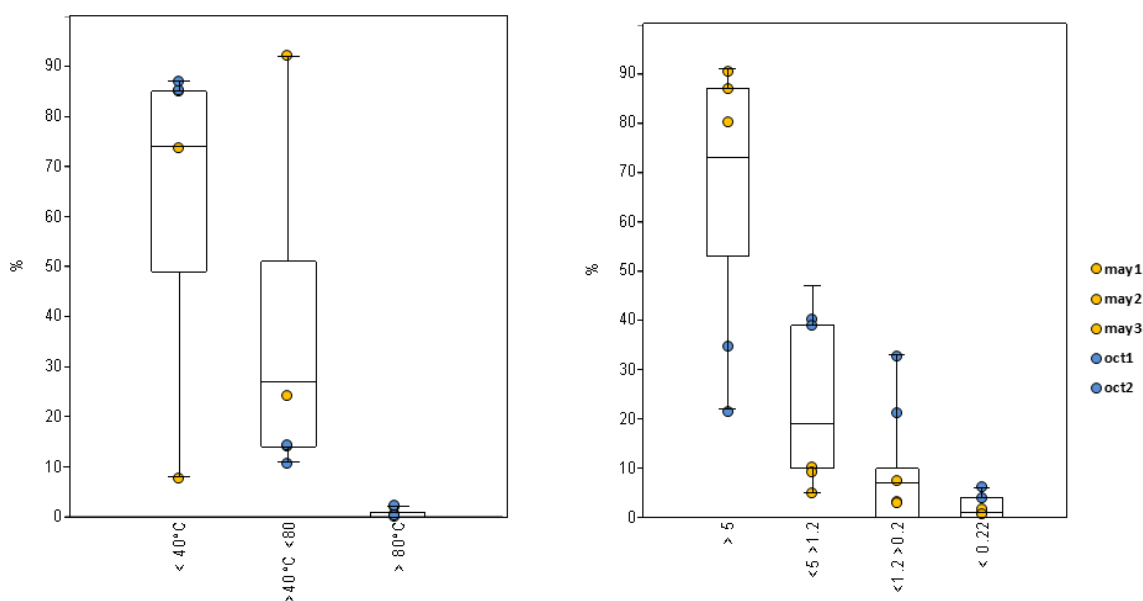


Figure 5S.1 Boxplots representing the loss of INPs.₈ due to thermal treatment (left panel, 10' in water bath at 40 °C and 80 °C) and filtration through progressively smaller meshes (right panel, 5 µm, 1.2 µm, 0.22 µm meshes), n=10. Dots representing specific values for a Sahara dust event (yellow) and for a storm from Northern Europe (blue) are overlapped.

5.5.2 Heat sensitivity of INPs._g

The results from progressive heating (figure 5S.1, left panel) clearly showed that more than 98 % of INPs._g was denatured at 80 °C, suggesting that INPs._g are of biological origin and based on molecular structures which get denatured at such temperature. The remaining 2 % can be considered to be expression either of other classes of biological INPs, like more heat-resistant molecules from pollen or fungi, or of mineral dust (Pummer et al., 2015).

More interestingly, around 73 % of INPs._g was on average lost already after heating at 40 °C for 10'. This aspect has a main strong implication: it seems that a large part of biological activity is due to proteins or glycoproteins which can be easily denatured, resembling those observed both for bacterial membranes and for the macromolecules produced by some fungal species (Pummer et al., 2015). The samples coming from air masses from Southern Europe containing desert dust and those from Northern Europe showed no significant differences in terms of susceptibility to temperature. This can indicate that several classes of biological INPs may be released from the same source region or close ones and progressively mixed during transportation, so that the final freezing spectra show similar temperature sensitivity.

5.5.3 Potential forms of aggregation of INPs._g

Some difference between Northern and Southern sources of air masses can be found in the dimensional composition of INPs._g. More than 80 % of INPs._g coming from air masses containing Sahara dust is bigger than 5 µm (coherently with Chuvochina et al., 2011), whereas from North Atlantic the dimensional fingerprint is more mixed and dominated by smaller fractions, mirroring the scarcity of coarse dust or soil particles (fig. 5S.1, right panel and fig. 5S.2). In the whole set of 10 samples analysed for the size distribution of INPs, 73 % of activity is due to particles or clumps of particles with an average diameter larger than 5 µm. The rest of activity (fraction < 5 µm) can be due either to fungal spores or bacterial cells or ice nucleation active macromolecules, freely floating or attached to fine mineral fractions.

This information on observed size distributions of INPs in environmental samples is just seminal, but can lead to important implications for assessing the role of biological aerosols on atmospheric processes. Firstly, modelling studies where INPs from biological origin are simulated should consider not only the release of single airborne cells, but also of macromolecules and clumps of biological films around mineral and soil particles of different sizes. Secondly, studies on the scavenging of biological aerosols through wash-out and rain-out processes should take into account of such aggregations of materials. Finally, sampling techniques based on cut-offs of particles of a certain diameter, i.e. analysis of particles smaller than 1 or 2 µm, may strongly underestimate the effective abundance of biological INPs in the air.

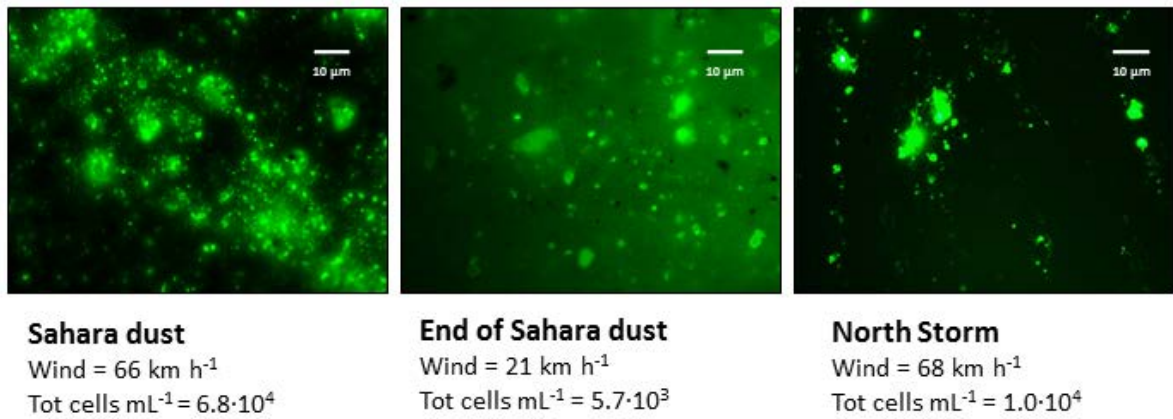


Figure 5S.2 Picture of precipitation samples, analysed with epifluorescence microscopy and SYBR green staining. They show the complexity of airborne biological material: bacterial cells may be either freely floating or associated to soil and mineral particles. Biofilms are also present. In the pictures it is possible to observe the decrease of bacterial abundance from the arrival of an air mass containing Sahara dust and its progressive extinction.

Clues that decaying leaves enrich Arctic air with ice nucleating particles

This chapter has been published as short communication:

Conen, F.¹, Stopelli, E.¹, and Zimmermann, L.¹: Clues that decaying leaves enrich Arctic air with ice nucleating particles, *Atmospheric Environment*, 129, 91–94, doi.org/doi:10.1016/j.atmosenv.2016.01.027, 2016.

¹ Environmental Geosciences, University of Basel, CH-4056 Basel, CH

Abstract

Decaying leaves from Arctic regions have previously been reported to produce large numbers of ice nucleating particles (IN). Their atmospheric relevance is unclear. Our initial observations at a coastal mountain observatory in northern Norway reveal a tripling in concentrations of IN active at $-15\text{ }^{\circ}\text{C}$ (IN_{-15}) in oceanic air after about one day of passage over land (from 1.7 and 4.9 $\text{IN}_{-15}\text{ m}^{-3}$, to 9.6 and 12.2 $\text{IN}_{-15}\text{ m}^{-3}$). Analysis of leaf litter collected near the observatory supports the earlier report of numerous IN associated with leaf litter on the ground ($2 \cdot 10^2\text{ IN}_{-15}\text{ }\mu\text{g}^{-1}$ litter particles $< 5\text{ }\mu\text{m}$). Together, both findings suggest that decaying leaves are a strong emission source of IN to the Arctic boundary layer.

6.1 Introduction

Ice nucleating particles (IN) enable the formation of ice in clouds warmer than $-36\text{ }^{\circ}\text{C}$. Concentrations of IN vary by orders of magnitude in time and space. In the Arctic, IN are rarer than in most other places. Reported concentrations of IN active at $-15\text{ }^{\circ}\text{C}$ (IN_{-15}) are around 1 m^{-3} winter and 10 m^{-3} in summer (Bigg, 1996; Bigg and Leck, 2001). The Arctic summer values are two orders of magnitude smaller than what is typically found over a much wider geographic range (DeMott et al., 2010). As a consequence, removal of water from the Arctic atmosphere through ice growth and precipitation is IN-limited (Prenni et al., 2007). This limitation contributes to the persistence of optically thin low-level clouds that cause surface warming in summer (Tjernström et al., 2014).

Marine biological material aerosolized by breaking waves and bubble bursting is commonly considered a source of IN in the Arctic boundary layer (Bigg, 1996; Bigg and Leck, 2001; Schnell and Vali, 1975; Wilson et al. 2015). Biological particles emitted from Arctic land surfaces are rarely considered, although Schnell and Vali (1973) had found that a large number of IN can be obtained from well decayed leaves of Arctic origin when they are suspended in water. The same authors demonstrated in a later experiment, with an enclosure placed above plant litters, that such IN become airborne (Schnell and Vali, 1976). Leaf-derived IN are produced by bacteria and saprophytic fungi, are of subcellular size ($< 0.2\text{ }\mu\text{m}$), and lose their activity when heated above $60\text{ }^{\circ}\text{C}$ (Fröhlich et al., 2015; Pummer et al., 2015; Schnell and Vali, 1972; Schnell and Vali, 1973; Vali et al., 1976). Frequent freeze-thaw cycles positively select for microorganisms that produce ice nucleating proteins (Wilson et al., 2012). Hence, their relative abundance in the Arctic is larger than in milder climate zones (Schnell and Vali, 1973). Contributions of marine and land surface sources to the concentration of IN in air depend on the duration of previous contact with each kind of surface and on the extent of aerosolization of IN within the boundary layer. Here we report on initial observations of atmospheric IN at a coastal site in northern Norway during days with little and greater land contact of sampled air masses, in order to evaluate whether air is noticeably enriched in IN through contact with vegetated land.

6.2 Material and methods

Atmospheric IN were collected between 02. and 06. July 2015 at Halde observatory (Finnmark county, $69^{\circ}55'45''\text{ N}$, $22^{\circ}48'30''\text{ E}$, 905 m a.s.l.). The observatory was established by Kristian Birkeland in 1899 to study polar lights (Birkeland, 1908). From 1918 to 1926 Hilding Köhler stayed there to study cloud droplet formation (Köhler, 1937). It is situated on the top of a natural pyramid of rocks, 150 m above other rocks at a horizontal distance of 500 m . A portable PM_{10} sampler (PQ100, BGI, Mesa Labs Inc., Butler, NJ, USA) was installed with its inlet 2 m above the observatory tower. We sampled four times for a period of 24 hours airborne particles on quartz-fiber filters (Pallflex® Tissuequartz, effective diameter 38 mm , Pall Corporation, Port Washington, NY, USA). The sampled air volume was 24 m^3 per filter at ambient conditions. Filters were analyzed at our laboratory in Basel following the method described in Conen et al. (2012).

Further, we collected a litter sample ($5 \times 2\text{ g}$, bulked) from the surface of a melting snowfield about 300 m below, 2 km East-northeast of the observatory. Litter had been transported from the surroundings by wind and accumulated in the more sheltered location where snow was still present

in July. The litter consisted of entire leaves and large fragments thereof, mainly from *Betula nana* and various grasses. Although they showed signs of decay to various degrees, their main structure was clearly discernible. We do not think this litter was any different from litter on snow-free surfaces. But, it was definitively easier to collect it there, than from other surfaces. At the laboratory we air dried it over night (23 °C), then gently moved it by hand over a sieve (63 µm) to separate small, loose particles. Total nitrogen (N) content was determined with an elemental analyser (model CN628, LECO Corporation, St. Joseph, MI, USA). Particles < 63 µm had a N content of 1.1 %, similar to that of larger recognizable leaves in the sample (1.4 % N) and very different from soil particles < 63 µm collected in the region (0.1 % N). We suspended 0.05 g of litter particles < 63 µm in 15 ml 0.1 % NaCl solution. The suspension was passed through a 5 µm mesh filter (sterile cellulose acetate syringe filters, Sterlitech Corporation, Kent, WA, USA), diluted and analyzed on a droplet freezing apparatus (Stopelli et al., 2014). Additionally, a subsample was heated for 10 minutes to 80 °C and another subsample passed through a 0.20 µm filter (same type and supplier as 5 µm filter) and analyzed for IN concentrations. The mass concentration of particles < 5 µm in the suspension was determined gravimetrically.

6.3. Results and discussion

Number concentrations of IN₁₅ in air above Halde observatory ranged from 1.7 to 12.2 m⁻³ (Table 6.1). The warmest temperature at which we observed freezing was -8 °C. At -10 °C we found an average of 0.6 IN m⁻³, an order of magnitude less than at -15 °C. Bigg (1996) and Bigg and Leck (2001) had observed about 2-3 times larger concentrations of IN₁₅ during summer at sea level further north. Differences between ice nucleation measurement techniques can be large (Hiranuma et al., 2015). But, smaller values measured at Halde might also be due to its greater elevation by 900 m and the fact that IN get activated in rising air from which they are efficiently removed by precipitation, which results in reduced IN concentrations at elevated sites (Conen et al., 2015; Stopelli et al., 2015).

Table 6.1 Numbers of ice nucleating particles (IN m⁻³) observed in the atmosphere above Halde observatory. Blank values are subtracted and numbers are adjusted to sea-level pressure. Blank values were on average 12 % of gross values. Ice nucleating particles found in the litter sample are indicated per unit mass of litter particles < 5 µm.

Temperature (°C)	-7	-8	-9	-10	-11	-12	-13	-14	-15
Date	IN (m ⁻³)								
02./03.07.15	0.0	0.3	0.6	1.3	1.6	2.6	4.1	7.2	12.2
04.07.15	0.0	0.2	0.2	0.2	0.4	0.8	1.3	2.0	4.9
05.07.15	0.0	0.0	0.0	-0.1	0.1	0.0	0.2	0.8	1.7
06.07.15	0.0	0.2	0.2	0.9	1.2	1.8	2.2	5.5	9.6
	IN (µg ⁻¹ particles < 5 µm)								
Litter	14	15	17	19	27	48	99	141	186

Sampled air masses had approached at low altitude (< 500 m a.s.l.) from the Arctic Ocean. Two-day back trajectories cover ocean surface between Spitsbergen and northern Norway and include shorter and longer passages over land before arrival at the observatory. On two days, air arrived almost directly from the sea, with land contact limited to a few hours before arrival (Figure 6.1b, 6.1c). Associated concentrations of IN_{-15} (4.9 and 1.7 m^{-3}) were similar to a recent estimate for surface level IN_{-15} of marine origin in the fetch region (1.2 to $2.4 \text{ IN}_{-15} \text{ m}^{-3}$; Figure 4a in Wilson et al., 2015). On the other two days, back trajectories indicate average land contact durations of around 30 hours (Figure 6.1a) and 15 hours (Figure 6.1d) prior to arrival at Halde. Prolonged land contact on average tripled concentrations of IN_{-15} (12.2 and 9.6 m^{-3}) compared to the two days with almost direct approach from the ocean. This observation suggests a substantial IN source at the land surface. Bigg (1996) had seen a similar rise in IN_{-15} concentration (from 4 to above $20 \text{ IN}_{-15} \text{ m}^{-3}$) during rapid advection of air from the Kola Peninsula to the central Arctic Ocean, presuming an industrial source of the additional IN. The closest major industrial air polluter to Halde observatory is the nickel smelter in Nikel, Russia, 290 km to the East-southeast (69.5°N , 30.2°E) and well outside the area covered by the back trajectories shown in Figure 6.1. Therefore, IN emitted from land surfaces in the region are probably not of industrial origin.

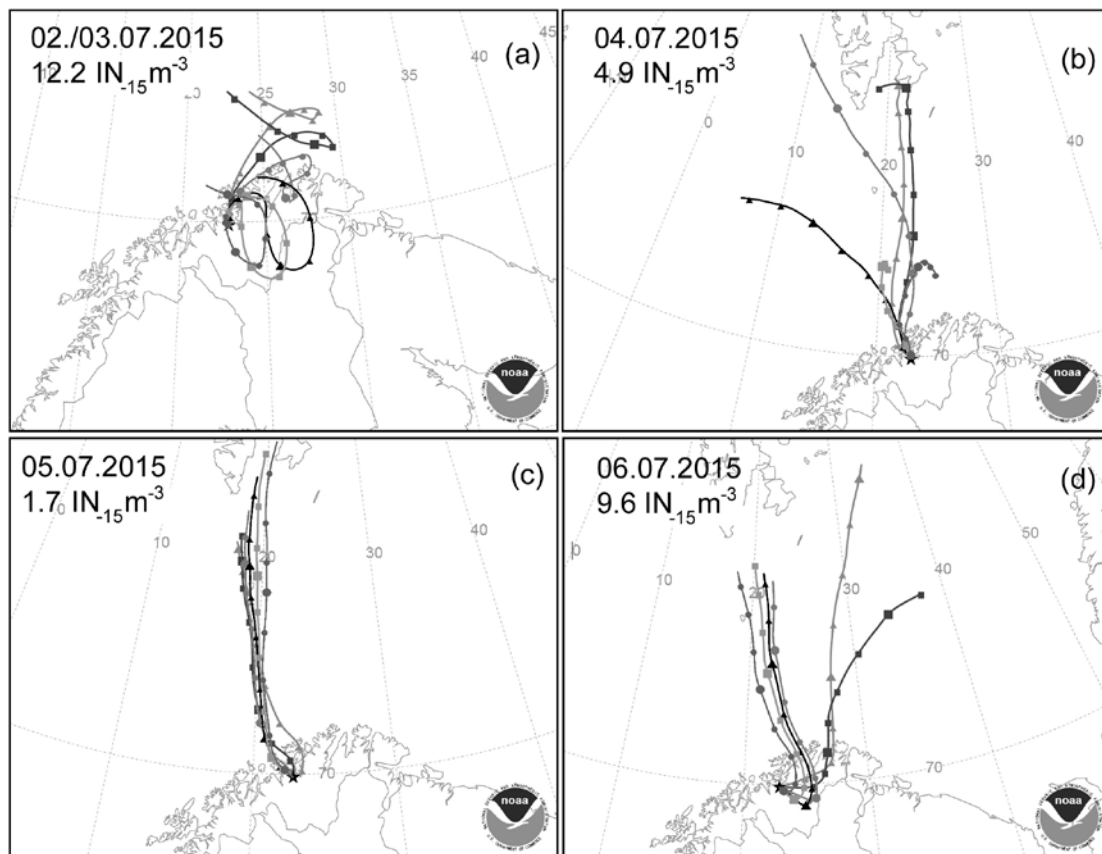


Figure 6.1 Back trajectories starting at Halde observatory every four hours during a 24-hour period of sampling aerosol on quartz-fiber filters (HYSPLIT Trajectory Model, NOAA, <http://ready.arl.noaa.gov/HYSPLIT.php>; 48-hour trajectories; markers every 6 hours; starting height 200 m above ground level). Sampling date and number of ice nucleating particles active at -15°C ($IN_{-15} \text{ m}^{-3}$) associated with each of the four 24-hour samples are shown in the panels.

6.4 Acknowledgements

Likely the most important source of IN₁₅ on Arctic land are microorganisms thriving on decaying leaves. The litter sample we had collected from the snow field below the observatory contained $2 \cdot 10^2$ IN₁₅ μg^{-1} particles $< 5 \mu\text{m}$. Heating to 80 °C deactivated at least 90 % of the IN active at -12 °C or warmer, and 70 % of IN₁₅. Heat resistant IN₁₅ could have been mineral particles, but also thermally more stable biological IN, such as rust spores or macromolecules released by birch pollen (Morris et al., 2013a; Pummer et al., 2012; Pummer et al., 2015). Hence, the fraction of biological IN₁₅ in our litter sample must have been between 70 and 100 %.

Results of our short visit to Halde observatory suggest that decaying leaves are a strong emission source of IN to the Arctic boundary layer over land. Leaf-derived IN were discovered in the 1970s, but little direct evidence for their atmospheric relevance has since been produced. Atmospheric research seems to have overlooked a biological source that could play a growingly important role in the Arctic environment. Climatic change is more rapid in the Arctic than elsewhere (Anisimov et al., 2007). Duration of snow cover in summer decreases and vegetation becomes more productive (Callaghan et al., 2011). Arctic greening increases the production of leaf litter, and probably of leaf-derived IN. The shorter duration of snow cover extends the time when such IN can be aerosolized. A judgement on whether a growing source of IN on Arctic land has the potential to affect regional cloud properties requires more data of the kind presented here. Further, it will be necessary to characterise in more detail IN caught on filter and to see whether numbers of atmospheric IN increase with the fall of leaves in autumn.

6.4 Acknowledgements

We very much thank Alta kommune, in particular Tor Helge Reinsnes Moen, for maintaining Halde observatory and for having given us access to it. Our travel was funded by the Swiss National Science Foundation (SNF) through grant no. 200021_140228. Calculations and plots of back trajectories were provided by the Air Resources Laboratory at NOAA through the HYSPLIT-WEB (internet based) resource. We are grateful to three anonymous reviewers for valuable comments that have greatly improved this short communication.

Conclusions and Outlooks

7.1 Conclusions

A total of 16 sampling campaigns have been carried out at the High Altitude Research Station Jungfraujoch to study the abundance and variability of INPs of biological origin in precipitation samples. Falling snow has been collected and analysed directly in the field with the new immersion freezing apparatus LINDA for the content of INPs active at moderate supercooling. Several meteorological and environmental parameters have been studied in association with the precipitation samples to define the best conditions to expect large abundance of INPs active at -8 °C. All these activities allowed us to fulfil all the major goals set by the research project:

- ✓ The abundance and variability of INPs active at moderate supercooling have been determined. Specifically, INPs active at -8 °C show measurable values from 0.21 up to 434 INPs₈ mL⁻¹ of precipitation. Large variability occurs not only over the year, but also within the same precipitation event;
- ✓ With three multiple linear regression models it was possible to describe up to 75 % of the observed variability in INPs₈ collected in precipitation at Jungfraujoch. All these models indicate that the variability of INPs₈ is determined by the coexistence of “source” and “sink” processes. Such drivers are best represented by wind speed, which is related to the potential for air masses to pick up and transport INPs₈ from several sources, and by the fraction of water vapour lost from an air mass as precipitation prior to sampling. The amount of precipitation lost has been derived by measuring $\delta^{18}\text{O}$ in snow samples and allowed us to demonstrate that INPs active at moderate supercooling are rapidly and selectively removed from clouds by precipitation;
- ✓ Bacterial cells range between $2.4 \cdot 10^3$ and $6.8 \cdot 10^4$ cells mL⁻¹ of precipitation, a narrow range which is coherent with observations done at several places around the world. The majority of

bacterial cells is living. Injections of bacteria are expected for wind speeds exceeding 50 km h^{-1} , while are not so sensitive to the amount of precipitation lost from an air mass prior to sampling. On average, entire bacterial cells can account for 15 % of the whole number of INPs_g, suggesting that cellular fragments and macromolecules, both freely floating and attached to mineral and soil fractions, must be addressed as important airborne INPs_g;

- ✓ *Pseudomonas syringae* has been successfully isolated at high-altitude and is associated with samples presenting large abundance of INPs_g. These findings indicate that, similarly to INP_g, also *P. syringae* may be picked up from infected crops with high wind speed and rapidly removed by precipitating clouds. This complements our understanding of the spreading mechanisms of this plant pathogenic bacterium, implementing the possibility to model, predict and contrast the development of crop diseases;
- ✓ Additionally, a set of observations done in North Norway on airborne INPs indicate that air masses with prolonged contact with land surfaces are enriched in INPs active at moderate supercooling. Still, it has been confirmed that the Arctic is generally characterised by a limited abundance of airborne INPs, despite the reservoir of INPs present in leaf litter. The Arctic is an intriguing “open air laboratory” to study the effect of climate change (warming) and land use change (greening) on the production of biological INPs and on their effect on clouds.

All these findings constitute a significant improvement of our understanding of the abundance, variability and nature of biological INPs in precipitation and point at the potential for biological INPs to impact cloud processes. Firstly, 10 % of precipitation samples contained more than $40 \text{ INPs}_{g} \text{ mL}^{-1}$, potentially corresponding to more than $10 \text{ INPs}_{g} \text{ per m}^3$ of air (with the median observed conversion factor of 0.25 mL of precipitation from 1 m^3 of air). According to the available case studies, a concentration of $10 \text{ INPs}_{g} \text{ m}^{-3}$ of air has been observed through in-cloud measurement as a sufficient number to promote the onset of the ice phase (Crawford et al., 2012; Mason, 1996). Secondly, based on the results of the models employed to describe the variability of INPs_g, it is possible to expand the number of contexts where and when the conditions are favourable for having large numbers of biological INPs. In fact, a coincidence of first precipitation and high wind speed is ideal for expecting a lot of INPs_g. Therefore, sampling effort to study the effect of INPs_g on precipitation should concentrate at the passage of a front, where this coincidence is expected and where the meteorological conditions are also favourable for the onset of precipitation. Thirdly, part of INPs_g can be made of entire ice nucleating bacterial cells, but the majority seems to depend on cellular fragments and molecules, floating or attached to mineral and soil particles of several sizes. This multiplies the nucleating potential of living organisms: from a single ice nucleating cell several INPs can be released as molecules or as cellular fragments once the cell dies. Such information also highlights the necessity to update modelling studies to include these forms of biological INPs. Furthermore, INPs are more efficiently removed by precipitation than bacterial cells. This means that INPs_g have a larger variability, a shorter residence time in the atmosphere and a shorter range of dispersal, while bacterial cells tend to persist longer in the atmosphere and mix over longer distances, which justifies also more constant concentrations. Also these findings sustain the necessity to update modelling studies.

7.2 Outlooks

The findings derived from the thesis open new perspectives for improving top-down approaches to study the relevance of biological INPs. High priority outlooks will be treated with detail in the following paragraphs.

7.2.1 Networking observatories to study the spatial variability of INPs

Results on precipitation collected at Jungfraujoch indicate that a coincidence of first precipitation and high wind speed accounts for large abundance of INPs₈. We can therefore expect an increase in the number of airborne INPs active at warm temperatures at the passage of a front, when an increase in wind speed can promote the release of biological particles which are successively removed by the first precipitation formed along the front. To test such hypothesis and to get better information on the spatial variability of biological INPs a network of observatories making regular measurements must be created. This will allow a more detailed understanding on the evolution of INPs over trajectories followed by air masses and a better connection of the spatial patterns of airborne INPs with the development of precipitation events.

A simple method to connect observatories is to measure INPs on PM₁₀ filters. A project took place in October 2015 to test this approach connecting 3 observatories: Monte Cimone (2165 m a.s.l., IT), Jungfraujoch (3580 m a.s.l., CH) and Puy de Dôme (1465 m a.s.l., FR). Preliminary results are presented in paragraph A1 of Additional Contents.

7.2.2 Shape of the freezing profiles and source region fingerprints

When assessing the role of INPs on climate, it is important to know which particles are dominantly emitted by which source region. This allows not only a better connection between bottom-up and top-down approaches, but also an improved understanding of how climate and land use change can modify the local and global budget of airborne INPs. Such information is difficult to derive in top-down studies, where the mix of INPs present in a sample is the sum of several INPs released from multiple source regions integrated over the trajectory of an air mass.

The shape of the freezing profiles of a precipitation sample could provide important information on the groups of INPs present in it. We can hypothesise that the dominant input of INPs from a specific source region of particles can be detected in the shape of the freezing profiles, with characteristic “peaks” of activity. This is based mainly on the knowledge that INPs of biological origin are dominant at moderate supercooling, followed by more abundant dust, soot, salts which are active at lower temperatures. Each source region may offer a different release of these INPs, therefore a specific fingerprint of peak temperatures of ice nucleation activity.

Some seminal results on a subset of precipitation samples collected at Jungfraujoch are presented in paragraph A3 of Additional Contents.

7.2.3 Approaches to distinguish groups of biological INPs

A further outlook concerns the improvement of the distinction of different groups of biological INPs in an environmental sample. This can help individuating the main organisms responsible for

the airborne biological INPs, studying in which forms biological INPs tend to be present in environmental samples and to predict how their contribution could change according to climate and land-use change.

In the supplementary material of chapter 5 the approach based on the progressive heating and filtration of a sample has been presented and discussed. The treatment with enzymes or chemicals is a good laboratory approach to study the nature of a specific ice nucleating substance. Its application in field is trickier, given the complexity and diversity of biological INPs in an environmental sample. The largest difficulty is to selectively remove the activity of a group of organisms and the INPs they produce just with a single enzyme.

A promising approach appears to be immunostaining of biological INPs. It is based on the addition to a sample of a specific antibody for the ice nucleating molecule and to the further marking of the bound antibody with a staining agent to make it visible. To my knowledge, antibodies exist for the protein produced by *Pseudomonas syringae* and are currently employed to check the mechanisms expression of such protein (Šantl-Temkiv et al., 2016). Knowing more on the structure of ice nucleating molecules produced by species of fungi and plants will allow the development of specific antibodies for these groups of organisms. We can therefore imagine to collect a precipitation or cloud water sample and to add SYBR green to it first to make cells visible. Secondly, a kit of antibodies specific for the ice nucleating molecules produced by different groups of organisms could be added to the sample and labelled with staining agents of different colours. This will allow the detection and distinction of the main groups of organisms responsible for producing the biological INPs in this sample. Their location could be compared with that of cells (stained with SYBR green) to prove if such molecules tend to be attached to cells, or are present as fragments thereof, or are freely released molecules, either floating or attached to soil and dust particles.

7.2.4 Strategies to link biological INPs to the development of precipitation

There is a final open question to treat, which constitutes also one of the most important outlooks of this work. An enhanced release of INPs_g is expected at the passage of a front where also meteorological conditions are favourable to the onset of precipitation. A lot of INPs_g can be found in the first precipitation collected during the frontal passage: how can we demonstrate a link between the presence of INPs_g in the air and then in rainfall with the onset of precipitation? In other words, and more generally, is it possible to conceive a field experiment to ultimately assess which particles are dominantly originating precipitation at the moment of sampling?

A necessary implementation of the top-down field studies is to enrich the portfolio of measurements on INPs and on environmental parameters. First of all, measurement of INPs in precipitation is highly informative, but several processes like the scavenging of INPs, riming, and crystal growth by water vapour deposition can alter the final concentration of INPs in solution. Secondly, more parameters are needed to better constrain the cases where and when INPs of biological origin are reasonably suspected to have impacted precipitation. Thirdly, such datasets could provide valuable information for cloud modellers to describe more in detail the processes occurring in clouds. During the recent meeting MILAF (Microorganisms at the Interface of Land-Atmosphere Feedbacks, EURAC, Bolzano, March 2016) a list of parameters were pointed at as necessary measurements to carry out whenever going for field measurements:

-
- The abundance of INPs both in the air/clouds and in precipitation;
 - The abundance of cloud condensation nuclei CCN;
 - The number of ice crystals and the number of water droplets inside clouds;
 - The vertical development of temperature and relative humidity;
 - The cloud type;
 - The reconstruction of precipitation history of the air mass.

To do that, quite a lot of equipment and skills are needed at the same place at the same time, which can hamper the development of regular measurements at several places observatories to individuate the regions and the circumstances most favourable for biological INPs to impact precipitation. Therefore, a successful strategy could be to rely on a “reduced” set of data for each parameter or “proxies” which can be easily measured. For instance, some strategies can be drawn:

- Further information can be derived from ^{18}O and is the approximate temperature of nucleation of hydrometeors, as described in the paper of Lowenthal et al., 2011. The method is particularly suitable for high-altitude observatories and is based on the comparison of values of $\delta^{18}\text{O}$ in precipitation AND cloud water collected at the same place. Both values are equally impacted by the previous amount of precipitation lost from an air mass and the difference is linked to a difference of temperature between cloud water at the bottom of the cloud (which coincides with the sampling point at the high-altitude observatory) and the temperature at which precipitation dominantly formed. Interestingly, the same article from Lowenthal et al., 2011 provides also an approach to estimate the mass fraction of precipitation originated by riming. It is based on the measurement of the abundance of sulphate both in cloud water and in precipitation. The rimed fraction is obtained dividing sulphate concentration in rimed precipitation with that in cloud droplets, under the assumption that sulphate is found only in aerosols acting as CCN and incorporated in precipitation only by riming. This approach can be used not only to correct the values of $\delta^{18}\text{O}$ in precipitation for riming, but also to correct the data for the concentrations of INPs measured in rain and snow and provide a more precise estimate the abundance of INPs in “pristine” precipitation as it formed. At high-altitude, the measurements of INPs in precipitation can be integrated with the analysis of the abundance of INPs in air masses collected with filters and in cloud water collected with droplet impactors;
- Concerning the temperature and the presence of the ice phase, measurements may be limited to cloud top and cloud bottom values, at least to limit the range of plausible local values inside the cloud. Ideally lidar-radar system should be installed on site to retrieve such parameter. Approximate values may be derived from databases of lidar-radar observations of satellites, with the caveat that the temporal and spatial detail of satellite information may be limited to the resolution of satellite data retrieval and the frequency of their passage over the same areas;
- For low-altitude sites an option is to collect information on the vertical distribution of these parameters with unmanned vehicles like drones equipped with sensors and cameras. An interesting technical challenge is to find light and efficient ways to equip drones with samplers for CCN and INPs, specifically knowing that large volumes of air must be filtered to collect enough INPs of biological origin. Considering that air masses are moving while sampling, even better would be to vertically stack many drones to contemporarily measure the same parameters at several heights. This could be employed for instance to derive a vertical profile of airborne particles and meteorological parameters before, during and after a frontal passage and link such data with measurements on precipitation collected on the ground.

The challenge is now double and equally fascinating: finding smart solutions to easily measure the minimum set of parameters described before (either at low-altitude or high-altitude), and expanding the number of sites and conditions where such measurements can be carried out. This will ultimately allow the detection of the best cases when and where biological INPs directly impact the development of precipitation.

Additional contents

A1 NICE project and airborne INPs

From the 5th to the 12th October 2015 the project NICE (Nucleators of Ice at monte Cimone) took place, thanks to funding for mobility from the European Project ACTRIS (within Horizon 2020 research and innovation program under grant agreement N° 654109). My activity consisted in collecting samples of airborne particles on PM₁₀ filters at observatory of Monte Cimone in Italy (2165 m a.s.l.). Thanks to the support of Angela Marinoni (CNR Bologna, Italy), a portable PM₁₀ sampler (PQ100, BGI, Mesa Labs INC., Butler, NJ, USA) was installed on site, air samples collected daily on quartz fibre filters with an average volume of 24 m³ of air on each filter. The filters were successively brought back to Basel and the content of INPs m⁻³ of air active at -15 °C or warmer temperatures was determined by immersion freezing (fig. A.1). Two blanks were collected by assembling and disassembling a PM₁₀ filter on the sampler, their content of INPs was subtracted to that of the samples. The main scientific objectives of the project were:

- to study the presence of INPs of biological origin at Monte Cimone;
- to test the general validity of the results obtained at Jungfraujoch on the temporal variations of INPs active at warm temperatures;
- to compare the data on the INPs measured at Monte Cimone with those measured at Jungfraujoch (3580 m a.s.l.) and at Puy de Dôme (1465 m a.s.l.) for the same week of observations and relate them with the meteorological conditions over Europe at the beginning of October 2015 (fig. A.2). Monte Cimone constitutes an interesting site to study the emissions of INPs from Northern Italy and the evolution of INPs released in the Mediterranean basin as air masses proceed towards the Alps. Puy de Dôme is an important point to study the evolution of air masses originating on the Atlantic Ocean and proceeding over the European continent.

I would like to thank Stephan Reimann (Empa, Switzerland) and Pierre Amato (Université Blaise Pascal, France) for kindly providing the filters for Jungfrauoch and Puy de Dôme.

The results for the filters collected at Monte Cimone show an increase of airborne INPs between the 6th and the 8th of October (fig. A.3). During those days a front originated over the Atlantic Ocean was passing over Europe and reached Monte Cimone, confirming the hypothesis that the passage of a front represents the best condition to have an enhanced abundance of airborne INPs. Another front reached Monte Cimone on the 10th of October, this time originating precipitation. In this case, no INPs were found on the filter collected during the storm event. This suggests that the determination of airborne INPs by means of PM₁₀ filters necessitates to take into account biases related to days with rain, given that droplets containing INPs may be too large (> 10 µm) to be captured on filters.

The median values of airborne INPs measured at Cimone were furtherly compared with the median values obtained for the filters from Jungfrauoch and with the sole filter available for Puy de Dôme for the week under study. Interestingly, not that much variability in the abundance of INPs is measurable for the 3 stations, despite different geographical position and different altitudes (fig. A.4). This can be explained by some factors:

- The sampling time for the PM₁₀ filters was at least 24 hours. This may have caused the averaging of events of “peak” injections of airborne INPs with more frequent background values, facilitating a larger comparability among sites;
- During the week from the 6th to the 12th of October all Europe was affected by the passage of the same fronts originated on the Atlantic Ocean;

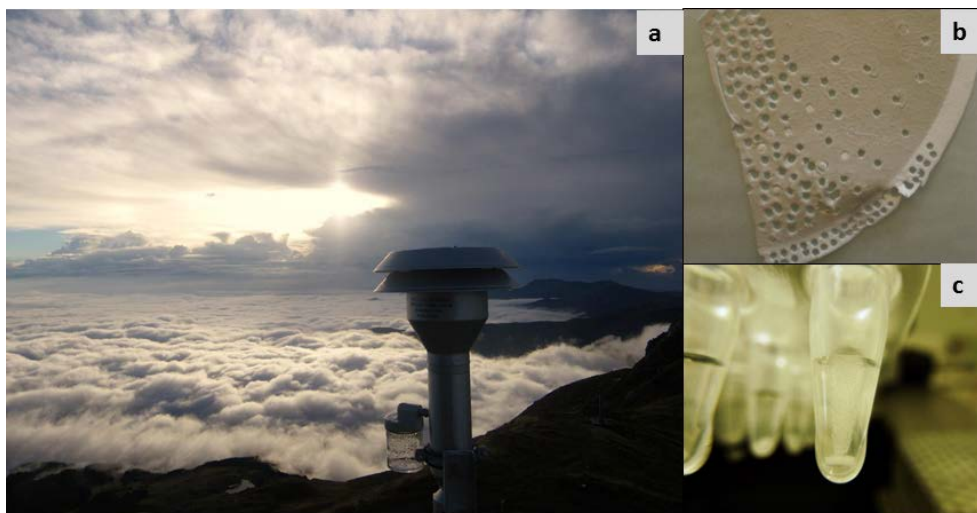


Figure A.1 a) PM₁₀ portable sampler on terrace of the observatory Monte Cimone; b) example of how filters are analysed: small cuts (corresponding to a known volume of air sampled) are taken from the filter and put into 108 x 500 µl Eppendorf safelock tubes containing 100 µl of Milli-Q water each. The tubes are successively immersed into a cooling bath where the temperature is progressively decreased. The freezing of each tube is detected optically (c). The number of the tubes frozen at a certain temperature is subsequently compared to the total number of tubes under analysis, related to the air volume collected on each cut and the concentration of INPs m⁻³ finally calculated (Conen et al, 2012).



Figure A.2 Location of Monte Cimone and the other observatories Jungfrauoch and Puy de Dôme, as network of stations measuring INPs of biological origin on PM₁₀ filters. The frequency of collection of PM₁₀ filters during NICE project is indicated.

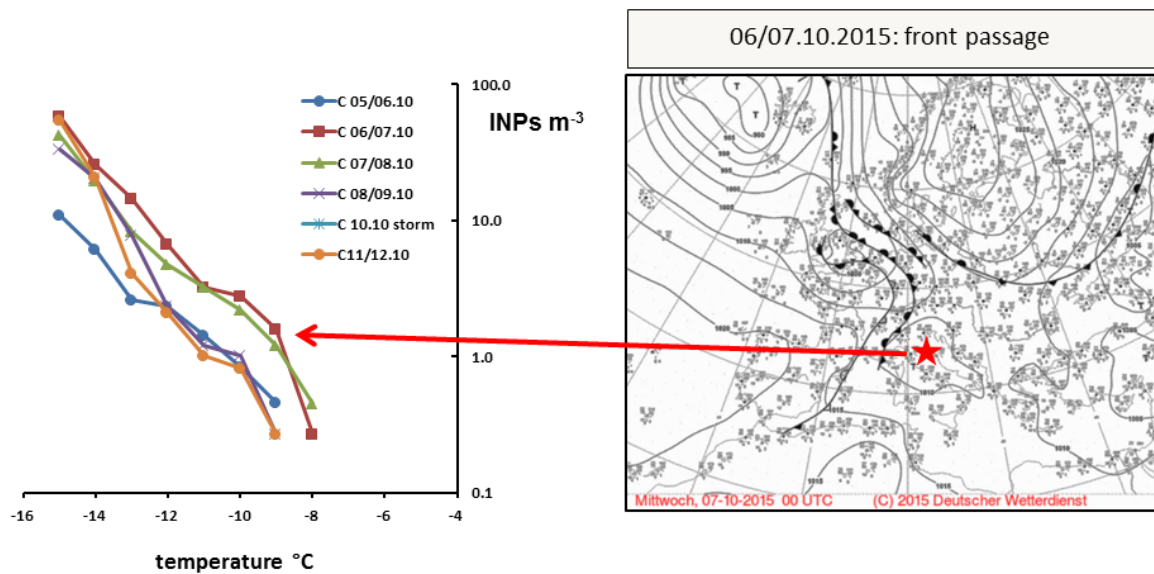


Figure A.3 Results of INPs m⁻³ measured in filters collected at Monte Cimone. The increase of INPs for the filters collected between the 6th and the 8th of October is related to the passage of a front over Europe (weather map available at the site www.wetter3.de).

- Looking for similar meteorological parameters (kindly provided by Angela Marinoni, Pierre Amato and MeteoSchweiz), the 3 observatories presented comparable values of wind speed only, pointing once more at the role of this parameter to explain concentrations of INPs. Furthermore, some rain samples were collected both at Monte Cimone and at Opme, a meteorological station close to Puy de Dôme, and analysed for their stable water isotope composition. Also in this case, for the days where both stations had rain events, water isotopes had a comparable range of values. This can indicate that the air masses coming from the Atlantic had a comparable precipitation development prior to arrival at Monte Cimone and Puy de Dôme.

The results presented here constitute the beginning of an activity of networking observatories to study the spatial variability of INPs of biological origin. Even if seminal, the results confirm what it was hypothesized based on the results from Jungfraujoch: wind speed and stable water isotope are helpful parameters to describe the abundance of INPs, while the passage of a front represents the best conditions to find an increase in the number of airborne INPs. The further development of this network will improve our understanding of the evolution of airborne biological INPs over trajectories followed by air masses both coming from the Atlantic (Puy-Jungfraujoch) and from Sahara desert and the Mediterranean basin (Cimone-Jungfraujoch).

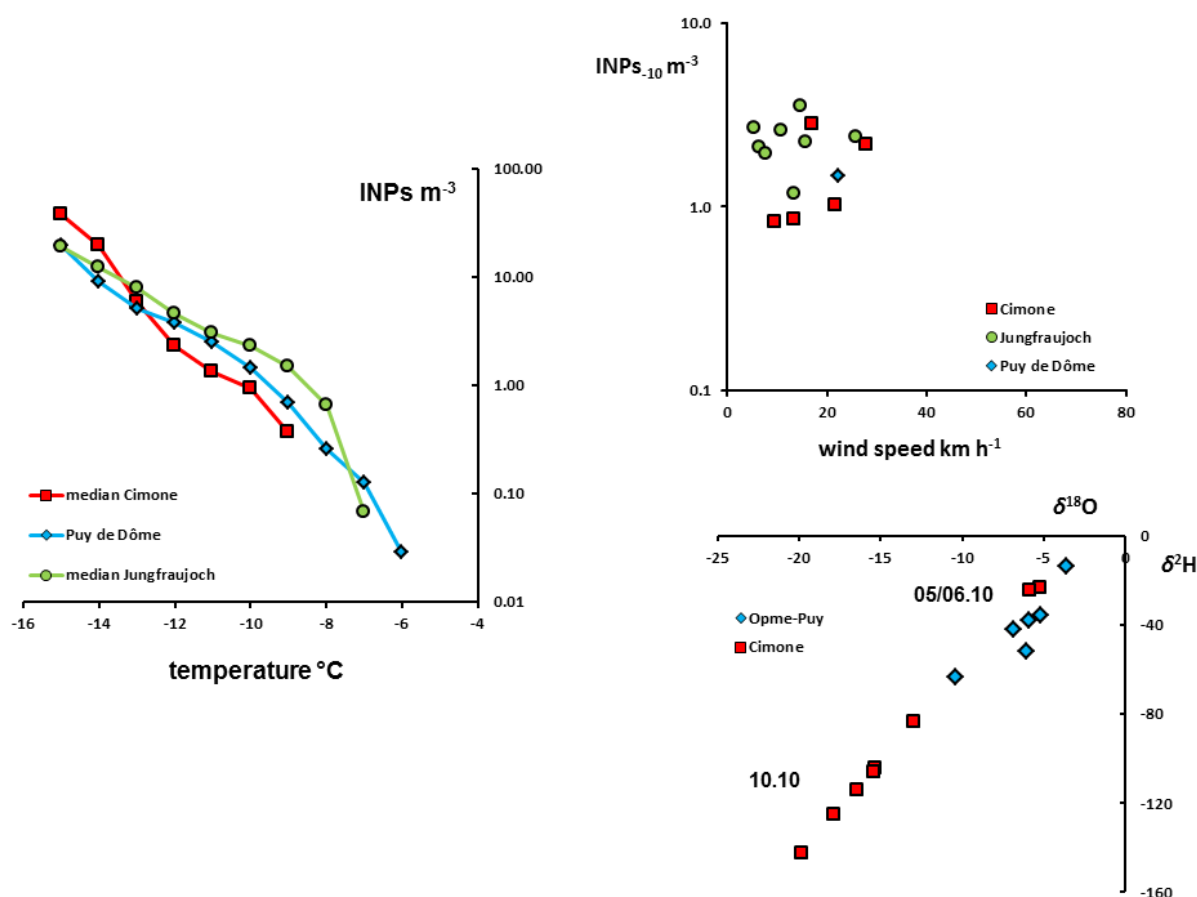


Figure A.4 Comparison of the median values of INPs m^{-3} measured at the 3 observatories Cimone, Jungfraujoch, Puy de Dôme during NICE project (on the left). Parameters presenting a comparable range of values at the 3 sites are represented on the right: wind speed and isotopic values of precipitation.

A2 Rain collection at the station Opme

In September 2015 an automatic rain sampler was installed at the meteorological station of Opme (680 m a.s.l., Central France), close to the observatory Puy de Dôme. The sampler opens automatically at the onset of precipitation and collects all precipitation occurring over a day in a single bottle. Pierre Amato from Université Blaise Pascal, Clermont Ferrand, has been doing the analysis of these precipitation samples for their content in INPs active at moderate supercooling and has been collecting meteorological information for rainy days. In Basel I am proceeding with the analysis of $\delta^{18}\text{O}$ values in these rain samples. The objective of this activity is to create a set of regularly collected data of INPs in precipitation and to study the validity of the results obtained at Jungfraujoch at a different site. Opme is a below-cloud site, therefore it offers a good opportunity to study the potential improvement of modelling INPs from stable water isotopes, specifically to account for the impact of the air column on precipitation samples between their formation in clouds and their collection at the ground level.

A3 Shape of the freezing profiles - first trials

A subset of $n = 13$ samples with potential source area clearly in the Mediterranean basin and $n = 14$ markedly originated from the North Atlantic were chosen to build composite freezing spectra. Given that each sample presented a specific absolute number of INPs, normalisation of the data was operated prior to the comparison of the freezing profiles. To normalise, the number of INPs active at each $1\text{ }^{\circ}\text{C}$ temperature step (i.e. between -7 and $-8\text{ }^{\circ}\text{C}$) was divided by the number of INPs frozen at $-12\text{ }^{\circ}\text{C}$. Potential source areas of the populations of INPs were obtained from the reconstruction of the trajectories of air masses with FLEXPART. The averaged source region plots were produced by Stephan Henne (Empa, Switzerland) and are shown in figure A.5, along with the composite normalised freezing spectra.

Samples from northern Europe have a relative increase of INPs active around $-7/-8\text{ }^{\circ}\text{C}$ and followed by a constant relative abundance of INPs active until $-12\text{ }^{\circ}\text{C}$, while samples from southern Europe present one peak of INPs active at $-8/-9\text{ }^{\circ}\text{C}$ and one at $-12\text{ }^{\circ}\text{C}$. This can be explained by the fact that samples from the Mediterranean basin can contain both biological INPs as well as important quantities of Sahara dust which could act as INPs around $-12\text{ }^{\circ}\text{C}$. Furthermore, the samples coming from South West were mainly collected in summer, those coming from North mainly in all other seasons. This means that seasonality may partly superimpose to the trends observed together with the different source region.

An important caution has to be considered. The freezing profiles have been normalised under the hypothesis that all groups of INPs have an equal chance to be released from a source and are equally removed by precipitating air masses. More measurements must be carried out to validate this assumption, at several sites, covering all the seasons and expanding the spectrum of freezing temperatures under study. It will be particularly interesting to study the shape of freezing profiles also at stations which are closer to sources emitting a dominant type of particles, like close to agricultural areas, urban areas, deserts, forests, on shores close to the ocean. Such more local fingerprints may constitute an important database of source-specific templates to be combined when interpreting freezing profiles measured at faraway sampling points.

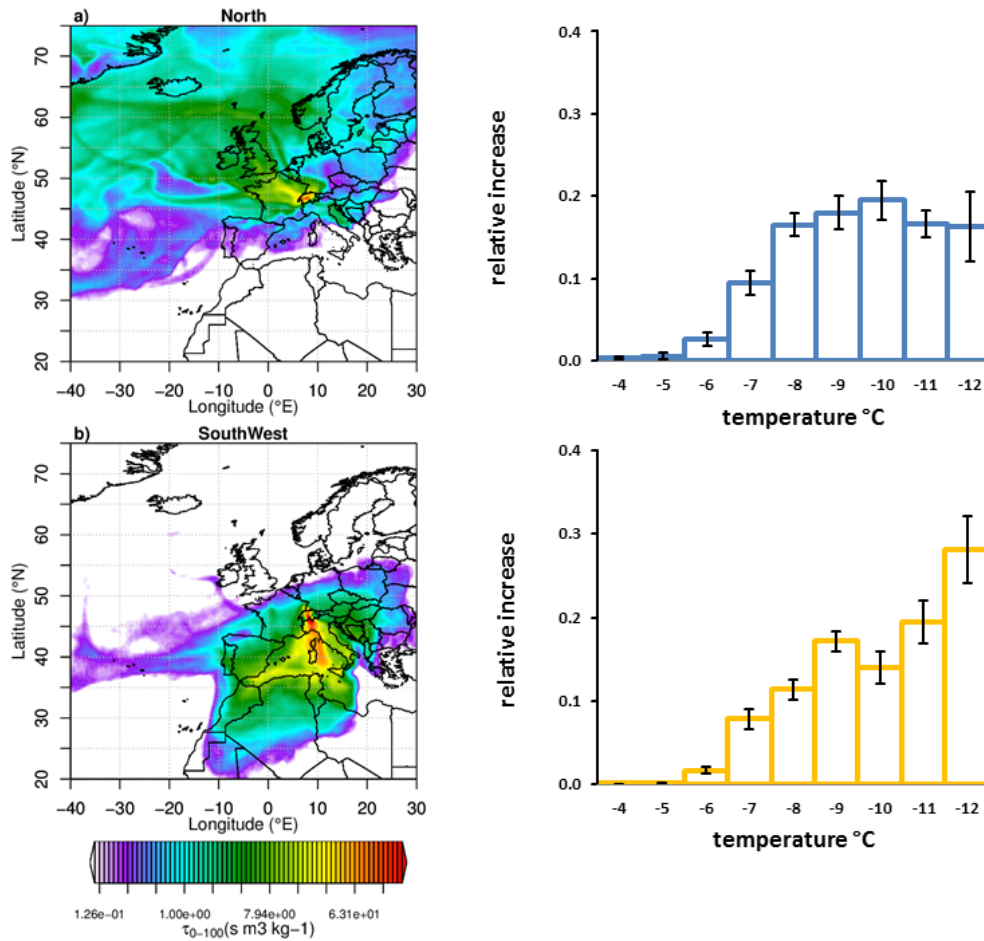


Figure A.5 Composite surface sensitivity plots for 14 samples from North Atlantic and 13 from the Mediterranean basin (left). Their corresponding composite normalised freezing spectra are presented on the right and indicate the relative increase of ice nucleating activity per °C temperature decrease.

A4 Table of data

This table presents a selection of the most important parameters measured in 14 out of 16 sampling campaigns at Jungfraujoch. They are relevant for this thesis and reported in the publications.

f_v represents the fraction of residual water vapour in a precipitating air mass (please refer to chapter 3 for details). Season values correspond to: 1 = winter; 2 = spring; 3 = autumn; 4 = summer. Source region values correspond to: 1 = North Europe; 2 = mixed; 3 = Southern Europe. Values of $N_{>0.5}$ derived from PM_{10} (as explained in paragraph 4.2.2 of the thesis) are reported in red

date of start sampling	start sampling (UTC)	end sampling (UTC)	INP _{s,8} mL ⁻¹	temperature (°C)	$\delta^{18}\text{O}_{\text{SNOW}}$	f_v	wind speed (km h ⁻¹)	precipitation (mm h ⁻¹)	log(N _{5.05} m ⁻³)	season	source region	log(NO _y /CO)	total bacteria mL ⁻¹	% living bacteria
07.12.2012	11.00 h	13.15 h	0.44	-15.0	-32.25	0.07	32.5	2.5	4.66	1	2	-2.50		
07.12.2012	13.20 h	15.30 h	0.22	-16.9	-27.84	0.10	27.8	1.6	4.97	1	2	-2.34		
07.12.2012	15.50 h	17.20 h	0.22	-18.9	-24.48	0.13	26.2	2.2	5.17	1	2	-2.14		
07.12.2012	17.30 h	21.00h	2.11	-20.5	-26.90	0.11	33.9	0.4	5.22	1	1	-2.18		
07.12.2012	22.00 h	05.30 h	0.89	-20.4	-31.47	0.07	37.4	1.5	4.81	1	1	-2.10		
08.12.2012	05.30 h	09.00 h		-20.7	-30.79	0.08	32.7	3.4	5.21	1	1	-1.83		
09.12.2012	17.15 h	19.00 h	1.36	-14.0	-22.82	0.15	54.9	2.3	4.76	1	2	-2.59		
09.12.2012	19.00 h	21.50 h	1.61	-14.5	-20.96	0.18	53.6	1.1	4.93	1	1	-2.61		
09.12.2012	22.30 h	05.00h	3.49	-15.9	-21.29	0.17	66.2	0.4	5.05	1	1	-2.46		
10.12.2012	05.30 h	08.00 h	4.09	-17.8	-17.00	0.25	58.3	1.8	4.82	1	1	-2.31		
10.12.2012	10.00 h	11.00 h	2.37	-19.0	-18.27	0.22	50.3	4.8	4.81	1	2	-2.05		
10.12.2012	11.15 h	13.30 h	6.88	-20.2	-19.47	0.20	51.0	1.2	4.92	1	2	-2.13		
10.12.2012	14.15 h	15.45 h	3.78	-20.7	-18.44	0.22	57.6	1.8	4.90	1	2	-2.09		
10.12.2012	16.00 h	17.30 h	4.72	-20.8	-19.91	0.19	57.5	3.2	6.68	1	2	-2.01		
19.01.2013	14.00 h	16.00h	0.44	-8.2	-26.20	0.11	18.1	0.5	4.25	1	3	-2.45		
19.01.2013	16.10 h	17.30 h		-8.7	-25.07	0.12	20.9	1.1	4.45	1	3	-2.43		
19.01.2013	17.30 h	20.00 h	1.12	-8.0	-22.77	0.14	31.2	0.3	4.39	1	2	-2.45		
19.01.2013	21.00 h	05.00 h	7.70	-9.7	-21.09	0.17	43.8	0.1	4.94	1	3	-2.31		
20.01.2013	05.00 h	11.00 h	5.34	-11.0	-17.35	0.23	41.6	0.1	5.69	1	3	-2.26		
20.01.2013	19.00 h	21.00 h	2.89	-13.7	-17.90	0.22	45.3	0.2	4.12	1	2	-2.28		
20.01.2013	22.00 h	04.30 h		-13.8	-19.95	0.18	38.3	0.3	3.94	1	2	-2.31		
21.01.2013	04.30 h	08.00 h	0.21	-13.8	-23.47	0.13	19.0	0.7	3.90	1	2	-2.36		
09.02.2013	02.00 h	05.00 h	0.43	-25.8	-26.06	0.12	29.4	1.4	5.00	1	1			
09.02.2013	05.00 h	07.45 h	0.65	-26.4	-25.10	0.13	31.9	1.4	5.23	1	1	-2.05		
09.02.2013	07.45 h	09.45 h	0.21	-27.0	-25.82	0.12	30.7	0.9	5.23	1	1	-2.03		
09.02.2013	09.45 h	12.15 h	0.21	-27.1	-27.50	0.11	22.6	0.7	5.44	1	1			
09.02.2013	14.00 h	18.30 h		-27.3	-25.40	0.12	24.0	0.5	5.44	1	1	-2.00		
10.02.2013	23.00 h	05.00 h		-14.9	-30.47	0.08	12.2	0.3	4.90	1	1	-2.68		
11.02.2013	05.00 h	09.30 h	0.88	-17.3	-28.13	0.09	26.4	0.1	4.99	1	2	-2.38		
11.02.2013	12.00 h	14.30 h	0.22	-15.4	-34.73	0.05	16.5	0.4	5.25	1	2	-2.37		
11.02.2013	14.30 h	17.00 h	1.11	-19.0	-36.05	0.05	23.7	0.4	5.12	1	2	-2.37		
11.02.2013	17.00 h	21.00 h	1.11	-19.8	-36.24	0.05	20.4	0.2	4.98	1	2	-2.32		
11.02.2013	21.30 h	04.30 h	0.43	-19.6	-34.62	0.05	20.8	0.8	5.04	1	2	-2.27		
12.02.2013	04.30 h	07.00 h	0.21	-20.2	-33.93	0.06	20.4	1.0	5.06	1	2	-2.16		
10.03.2013	23.00 h	06.00 h	0.21	-13.6	-16.38	0.27	13.0	0.1	5.49	2	2	-2.21	5285	
11.03.2013	07.00 h	11.00 h	0.21	-12.7	-17.18	0.25	10.3	0.4	4.85	2	2	-2.43	7689	78
11.03.2013	11.00 h	15.00 h		-12.0	-17.10	0.25	1.7	0.4	4.76	2	2	-2.42	3647	74
12.03.2013	06.00 h	09.30 h	0.21	-13.1	-22.20	0.16	6.7	0.1	4.92	2	2	-2.48	22817	
12.03.2013	16.00 h	18.00 h	2.35	-14.1	-18.73	0.22	11.7	0.2	5.24	2	2	-2.17	10383	74
13.03.2013	21.00 h	05.00 h	1.35	-22.4	-28.01	0.10	23.8	0.2	5.18	2	1	-1.84	9326	52

A4 Table of data

14.03.2013	05.00 h	08.00 h	2.09	-24.3	-29.26	0.09	38.7	0.4	5.63	2	1	-1.78	7461	54
19.04.2013	11.40 h	13.40 h	1.59	-6.2	-9.09	0.47	19.1	2.7	6.03	2	3		8082	69
19.04.2013	13.40 h	15.30 h	0.21	-7.1	-13.48	0.35	13.7	2.4	5.26	2	1		7772	48
19.04.2013	15.30 h	18.00 h	3.16	-10.9	-15.82	0.28	21.6	0.8	4.64	2	1		4974	56
19.04.2013	18.00 h	20.00 h	1.35	-12.8	-18.55	0.22	25.0	2.0	3.98	2	1			
19.04.2013	21.30 h	04.00 h	0.21	-11.6	-14.27	0.32	14.4	1.9	4.69	2	2		9948	56
20.04.2013	04.30 h	10.30 h	8.06	-10.0	-12.74	0.33	56.2	0.9	4.63	2	2		10258	52
20.04.2013	10.30 h	14.30 h	0.65	-8.5	-14.82	0.28	48.6	0.9	4.08	2	2		9637	61
20.04.2013	14.30 h	17.30 h	1.35	-8.1	-14.95	0.27	40.7	0.9	4.03	2	2		10258	61
20.04.2013	17.30 h	19.30 h	1.11	-8.4	-12.71	0.33	42.8	0.9	3.79	2	2			
22.05.2013	12.10 h	13.45 h		-8.4	-16.55	0.26	23.8	6.3	4.30	2	1		12901	52
22.05.2013	13.45 h	15.30 h	0.65	-9.3	-14.87	0.30	31.3	5.6	4.73	2	1		7927	61
22.05.2013	15.30 h	17.15 h	1.35	-9.9	-14.13	0.32	33.7	1.8	5.23	2	1		4197	63
22.05.2013	17.30 h	19.30 h	1.84	-10.0	-14.55	0.31	33.9	2.2	4.79	2	1			
22.05.2013	21.00 h	01.00 h	1.11	-11.3	-15.27	0.29	28.0	1.4	5.05	2	1		4507	55
23.05.2013	12.30 h	15.15 h	18.14	-11.1	-12.30	0.38	15.8	0.3	5.22	2	1		12124	
23.05.2013	15.15 h	16.15 h	4.04	-10.8	-13.43	0.34	19.4	3.9	5.07	2	1			
23.05.2013	16.15 h	17.45 h	0.65	-11.5	-14.83	0.30	19.4	3.6	4.75	2	1		5595	64
23.05.2013	17.45 h	19.00 h	0.43	-13.2	-18.14	0.23	17.1	2.1	4.90	2	1			
23.05.2013	20.45 h	04.00 h	1.35	-16.3	-16.19	0.26	27.7	0.6	5.38	2	1		4974	75
24.05.2013	04.00 h	06.00h	0.88	-17.2	-18.76	0.21	29.5	1.0	5.26	2	1		6528	64
20.06.2013	01.00 h	04.00 h	113.92	0.3	-4.94	0.67	66.3	0.2	6.37	4	3		67301	66
20.06.2013	04.00 h	08.00 h	68.09	-0.1	-7.14	0.55	61.9	0.7	6.27	4	3		66679	55
20.06.2013	09.00 h	11.00 h	94.55	0.0	-5.42	0.64	66.0	0.2	6.06	4	3			
20.06.2013	11.00 h	13.30 h	182.55	-0.8	-9.01	0.46	75.2	0.9	6.04	4	3		34972	67
20.06.2013	13.30 h	15.30 h	159.04	-1.3	-8.22	0.49	89.1	0.7	5.69	4	3			
20.06.2013	15.30 h	17.30 h	72.09	-1.5	-8.35	0.48	74.8	1.3	5.61	4	3		23081	35
20.06.2013	19.30 h	02.00 h	16.13	-1.0	-7.32	0.53	40.2	1.2	5.83	4	3		22460	45
21.06.2013	17.00 h	18.30 h	56.90	-0.5	-5.37	0.64	15.1	0.4	5.98	4	3			
21.06.2013	18.30 h	20.00 h	10.26	-0.6	-6.32	0.59	11.1	1.7	5.90	4	3			
21.06.2013	21.00 h	03.30 h	0.65	-2.6	-12.94	0.32	12.1	2.3	5.79	4	3			
07.08.2013	12.00 h	14.00 h	122.98	0.4	-3.22	0.78	59.8	0.6	6.21	4	3		53312	63
07.08.2013	14.00 h	16.10 h	68.09	0.1	-5.47	0.63	65.7	1.1	5.99	4	3	-2.07	67612	59
07.08.2013	16.10 h	19.20 h	434.64	-0.2	-5.42	0.63	76.3	0.9	6.08	4	3	-2.05	43365	56
07.08.2013	20.30 h	04.00 h	37.44	0.2	-6.99	0.54	60.0	0.7	6.25	4	3	-2.00	32174	63
08.08.2013	06.30 h	09.30 h	7.21	0.4	-8.59	0.47	30.3	0.9	6.20	4	2	-2.40	7772	40
08.08.2013	09.30 h	11.00 h	0.88	-1.1	-9.88	0.41	25.4	0.4	4.25	4	2	-2.23		
08.08.2013	11.00 h	15.00 h	7.21	-0.4	-9.29	0.43	33.6	0.9	4.62	4	2	-2.09	13989	51
08.08.2013	15.00 h	17.00 h	4.04	0.2	-7.50	0.52	21.0	0.3	5.40	4	2	-2.26	5751	70
08.08.2013	20.00 h	04.00 h	2.61	-1.3	-11.89	0.34	7.7	0.2	5.15	4	2	-2.48		
08.09.2013	02.00h	05.00 h	2.35	-0.8	-8.78	0.47	42.4	0.9	5.56	3	3	-2.40	3264	55
08.09.2013	12.00 h	14.00 h	6.39	-0.1	-7.78	0.52	27.6	1.4	5.30	3	3	-2.23	3109	58
08.09.2013	14.00 h	15.15 h	3.86	-0.4	-8.33	0.49	16.0	3.0	4.96	3	3		3886	48
08.09.2013	15.15 h	16.45 h	32.16	-0.5	-8.40	0.49	11.6	3.7	4.91	3	3	-2.30	4041	54
08.09.2013	17.10 h	18.30 h	1.11	-1.0	-9.00	0.46	12.6	0.7	4.94	3	3	-2.36		

08.09.2013	18.30 h	04.00 h	3.96	-3.2	-14.71	0.26	16.0	1.3	4.61	3	2	-2.37	2953	63
12.09.2013	10.50 h	13.50 h	1.84	-7.7	-9.00	0.48	17.1	0.3	4.83	3	1	-2.17	3264	62
12.09.2013	13.50 h	15.40 h	2.09	-7.5	-11.75	0.39	14.0	0.7	4.34	3	1	-2.16	2642	65
12.09.2013	15.40 h	17.00 h	1.59	-7.6	-13.73	0.33	17.1	1.4	4.50	3	1	-2.14	2953	63
12.09.2013	17.00 h	18.30 h	3.16	-8.0	-13.67	0.33	18.8	0.7	4.67	3	1	-2.15		
12.09.2013	19.30 h	01.00 h	2.89	-9.2	-13.33	0.34	19.8	0.2	5.10	3	1	-2.13	2875	54
22.05.2014	04.00h	12.00h	44.48	-3.2	-4.47	0.72	65.8	2.00	7.15	2	3	-2.13	52691	74
22.05.2014	12.00 h	20.00 h	12.01	-2.8	-8.81	0.49	55.3	1.95	5.74	2	3	-2.17	17874	69
22.05.2014	20.00h	04.00h	31.51	-5.1	-8.01	0.52	58.7	2.32	5.48	2	3	-2.37	15388	60
28.06.2014	20.00h	04.00h	5.00	-1.1	-9.96	0.47	26.2	0.90	5.45	4	2	-2.05	5285	53
29.06.2014	04.00h	10.00h	0.21	-1.8	-14.08	0.32	19.6	1.93	4.90	4	2	-2.27	3109	70
29.06.2014	10.00h	16.00h	6.29	-2.8	-12.69	0.36	14.6	1.18	4.94	4	2	-2.24	5595	56
29.06.2014	18.00h	04.00h	2.35	-7.4	-14.9	0.29	34.3	0.98	5.04	4	1	-2.31	2642	76
29.07.2014	04.00h	10.00h	0.43	-2.0	-17.6	0.23	26.2	2.00	4.13	4	2	-2.24	5751	70
29.07.2014	11.00h	15.30h	1.59	-1.6	-14.47	0.31	28.6	0.85	4.97	4	2		4041	77
30.07.2014	04.00h	12.00h	0.88	-0.4	-13.64	0.34	33.0	2.25	4.90	4	1	-2.22	29998	55
30.07.2014	17.00h	01.00h	0.88	3.2	-14.99	0.30	5.4	5.47	4.51	4	1	-2.22	7305	55
30.09.2014	13.00h	13.45h	0.21	-1.2	-10.34	0.41	7.6	0.59	5.07	3	3	-2.22	3575	
01.10.2014	05.00h	06.30h	1.59	-2.5	-11.17	0.38	17.0	0.73	4.70	3	3	-2.36	2409	45
21.10.2014	20.00h	04.00h	60.51	-12.8	-11.46	0.39	68.0	2.00	5.35	3	1		9948	61
22.10.2014	06.00h	13.00h	29.02	-17.0	-14.72	0.29	60.4	2.00	5.23	3	1		6839	48

References

Andronache C.: Estimated variability of below-cloud aerosol removal by rainfall for observed aerosol size distribution, *Atmos. Chem. Phys.*, 3, 131-143, doi:10.5194/acp-3-131-2003, 2003.

Anisimov, O.A., Vaughan, D.G., Callaghan, T.V., Furgal, C., Marchant, H. and co-authors: Polar regions (Arctic and Antarctic). *Climate Change 2007: Impacts, Adaptation and Vulnerability. Contribution of Working Group II to the Fourth Assessment Report of the Intergovernmental Panel on Climate Change*, M.L. Parry, O.F. Canziani, J.P. Palutikof, P.J. van der Linden and C.E. Hanson, Eds., Cambridge University Press, Cambridge, 653-685, 2007.

Attard, E., Yang, H., Delort, A. M., Amato, P., Pöschl U., Glaux, C., Koop, T., and Morris, C. E.: Effects of atmospheric conditions on ice nucleation activity of *Pseudomonas*, *Atmos. Chem. Phys.*, 12, 10667-10677, doi:10.5194/acp-12-10667-2012, 2012.

Bauer, H., Kasper-giebl, A., and Lo, M.: The contribution of bacteria and fungal spores to the organic carbon content of cloud water , precipitation and aerosols, *Atmos. Res.*, 64, 109–119, doi:10.1016/S0169-8095(02)00084-4, 2002.

Bigg, E. K.: Ice forming nuclei in the high Arctic, *Tellus B*, 48, 223-233, doi:10.1034/j.1600-0889.1996.t01-1-00007.x, 1996.

Bigg, E. K., and Leck, C.: Cloud-active particles over the central Arctic Ocean, *J. Geophys. Res.*, 106, 32155-32166, doi:10.1029/1999JD901152, 2001.

Birkeland, K.: The Norwegian aurora polaris expedition 1902-1903, Vol. 1: On the cause of magnetic storms and the origin of terrestrial magnetism, H. Aschehoug & Co., Christiania, available at: <https://archive.org/details/norwegianaurorap01chiririch> (last access: 22.02.2016), 1908.

Bowers, R. M., Lauber, C. L., Wiedinmyer, C., Hamady, M., Hallar, A. G., Fall, R., Knight, R., and Fierer, N.: Characterization of airborne microbial communities at a high-elevation site and their potential to act as atmospheric ice nuclei, *Appl. Environ. Microbiol.*, 75, 5121–5130, doi:10.1128/AEM.00447-09, 2009.

Brunner, D., Henne, S., Keller, C. A., Vollmer, M. K., Reimann, S., and Buchmann, B.: Estimating European Halocarbon Emissions Using Lagrangian Backward Transport Modeling and in Situ Measurements at the Jungfraujoch High-Alpine Site, *Lagrangian Modeling of the Atmosphere* (eds J. Lin, D. Brunner, C. Gerbig, A. Stohl, A. Luhar and P. Webley), American Geophysical Union, Washington DC, 207-221, doi:10.1029/2012GM001258, 2013.

Burrows, S. M., Butler, T., Jöchel, P., Tost, H., Kerkweg, H., Pöschl, U., and Lawrence, M. G.: Bacteria in the global atmosphere – Part 2 : Modeling of emissions and transport between different ecosystems., *Atmos. Chem. Phys.*, 9, 9281–9297, doi:10.5194/acp-9-9281-2009, 2009.

Callaghan, T. V., Johansson, M., Brown, A. D., Groisman, P. Y., Labba, N, Radionov, V., Bradley, R. S., Blangy, S., Bulygina, O. B., Christensen, T. R., Colman, J. E., Essery, R. L. H., Forbes, B. C., Forchhammer, M. C., Golubev, V. N., Honrath, R. E., Juday, G. P., Meshcherskaya, A. V., Phoenix, G. K., Pomeroy, J., Rautio, A., Robinson, D. A., Schmidt, N. M., Serreze, M. C., Shevchenko, V. P., Shiklomanov, A. I., Shmakin, A. B., Sköld, P., Sturm, M., Woo, M., and Wood, E. F.: Multiple effects of changes in Arctic snow cover, *Ambio*, 40, 32-45, doi:10. 1007/s13280-011-0213-x, 2011.

Cantrell, W., and Heymsfield, A.: Production of Ice in Tropospheric Clouds: A Review, *B. Am. Meteorol. Soc.*, 86, 795–807, doi:10.1175/BAMS-86-6-795, 2005.

Chongyi, E., Yong, W., Taibao, Y., Jiankang, H., Hongchang, H., and Fengmei, Y.: Different responses of different altitudes surrounding Taklimakan Desert to global climate change, *Environ. Geol.*, 56, 1281–1293, doi:10.1007/s00254-008-1227-y, 2008.

Christner, B. C., Cai, R., Morris, C. E., McCarter, K. S., Foreman, C. M., Skidmore, M. L., Montross, S. N., and Sands, D. C.: Geographic, seasonal, and precipitation chemistry influence on the abundance and activity of biological ice nucleators in rain and snow, *P. Natl. Acad. Sci. USA*, 105, 18854–18859, doi:10.1073/pnas.0809816105, 2008a.

Christner, B. C., Morris, C. E., Foreman, C. M., Cai, R., and Sands, D. C.: Ubiquity of biological ice nucleators in snowfall, *Science*, 319, 1214, doi:10.1126/science.1149757, 2008b.

Chuvochina, M. S., Marie, D., Chevaillier, S., Petit, J. -R., Normand, P., Alekhina, I. A., and Bulat, S. A.: Community Variability of Bacteria in Alpine Snow (Mont Blanc) Containing Saharan Dust Deposition and Their Snow Colonisation Potential, *Microbes Environ.*, 26, 237-247, doi:10.1264/jsme2.ME11116, 2011.

Collaud Coen, M., Weingartner, E., Furger, M., Nyeki, S., Prévôt, a. S. H., Steinbacher, M., and Baltensperger, U.: Aerosol climatology and planetary boundary influence at the Jungfraujoch analyzed by synoptic weather types, *Atmos. Chem. Phys.*, 11, 5931–5944, doi:10.5194/acp-11-5931-2011, 2011.

Conen, F. and Leifeld, J.: A new facet of soil organic matter, *Agric. Ecosyst. Environ.*, 185, 186–187, doi:10.1016/j.agee.2013.12.024, 2014.

Conen, F., Morris, C. E., Leifeld, J., Yakutin, M. V., and Alewell, C.: Biological residues define the ice nucleation properties of soil dust, *Atmos. Chem. Phys.*, 11, 9643–9648, doi:10.5194/acp-11-9643-2011, 2011.

Conen, F., Henne, S., Morris, C. E., and Alewell, C.: Atmospheric ice nucleators active ≥ -12 °C can be quantified on PM₁₀ filters, *Atmos. Meas. Tech.*, 5, 321-327, doi:10.5194/amt-5-321-2012, 2012.

Conen, F., Rodriguez, S., Hüglin, C., Henne, S., Herrmann, E., Bukowiecki, N., and Alewell, C.: Atmospheric ice nuclei at the high-altitude observatory Jungfraujoch, Switzerland, *Tellus B*, 67, 1–10, doi:10.3402/tellusb.v67.25014, 2015.

Crawford, I., Bower, K. N., Choularton, T. W., Dearden, C., Crosier, J., Westbrook, C., Capes, G., Coe, H., Connolly, P. J., Dorsey, J. R., Gallagher, M. W., Williams, P., Trembath, J., Cui, Z., and Blyth, A.: Ice formation and development in aged, wintertime cumulus over the UK: observations and modelling, *Atmos. Chem. Phys.*, 12, 4963–4985, doi:10.5194/acp-12-4963-2012, 2012.

Creamean, J. M., Suski, K. J., Rosenfeld, D., Cazorla, A., DeMott, P. J., Sullivan, R. C., White, A. B., Ralph, F. M., Minnis, P., Comstock, J. M., Tomlinson, J. M., and Prather, K. A.: Dust and biological aerosols from the Sahara and Asia influence precipitation in the western U.S., *Science*, 339, 1572–1578, doi:10.1126/science.1227279, 2013.

Deguillaume, L., Charbouillot, T., Joly, M., Vaïtilingom, M., Parazols, M., Marinoni, A., Amato, P., Delort, A.-M., Vinatier, V., Flossmann, A., Chaumerliac, N., Pichon, J. M., Houdier, S., Laj, P., Sellegri, K., Colomb, A., Brigante, M., and Mailhot, G.: Classification of clouds sampled at the puy de Dôme (France) based on 10 yr of monitoring of their physicochemical properties, *Atmos. Chem. Phys.*, 14, 1485–1506, doi:10.5194/acp-14-1485-2014, 2014.

DeMott, P. J. and Prenni, A. J.: New directions: need for defining the numbers and sources of biological aerosols acting as ice nuclei, *Atmos. Environ.*, 44, 1944-1945, doi:10.1016/j.atmosenv.2010.02.032, 2010.

DeMott, P. J., Prenni, A. J., Liu, X., Kreidenweis, S. M., Petters, M. D., Twohy, C. H., Richardson, M. S., Eidhammer, T., and Rogers, D. C.: Predicting global atmospheric ice nuclei distributions and their impacts on climate, *P. Natl. Acad. Sci. USA*, 107, 11217–11222, doi.org/10.1073/pnas.0910818107, 2010.

DeMott, P. J., Möhler, O., Stetzer, O., Vali, G., Levin, Z., Petters, D. M., Murakami, M., Leisner, T., Bundke, U., Klein, H., Kanji, A. Z., Cotton, R., Jones, H., Benz, S., Brinkmann, M., Rzesanke, D., Saathoff, H., Nicolet, M., Saito, A., Nillius, B., Bingmer, H., Abbatt, J., Ardon, K., Ganor, E., Georgakopoulos, D. G. and Saunders, C.: Resurgence in ice nuclei measurement research, *B. Am. Meteorol. Soc.*, 92, 1623-1635, doi:10.1175/2011BAMS3119.1, 2011.

DeMott, P. J., Hill, T. C. J., McCluskey, C. S., Prather, K. A., Collins, D. B., Sullivan, R. C., Ruppel, M. J., Mason, R. H., Irish, V. E., Lee, T., Hwang, C. Y., Rhee, T. S., Snider, J. R., McMeeking, G. R., Dhaniyala, S., Lewis, E. R., Wentzell, J. J. B., Abbatt, J., Lee, C., Sultana, C. M., Ault, A. P., Axson, J. L., Martinez, M. D., Venero, I., Santos-Figueroa, G., Dale Stokes, M., Deane, G. B., Mayol-Bracero, O. L., Grassian, V. H., Bertram, T. H., Bertram, A. K., Moffett, B. F., and Franc, G. D.: Sea spray aerosol as a unique source of ice nucleating particles. *P. Natl. Acad. Sci. USA Early Edition*, doi:10.1073/pnas.1514034112, 2015.

Després, V. R., Huffman, J. A., Burrows, S. M., Hoose, C., Safatov, A. S., Buryak, G., Fröhlich-Nowoisky, J., Elbert, W., Andreae, M. O., Pöschl, U., and Jaenicke, R.: Primary biological aerosols particles in the atmosphere: a review, *Tellus B*, 64, doi.org/10.3402/tellusb.v64i0.15598, 2012.

Favet, J., Lapanje, A., Giongo, A., Kennedy, S., Aung, Y. Y., Cattaneo, A., Davis-Richardson, A. G., Brown, C. T., Kort, R., Brumsack, H. -J., Schnetger, B., Chappell, A., Kroijenga, J., Beck, A., Schwibbert, K., Mohamed, A. H., Kirchner, T., Dorr de Quadros, P., Triplett, E. W., Broughton, W. J., and Gorbushina, A. A.: Microbial hitchhikers on intercontinental dust: catching a lift in Chad, *The ISME Journal*, 7, 850-867, doi:10.1038/ismej.2012.152, 2013.

Fröhlich, R., Cubison, M. J., Slowik, J. G., Bukowiecki, N., Canonaco, F., Croteau, P. L., Gysel, M., Henne, S., Herrmann, E., Jayne, T. J., Steinbacher, M., Worsnop, D. R., Baltensperger, U., and Prévôt, A. S. H.: Fourteen months of on-line measurements of the non-refractory submicron aerosol at the Jungfraujoch (3580m a.s.l.) - chemical composition, origins and organic aerosol sources, *Atmos. Chem. Phys.*, 15, 11373-11398, doi:10.5194/acp-15-11373-2015, 2015.

Fröhlich-Nowoisky, J., Hill, T. C. J., Pummer, B. G., Yordanova, P., Franc, G. D., and Pöschl, U.: Ice nucleation activity in the widespread soil fungus *Mortierella alpina*, *Biogeosciences*, 12, 1057–1071, doi:10.5194/bg-12-1057-2015, 2015.

Gao, W., Zhang W., and Meldrum, D. R.: RT-qPCR based quantitative analysis of gene expression in single bacterial cells, *J. Microbiol. Meth.*, 85, 221-227, doi:10.1016/j.mimet.2011.03.008, 2011.

Gayet, J. F., Treffeisen, R., Helbig, A., Bareiss, J., Matsuki, A., Herber, A., and Schwarzenboeck, A.: On the onset of the ice phase in boundary layer Arctic clouds, *J. Geophys. Res.*, 114, 1–15, doi:10.1029/2008JD011348, 2009.

Griffiths, A. D., Conen, F., Weingartner, E., Zimmermann, L., Chambers, S. D., Williams, A. G., and Steinbacher, M.: Surface-to-mountaintop transport characterised by radon observations at the Jungfraujoch, *Atmos. Chem. Phys.*, 14, 12763-12779, doi:10.5194/acp-14-12763-2014, 2014.

Guilbaud, C., Morris, C. E., Barakat, M., Ortet, P., and Berge, O.: Isolation and identification of *Pseudomonas syringae* facilitated by a PCR targeting the whole *P. syringae* group, *FEMS Microbiol. Ecol.*, 92, doi: 10.1093/femsec/fiv146, 2016.

Hallett, J. and Mossop, S.: Production of secondary ice particles during the riming process, *Nature*, 249, 26-28, 1974.

Hammer, E., Bukowiecki, N., Gysel, M., Jurányi, Z., Hoyle, C. R., Vogt, R., Baltensperger, U., and Weingartner, E.: Investigation of the effective peak supersaturation for liquid-phase clouds at the high-alpine site Jungfraujoch, Switzerland (3580 m a.s.l.), *Atmos. Chem. Phys.*, 14, 1123–1139, doi:10.5194/acp-14-1123-2014, 2014.

Hammer, Ø., Harper, D. A., and Ryan, P. D.: PAST: PAleontologi- cal STatistics software package for education and data analysis, *Palaeontol. Electron.*, 4, available at: http://www.uv.es/pe/2001_1/past/past.pdf (last access: 12.02.2015), 2001.

Hiranuma, N., Augustin-Bauditz, S., Bingemer, H., Budke, C., Curtius, J., Danielczok, A., Diehl, K., Dreischmeier, K., Ebert, M., Frank, F., Hoffmann, N., Kandler, K., Kiselev, A., Koop, T., Leisner, T., Mohler, O., Nillius, B., Peckhaus, A., Rose, D., Weinbruch, S., Wex, H., Boose, Y., DeMott, P. J., Hader, J. D., Hill, T. C. J., Kanji, Z. A., Kulkarni, G., Levin, E. J. T., McCluskey, C. S., Murakami, M., Murray, B. J., Niedermeier, D., Petters, M. D., O'Sullivan, D., Saito, A., Schill, G. P., Tajiri, T., Tolbert, M. A., Welti, A., Whale, T. F., Wright, T. P., and Yamashita, K.: A comprehensive laboratory study on the immersion freezing behavior of illite NX particles: a comparison of 17 ice nucleation measurement techniques, *Atmos. Chem. Phys.*, 15, 2489-2518, doi:10.5194/acp-15-2489-2015, 2015.

Hoose, C. and Möhler, O.: Heterogeneous ice nucleation on atmospheric aerosols: a review of results from laboratory experiments, *Atmos. Chem. Phys.*, 12, 9817-9854, doi:10.5194/acp-12-9817-2012, 2012.

Hoose, C., Kristjánsson, J. E., and Burrows, S. M.: How important is biological ice nucleation in clouds on a global scale?, *Environ. Res. Lett.*, 5, 1-7, doi:10.1088/1748-9326/5/2/024009, 2010a.

Hoose, C., Kristjánsson, J. E., Chen, J.-P., and Hazra, A.: A Classical-Theory-Based Parameterization of Heterogeneous Ice Nucleation by Mineral Dust, Soot, and Biological Particles in a Global Climate Model, *J. Atmos. Sci.*, 67, 2483–2503, doi:10.1175/2010JAS3425.1, 2010b.

Huffman, J. A., Prenni, A. J., DeMott, P. J., Pöhlker, C., Mason, R. H., Robinson, N. H., Fröhlich-Nowoisky, J., Tobo, Y., Després, V. R., Garcia, E., Gochis, D. J., Harris, E., Müller-Germann, I., Ruzene, C., Schmer, B., Sinha, B., Day, D. A., Andreae, M. O., Jimenez, J. L., Gallagher, M., Kreidenweis, S. M., Bertram, A. K., and Pöschl, U.: High concentrations of biological aerosol particles and ice nuclei during and after rain, *Atmos. Chem. Phys.*, 13, 6151–6164, doi:10.5194/acp-13-6151-2013, 2013.

IAEA International Atomic Energy Agency: Environmental isotopes in the hydrological cycle. Principles and applications. Vol. 2. Atmospheric Water, available at: http://www-naweb.iaea.org/napc/ih/IHS_resources_publication_hydroCycle_en.html (last access: 12.02.2015), 2001a.

IAEA International Atomic Energy Agency: Environmental isotopes in the hydrological cycle. Principles and applications. Vol. 3. Surface Water, available at: http://www-naweb.iaea.org/napc/ih/IHS_resources_publication_hydroCycle_en.html (last access: 12.02.2015), 2001b.

Iannone, R., Chernoff, D. I., Pringle, A., Martin, S. T., and Bertram, A.K.: The ice nucleation ability of one of the most abundant types of fungal spores found in the atmosphere, *Atmos. Chem. Phys.*, 11, 1191-1201, doi:10.5194/acp-11-1191-2011, 2011.

IPCC Intergovernmental Panel on Climate Change: The Physical Science Basis, Summary for Policymakers of Working Group 1, available at: http://www.ipcc.ch/pdf/assessment-report/ar5/wg1/WGIAR5_SPM_brochure_en.pdf, (last access: 18.05.2016), 2013a.

IPCC Intergovernmental Panel on Climate Change: The Physical Science Basis, Full Report of Working Group 1, available at: http://www.climatechange2013.org/images/report/WGIAR5_ALL_FINAL.pdf, (last access: 18.05.2016), 2013b.

Jiang, H., Yin, Y., Yang, L., Yang, S., Su, H., and Chen, K.: The Characteristics of Atmospheric Ice Nuclei Measured at Different Altitudes in the Huangshan Mountains in the Southwest China, *Adv. Atmos. Sci.*, 31, 396-406, doi:10.1007/s00376-013-3048-5, 2014.

Joly, M., Attard, E., Sancelme, M., Deguillame, L., Guilbaud, C., Morris, C. E., Amato, P., and Delort, A. M.: Ice nucleation activity of bacteria isolated from cloud water, *Atmos. Environ.*, 70, 392-400, doi:10.1016/j.atmosenv.2013.01.027, 2013.

Joly, M., Amato, P., Deguillaume, L., Monier, M., Hoose, C., and Delort, A. M.: Quantification of ice nuclei active at near 0 °C temperatures in low-altitude clouds at the Puy de Dôme atmospheric station, *Atmos. Chem. Phys.*, 14, 8185–8195, doi:10.5194/acp-14-8185-2014, 2014.

Jones, A. M. and Harrison, R. M.: The effects of meteorological factors on atmospheric bioaerosol concentrations-a review, *Sci. Total Environ.*, 326, 151–180, doi:10.1016/j.scitotenv.2003.11.021, 2004.

Kellogg, C. A. and Griffin, D. W.: Aerobiology and the global transport of desert dust, *Trends Ecol. Evol.*, 21, 638–644, doi:10.1016/j.tree.2006.07.004, 2006.

Ketterer, C., Zieger, P., Bukowiecki, N., Collaud Coen, M., Maier, O., Ruffieux, D., and Weingartner, E.: Investigation of the Planetary Boundary Layer in the Swiss Alps Using Remote Sensing and In Situ Measurements, *Bound-Lay. Meteorol.*, 151, 317–334, doi:10.1007/s10546-013-9897-8, 2014.

Köhler, H.: Studien über Nebelfrost und Schneebildung und über den Chlorgehalt des Nebelfrostes, des Schnees und des Seewassers im Halddegebiet, *Bull. Geol. Inst. Univ. Upsala*, 26, 279-308, 1937.

Lau, K. M., and Wu, H. T.: Warm rain processes over tropical oceans and climate implications, *Geophys. Res. Lett.*, 30, 2290, doi:10.1029/2003GL018567, 2003.

-
- Limpert, E., Burke, J., Galan, C., Trigo, M. D. M., West, J. S., and Stahel, W. A.: Data, not only in aerobiology: how normal is the normal distribution?, *Aerobiologia*, 24, 121–124, doi:10.1007/s10453-008-9092-4, 2008.
- Lindemann, J., Constantinidou, H. A., Barchet, W. R., and Upper, C. D.: Plants as sources of airborne bacteria, including ice nucleation-active bacteria, *Appl. Environ. Microb.*, 44, 1059–1063, 1982.
- Lindow, S. E., Arny, D. C., and Upper, C. D.: Distribution of ice nucleation-active bacteria on plants in nature, *Appl. Environ. Microb.*, 36, 831–838, 1978.
- Lindow, S. E.: The role of bacterial ice nucleation in frost injury to plants, *Ann. Rev. Phytopathol.*, 21, 363–384, 1983.
- Lowenthal, D. H., Borys, R. D., Cotton, W., Saleeby, S., Cohn, S. A., and Brown, W. O.J.: The altitude of snow growth by riming and vapor deposition in mixed-phase orographic clouds, *Atmos. Environ.*, 45, 519–522, doi:10.1016/j.atmosenv.2010.09.061, 2011.
- Majoube, M.: Fractionnement en oxygène-18 et en deuterium entre l'eau et sa vapeur, *J. Chem. Phys.*, 197, 1423–1436, 1971.
- Maki, L. R., Galyan, E. L., and Caldwell, D. R.: Ice Nucleation Induced by *Pseudomonas syringae*, *Appl. Environ. Microb.*, 28, 456–459, 1974.
- Mason, B. J.: *The Physics of Clouds*, Oxford University Press, 1957.
- Mason, B. J.: The rapid glaciation of slightly supercooled cumulus clouds, *Q. J. Roy. Meteor. Soc.*, 122, 357–365, 1996.
- Moffett, B. F., Getti, G., Henderson-Begg, K., and Hill, T. C. J.: Ubiquity of ice nucleation in lichen – possible atmospheric implications, *Lindbergia*, 38, 39–43, 2015.
- Möhler, O., DeMott, P. J., Vali, G., and Levin, Z.: Microbiology and atmospheric processes: the role of biological particles in cloud physics, *Biogeosciences*, 4, 1059–1071, doi:10.5194/bg-4-1059-2007, 2007.
- Monteil, C. L., Guilbaud, C., Glaux, C., Lafolie, F., Soubeyrand, S., and Morris, C. E.: Emigration of the plant pathogen *Pseudomonas syringae* from leaf litter contributes to its population dynamics in alpine snowpack, *Environ. Microbiol.*, 14, 2099–2112, doi:10.1111/j.1462-2920.2011.02680.x, 2012.
- Monteil, C. L., Bardin, M., and Morris, C. E.: Features of air masses associated with the deposition of *Pseudomonas syringae* and *Botrytis cinerea* by rain and snowfall, *The ISME Journal*, 8, 2290–2304, doi:10.1038/ismej.2014.55, 2014.
- Moran, T. A., Marshall, S. J., Evans, E. C., and Sinclair, K. E.: Altitudinal Gradients of Stable Isotopes in Lee-Slope Precipitation in the Canadian Rocky Mountains, *Arct. Antarct. Alp. Res.*, 39, 455–467, doi:10.1657/1523-0430(06-022), 2007.
- Morris, C. E., Sands, D. C., Vinatzer, B. A., Glaux, C., Guilbaud, C., Buffière, A., Yan, S., Dominguez, H., and Thompson, B. M.: The life history of the plant pathogen *Pseudomonas syringae* is linked to the water cycle, *The ISME Journal*, 2, 321–334, doi:10.1038/ismej.2007.113, 2008.
- Morris, C. E., Sands, D. C., Vanneste, J. L., Montarry, J., Oakley, B., Guilbaud, C., and Glaux, C.: Inferring the Evolutionary History of the Plant Pathogen *Pseudomonas syringae* from Its Biogeography in Headwaters of Rivers in North America, Europe, and New Zealand, *mBio*, 1, e00107–10, doi:10.1128/mBio.00107-10, 2010.
- Morris, C. E., Sands, D. C., Bardin, M., Jaenicke, R., Vogel, B., Leyronas, C., Ariya, P. A. and Psenner, R.: Microbiology and atmospheric processes: research challenges concerning the impact of airborne microorganisms on the atmosphere and climate, *Biogeosciences*, 8, 17–25, doi:10.5194/bg-8-17-2011, 2011.

Morris, C. E., Sands, D. C., Glaux, C., Samsatly, J., Asaad, S., Moukahel, A. R., Goncalves, F. I. T., and Bigg, K. E.: Urediospores of rust fungi are ice nucleation active at > -10 °C and harbor ice nucleation active bacteria, *Atmos. Chem. Phys.*, 13, 4223-4233, doi:10.5194/acp-13-4223-2013, 2013a.

Morris, C. E., Monteil, C. L., and Berge, O.: The life history of *Pseudomonas syringae*: Linking agriculture to Earth system processes, *Annu. Rev. Phytopathol.*, 51, 85-104, doi:10.1146/annurev-phyto-082712-102402, 2013b.

Morris, C. E., Conen, F., Huffman, J. A., Phillips, V., Pöschl, U., and Sands, D. C.: Bioprecipitation: a feedback cycle linking earth history, ecosystem dynamics and land use through biological ice nucleators in the atmosphere, *Glob. Change Biol.*, 20, 341-351, doi:10.1111/gcb.12447, 2014.

Mühlbauer, A., Hashino, T., Xue, L., Teller, A., Lohmann, U., Rasmussen, R. M., Geresdi, I., and Pan, Z.: Intercomparison of aerosol-cloud-precipitation interactions in stratiform orographic mixed-phase clouds. *Atmos. Chem. Phys.*, 10, 8173-8196, doi:10.5194/acp-10-8173-2010, 2010.

Mülmenstädt, J., Sourdeval, O., Delanoë, J., and Quaas, J.: Frequency of occurrence of rain from liquid-, mixed-, and ice-phase clouds derived from A-Train satellite retrievals, *Geophys. Res. Lett.*, 42, 6502-6509, doi:10.1002/2015GL064604, 2015.

Murray, B. J., O'Sullivan, D., Atkinson, J. D., and Webb, M. E.: Ice nucleation by particles immersed in supercooled cloud droplets, *Chem. Soc. Rev.*, 41, 6519-6554, doi:10.1039/C2CS35200A, 2012.

Nemecek-Marshall, M., LaDuca, R., and Fall, R.: High-level expression of ice nuclei in a *Pseudomonas syringae* strain is induced by nutrient limitation and low temperature, *J. Bacteriol.*, 175, 4062-4070, 1993.

O'Sullivan, D., Murray, B. J., Malkin, T. L., Whale, T. F., Umo, N. S., Atkinson, J. D., Price, H. C., Baustian, K. J., Browse, J., and Webb, M. E.: Ice nucleation by fertile soil dusts: relative importance of mineral and biogenic components, *Atmos. Chem. Phys.*, 14, 1853-1867, doi:10.5194/acp-14-1853-2014, 2014.

O'Sullivan, D., Murray, B. J., Ross, J. F., Whale, T. F., Price, H. C., Atkinson, J. D., Umo, N. S., and Webb, M. E.: The relevance of nanoscale biological fragments for ice nucleation in clouds, *Sci. Rep.*, 5, 8082, doi:10.1038/srep08082, 2015.

Pandey Deolal, S., Staehelin, J., Brunner, D., Cui, J., Steinbacher, M., Zellweger, C., Henne, S., and Vollmer, M. K.: Transport of PAN and NO_y from different source regions to the Swiss high alpine site Jungfraujoch, *Atmos. Environ.*, 64, 103-115, doi:10.1016/j.atmosenv.2012.08.021, 2013.

Perovich, D. K.: Complex yet translucent: the optical properties of sea ice, *Physica B*, 338, 107-114, doi:10.1016/S0921-4526(03)00470-8, 2003.

Peter, H., Hörtnagl, P., Reche, I., and Sommaruga, R.: Bacterial diversity and composition during rain events with and without Saharan dust influence reaching a high mountain lake in the Alps, *Environ. Microbiol. Rep.*, 6, 618-624, doi:10.1111/1758-2229.12175, 2014.

Petters, M. D. and Wright, T. P.: Revisiting ice nucleation from precipitation samples, *Geophys. Res. Lett.*, 42, 8758-8766, doi:10.1002/2015GL065733, 2015.

Pfahl, S., and Sodemann, H.: What controls deuterium excess in global precipitation?, *Clim. Past.*, 10, 771-781, doi:10.5194/cp-10-771-2014, 2014.

Phillips, V. T. J., Choulaton, T. W., Illingworth, A. J., Hogan, R. J., and Field, P. R.: Simulations of the glaciation of a frontal mixed-phase cloud with the Explicit Microphysics Model, *Q. J. R. Meteorol. Soc.*, 129, 1351-1371, doi:10.1256/qj.02.100, 2003.

Phillips, V. T. J., DeMott, P. J., and Andronache, C.: An Empirical Parameterization of Heterogeneous Ice Nucleation for Multiple Chemical Species of Aerosol, *J. Atmos. Sci.*, 65, 2757-2783, doi:10.1175/2007JAS2546.1, 2008.

-
- Pöschl, U., Martin, S. T., Sinha, B., Chen, Q., Gunthe, S. S., Huffman, J. A., Borrmann, S., Farmer, D. K., Garland, R. M., Helas, G., Jimenez, J. L., King, S. M., Manzi, A., Mikhailov, E., Pauliquevis, T., Petters, M. D., Prenni, A. J., Roldin, P., Rose, D., Schneider, J., Su, H., Zorn, S. R., Artaxo, P., and Andreae, M. O.: Rainforest Aerosols as Biogenic Nuclei of Clouds and Precipitation in the Amazon, *Science*, 329, 1513–1516, doi:10.1126/science.1191056, 2009.
- Pratt, K. A., DeMott, P. J., French, J. R., Wang, Z., Westphal, D. L., Heymsfield, A. J., Twohy, C. H., Prenni, A. J., and Prather, K. A.: In situ detection of biological particles in cloud ice-crystals, *Nat. Geosci.*, 2, 398–401, doi:10.1038/ngeo521, 2009.
- Prenni, A. J., Harrington, J. Y., Tjernström, M., DeMott, P. J., Avramov, A., Long, C. N., Kreidenweis, S. M., Olsson, P. Q., and Verlinde, J.: Can ice-nucleating aerosols affect Arctic seasonal climate?, *Bull. Amer. Meteor. Soc.*, 88, 541–550, doi:10.1175/BAMS-88-4-541, 2007.
- Prenni, A. J., Petters, M. D., Kreidenweis, S. M., Heald, C. L., Martin, S. T., Artaxo, P., Garland, R. M., Wollny, A. G., and Pöschl, U.: Relative roles of biogenic emissions and Saharan dust as ice nuclei in the Amazon basin, *Nature Geosci.*, 2, 402–405, doi:10.1038/ngeo517, 2009.
- Prenni, A. J., Tobo, Y., Garcia, E., DeMott, P. J., Huffman, J. A., McCluskey, C. S., Kreidenweis, S. M., Prenni, J. E., Pöhlker, C., and Pöschl, U.: The impact of rain on ice nuclei populations at a forested site in Colorado, *Geophys. Res. Lett.*, 40, 227–231, doi:10.1029/2012GL053953, 2013.
- Pummer, B. G., Bauer, H., Bernardi, J., Bleicher, S., and Grothe, H.: Suspendable macromolecules are responsible for ice nucleation activity of birch and conifer pollen, *Atmos. Chem. Phys.*, 12, 2541–2550, doi:10.5194/acp-12-2541-2012, 2012.
- Pummer, B. G., Budke, C., Augustin-Bauditz, S., Niedermeier, D., Felgitsch, L., Kampf, C. J., Huber, R. G., Liedl, K. R., Loerting, T., Moschen, T., Schauerl, M., Tollinger, M., Morris, C. E., Wex, H., Grothe, H., Pöschl, U., Koop, T., and Fröhlich-Nowoisky, J.: Ice nucleation by water-soluble macromolecules, *Atmos. Chem. Phys.*, 15, 4077–4091, doi:10.5194/acp-15-4077-2015, 2015.
- R Core Team: R: A Language and Environment for Statistical Computing, R Foundation for Statistical Computing, Vienna, Austria, available at: <http://www.R-project.org> (last access: 12.02.2015), 2011.
- Rowley, D. B., Pierrehumbert, R. T., and Currie, B. S.: A new approach to stable isotope-based paleoaltimetry: implications for paleoaltimetry and paleohypsometry of the High Himalaya since the Late Miocene, *Earth Planet. Sci. Lett.*, 188, 253–268, doi:10.1016/S0012-821X(01)00324-7, 2001.
- Ruggles, J. A., Nemecek-Marshall, M. and Fall, R.: Kinetics of appearance and disappearance of classes of bacterial ice nuclei support an aggregation model for ice nucleus assembly, *J. Bacteriol.*, 175, 7216–7221, 1993.
- Santachiara, G., Prodi, F., and Belosi, F.: Atmospheric aerosol scavenging processes and the role of thermo- and diffusion-phoretic forces, *Atmos. Res.*, 128, 46–56, doi:10.1016/j.atmosres.2013.03.004, 2013.
- Šantl-Temkiv, T., Finster, K., Dittmar, T., Hansen, B. M., Thyraug, R., Nielsen, N. W., and Karlson, U. G.: Hailstones: a window into the microbial and chemical inventory of a storm cloud, *PLoS*, 8, e53550, doi:10.1371/journal.pone.0053550, 2013.
- Šantl-Temkiv, T., Sahyoun, M., Finster, K., Hartmann, S., Augustin-Bauditz, S., Stratmann, F., Wex, H., Clauss, T., Nielsen, N. W., Havskov Sørensen, J., Smith Korsholm, U., Wick, L. Y., and Gosewinkel Karlson, U.: Characterization of airborne ice-nucleation-active bacteria and bacterial fragments, *Atmos. Environ.*, 109, 105–117, doi:10.1016/j.atmosenv.2015.02.060, 2015.
- Šantl-Temkiv, T., Ling, M., Holm, S., Finster, K., and Boesen, T.: The presence of INA proteins on the surface of single cells of *Pseudomonas syringae* R10.79 isolated from rain, *Geophys. Res. Abstracts*, EGU2016-15510, 2016.
- Sattler, B., Puxbaum, H., and Psenner, R.: Bacterial growth in supercooled cloud droplets, *Geophys. Res. Lett.*, 28, 239–242, 2001.
-

-
- Schmale, D. G., and Ross, S. D.: Highways in the sky: scales of transport of plant pathogens, *Annu. Rev. Phytopathol.*, 53, 591-611, doi:10.1146/annurev-phyto-080614-115942, 2015.
- Schnell, R. C. and Vali, G.: Atmospheric ice nuclei from decomposing vegetation, *Nature*, 236, 163-165, doi:10.1038/236163a0, 1972.
- Schnell, R. C. and Vali, G.: World-wide source of leaf-derived freezing nuclei, *Nature*, 246, 212-213, doi:10.1038/246212a0, 1973.
- Schnell, R. C. and Vali, G.: Freezing nuclei in marine waters, *Tellus*, 27, 321-323, doi:10.1111/j.2153-3490.1975.tb01682.x, 1975.
- Schnell, R. C., and Vali, G.: Biogenic ice nuclei: Part I. Terrestrial and marine sources, *J. Atmos. Sci.*, 33, 1554-1564, doi:10.1175/1520-0469(1976)033<1554:BINPIT>2.0.CO;2, 1976.
- Schumann, T.: Aerosol and hydrometeor concentrations and their chemical composition during winter precipitation along a mountain slope-III. Size-differentiated in-cloud scavenging efficiencies, *Atmos. Environ.*, 25A, 809-824, doi:10.1016/0960-1686(91)90079-M, 1991.
- Sesartic, A., Lohmann, U., and Storelvmo, T.: Bacteria in the ECHAM5-HAM global climate model. *Atmos. Chem. Phys.*, 12, 8645-8661, doi:10.5194/acp-12-8645-2012, 2012.
- Sinclair, K. E., Marshall, S. J., and Moran, T. A.: A Lagrangian approach to modelling stable isotopes in precipitation over mountainous terrain, *Hydrol. Process.*, 25, 2481-2491, doi:10.1002/hyp.7973, 2011.
- Sodemann, H. and Zubler, E.: Seasonal and inter-annual variability of the moisture sources for Alpine precipitation during 1995-2002, *Int. J. Climatol.*, 30, 974-961, doi:10.1002/joc.1932, 2010.
- Stan, C. A., Schneider, G. F., Shevkoplyas, S. S., Hashimoto, M., Ibanescu, M., Wiley, B. J. and Whitesides, G. M.: A microfluidic apparatus for the study of ice nucleation in supercooled water drops, *Lab. Chip*, 9, 2293-2305, doi:10.1039/B906198C, 2009.
- Stohl, A., Forster, C., Frank, A., Seibert, P., and Wotawa, G.: Technical note: the Lagrangian particle dispersion model FLEXPART version 6.2, *Atmos. Chem. Phys.*, 5, 2461-2474, doi:10.5194/acp-5-2461-2005, 2005.
- Stopelli, E., Conen, F., Zimmermann, L., Alewell, C., and Morris, C. E.: Freezing nucleation apparatus puts new slant on study of biological ice nucleators in precipitation, *Atmos. Meas. Tech.*, 7, 129-134, doi:10.5194/amt-7-129-2014, 2014.
- Stopelli, E., Conen, F., Morris, C. E., Herrmann, E., Bukowiecki, N., and Alewell, C.: Ice nucleation active particles are efficiently removed by precipitating clouds, *Sci. Rep.*, 5, 16433, doi:10.1038/srep16433, 2015.
- Stopelli, E., Conen, F., Morris, C. E., Herrmann, E., Henne, S., Steinbacher, M., and Alewell, C.: Predicting abundance and variability of ice nucleating particles in precipitation at the high-altitude observatory Jungfraujoch, *Atmos. Chem. Phys.*, 16, 8341-8351, doi:10.5194/acp-16-8341-2016, 2016.
- Szyrmer, W., and Zawadzki, I.: Snow Studies. Part II: Average Relationship between Mass of Snowflakes and Their Terminal Fall Velocity, *J. Atmos. Sci.*, 67, 3319-3335, doi:10.1175/2010JAS3390.1, 2010.
- Tjernstrom, M., Leck, C., Birch, C. E., Bottenheim, J. W., Brooks, B. J., Brooks, I. M., Backlin, L., Chang, Y. W., de Leeuw, G., Di Liberto, L., de la Rosa, S., Granath, E., Graus, M., Hansel, A., Heintzenberg, J., Held, A., Hind, A., Johnston, P., Knulst, J., Martin, M., Matrai, P. A., Mauritsen, T., Müller, M., Norris, S. J., Orellana, M. V., Orsini, D. A., Paatero, J., Persson, P. O. G., Gao, Q., Rauschenberg, C., Ristovski, Z., Sedlar, J., Shupe, M. D., Sierau, B., Sirevaag, A., Sjogren, S., Stetzer, O., Swietlicki, E., Szczodrak, M., Vaattovaara, P., Wahlberg, N., Westberg, M., and Wheeler, C. R.: The Arctic Summer Cloud Ocean Study (ASCOS): overview and experimental design, *Atmos. Chem. Phys.*, 14, 2823-2869, doi:10.5194/acp-14-2823-2014, 2014.
-

Vařilingom, M., Attard, E., Gaiani, N., Sancelme, M., Deguillaume, L., Flossmann, A. I., Amato, P., and Delort, A.-M.: Long-term features of cloud microbiology at the puy de Dôme (France), *Atmos. Environ.*, 56, 88–100, doi:10.1016/j.atmosenv.2012.03.072, 2012.

Vali, G.: Quantitative evaluation of experimental results on the heterogeneous freezing nucleation of supercooled liquids, *J. Atmos. Sci.*, 28, 402–409, 1971.

Vali, G.: Principles of ice nucleation, in: *Biological ice nucleation and its applications*, American Phytopathological Society; Lee, E. R. Jr., Warren, G. J. and Gusta, L.V., APS Press, St. Paul, Minnesota, USA, 1–28, 1995.

Vali, G.: Repeatability and randomness in heterogeneous freezing nucleation, *Atmos. Chem. Phys.*, 8, 5017–5031, doi:10.5194/acp-8-5017-2008, 2008.

Vali, G. and Stansbury E. J.: Time-dependent characteristics of the heterogeneous nucleation of ice, *Can. J. Phys.*, 44, 477–502, 1966.

Vali, G., Christensen, M., Fresh, R. W., Galyan, E. L., Maki, L. R., and Schnell, R. C.: Biogenic ice nuclei. Part II: Bacterial sources, *J. Atmos. Sci.*, 33, 1565–1570, doi:10.1175/1520-0469(1976)033<1565:BINPIB>2.0.CO;2, 1976.

Weingartner, E., Nyeki, S., and Baltensperger, U.: Seasonal and diurnal variation of aerosol size distributions ($10 < D < 750$ nm) at a high-alpine site (Jungfraujoch 3580 m asl), *J. Geophys. Res.*, 104, 809–826, doi:10.1029/1999JD900170, 1999.

Wilson, S. L., Grogan, P., and Walker, V. K.: Prospecting for ice association: characterization of freeze–thaw selected enrichment cultures from latitudinally distant soils, *Can. J. Microbiol.*, 58, 402–412, doi:10.1139/w2012-010, 2012.

Wilson, T. W., Ladino, L. A., Alpert, P. A., Breckels, M. N., Brooks, I. M., Browse, J., Burrows, S. M., Carslaw, K. S., Huffman, J. A., Judd, C., Kilhau, W. P., Mason, R. H., McFiggans, G., Miller, L. A., Nájera, J. J., Polishchuk, E., Rae, S., Schiller, C. L., Si, M., Vergara Temprado, J., Whale, T. F., Wong, J. P. S., Wurl, O., Yakobi-Hancock, J. D., Abbatt, J. P. D., Aller, J. Y., Bertram, A. K., Knopf, D. A., and Murray, B. J.: A marine biogenic source of atmospheric ice nucleating particles, *Nature*, 525, 234–238, doi:10.1038/nature14986, 2015.

WMO/GAW World Meteorological Organisation/ Global Atmospheric Watch: Aerosol Measurements Procedures. Guidelines and Recommendations, available at: <https://www.wmo.int/pages/prog/gcos/documents/gruanmanuals/GAW/gaw143.pdf> (last access: 12.02.2015), 2003.

Wright, T. P., Hader, J. D., McMeeking, G. R., and Petters, M. D.: High Relative Humidity as a Trigger for Widespread Release of Ice Nuclei, *Aerosol Sci. Tech.*, 48, i–v, doi:10.1080/02786826.2014.968244, 2014.

Xia, Y., Conen, F., and Alewell, C.: Total bacterial number concentration in free tropospheric air above the Alps, *Aerobiologia*, 29, 153–159, doi:10.1007/s10453-012-9259-x, 2012.

Yamanaka, T., Tsujimura, M., Oyunbaatar, D., and Davaa, G.: Isotopic variation of precipitation over eastern Mongolia and its implication for the atmospheric water cycle, *J. Hydrol.*, 333, 21–34, doi:10.1016/j.jhydrol.2006.07.022, 2007.

Zawadzki, I., Jung, E., and Lee G.: Snow Studies. Part I: A Study of Natural Variability of Snow Terminal Velocity, *J. Atmos. Sci.*, 67, 1591–1604, doi:10.1175/2010JAS3342.1, 2010.

Acknowledgements/Ringraziamenti

Thank you Franz for being a present and motivated supervisor, for the scientific discussions we have had, which have significantly improved the quality of this job. I consider you as a model of scientific thinking.

Thank you Christine and Cindy for following my work, for having given me the chance, along with Franz, to take the lead of this interesting research project, for motivating me and being present also from a personal point of view all these years.

I am grateful to Benjamin Murray for taking part into the PhD committee.

I would like to thank SNF for funding my PhD project and the European Project ACTRIS for funding the measurements at Monte Cimone.

Thank you Axel, Thomas, Judith, Mark, Marianne, Caroline, Odile for your feedbacks and for your precious support in the laboratory.

Thank you Maria, Urs, Joan and Martin for the support at Jungfrauoch.

Thank you and a big hug to all of you UGW colleagues, for your feedbacks and suggestions, for the nice conversations we have had during these years, at lunch, during coffee breaks, at EGU. Jan Paul, Laura and Stefan you have been great office mates.

Thank you Pierre, Angela, MILAFers, co-authors of the articles.

Thank you Corinne, Samira and Michael for your work and for making me think about the importance of being a supervisor.

Thanks to all the friends known in Basel, for their nice words of encouragement.

Thank you to those who everyday stand up and decide to do even a small thing to change the world and thank you to every passionate person I have had the chance to meet.

Grazie alla mamma Milena (che è la persona più forte che conosco) e al babbo Giuseppe, per la vita che mi muove e per la libertà di scegliere, e grazie alle loro mamme e ai loro papà.

Grazie Jacopo per essere amico presente e solido.

Grazie Vale per le nostre vite parallele, grazie Hati per le risate insieme e grazie a Ennio e Andrea per il supporto a distanza.

Grazie Herbert per tutto.

Thank you everyone for your help and support, scientific and personal, and for your smiles.

Grazie a tutti voi per il vostro aiuto e supporto, scientifico e personale, e per i vostri sorrisi.

All of these lines across my face, tell you the story of who I am. So many stories of where I've been, and how I got to where I am. But these stories don't mean anything, when you've got no one to tell them to...

